THE AUTOCAUSTICIZING OF SODIUM CARBONATE WITH COLEMANITE

By

GULGUN SOZEN

B.Sc., Middle East Technical University, Turkey, 1981

A THESIS SUBMITTED IN PARTIAL FULFILLMENT OF

THE REQUIREMENTS FOR THE DEGREE OF

MASTER OF APPLIED SCIENCE

in

THE FACULTY OF GRADUATE STUDIES

(Department of Chemical Engineering)

We accept this thesis as conforming

to the required standard

THE UNIVERSITY OF BRITISH COLUMBIA

January 1985

Department of _Chemical Engineering_

The University of British Columbia
1956 Main Mall
Vancouver, Canada
V6T 1Y3

Date _Jan 22nd, 1985_

ABSTRACT

Autocausticizing, a new method to regenerate sodium hydroxide from the sodium carbonate, is intended to replace the conventional Kraft Recovery System which uses calcium hydroxide produced in a lime kiln for this purpose. It is defined as the self-induced expulsion of carbon dioxide bound in the smelt by using certain amphoteric oxides. Thus autocausticizing can eliminate the need for a lime cycle and hence reduce the Kraft process capital and operating costs.

The reactions between sodium carbonate and a number of amphoteric oxides have been reported in the literature. Patents have been issued on the use of titanium dioxide, iron oxide and sodium borates for this purpose.

The sodium borates have the advantage of a high reaction rate, but are totally soluble and must be carried throughout the whole Kraft cycle. In this research colemanite (calcium borate) which is mined as a cheap mineral in California and in Turkey was studied as an autocausticizing agent. Since it is partially soluble and most likely can be recycled, it would eliminate the problems associated with the use of soluble borates.

Experiments were performed both isothermally and under constant heating rate conditions. Isothermal studies were made with TiO_2, alumina and colemanite to compare their performances as autocausticizing agents at 900°C and 1000°C for various reaction times in an electric furnace.

The second group of experiments was made using a differential thermogravimetric (TG) analyzer. In these experiments mixtures with 20 to 80 weight percent colemanite in sodium carbonate were heated at a constant heating rate of 10°K/min in the range of 190-1000°C. The results indicate that two reaction were involved. Above the stoichiometric colemanite concentration the colemanite and sodium carbonate had reacted completely by a temperature of about 700°C. Above that temperature the impurities in the colemanite appeared to catalyze the decomposition of sodium carbonate if the colemanite concentration was less than the stoichiometric amount needed.

TG data were analyzed for the first and second reactions between the temperature ranges of 190-700°C and 700-1000°C respectively. Kinetic models were developed in terms of the reaction order, activation energy and frequency factor. The first reaction was found to be zero order on sodium carbonate concentration. The results also showed that the activation energy and frequency factor were functions of the colemanite concentration in the mixtures. As a result the rate was affected by the amount of colemanite used. The same was true for the second reaction except the reaction was first order. The concentrations predicted for the isothermal tests by the model were compared with the results of the isothermal study for various colemanite concentrations. Reasonable agreement was found except for the values at lower conversions, which might be due to the increased importance of the diffusion of CO_2 from the mixtures in the case of isothermal runs. It was also found that it is possible to obtain conversions as high as 85 percent with 40 percent colemanite in 20 minutes. Promising results were obtained from the recycle tests as well.

TABLE OF CONTENTS

LIST OF TABLES

LIST OF FIGURES

ACKNOWLEDGEMENTS

1. INTRODUCTION

Kraft pulping is the main pulping method used today. This process uses sodium hydroxide and sodium sulfide as a cooking agent. The former is converted to sodium carbonate when the alkaline spent pulping liquors are burned to yield chemicals and heat in a recovery furnace. Since sodium carbonate is not sufficiently alkaline to pulp wood to an adequate degree it must consequently be transformed into hydroxide. This process is called causticization, and is conducted with the aid of calcium hydroxide which is generated in a lime kiln. The major disadvantage of the Kraft process is the cost, complexity and the inflexibility of this recovery system. The lime kiln is the last major user of fossil fuel in a Kraft mill and the causticizing area is difficult to maintain in a clean non-polluting state.

Autocausticizing is proposed to replace the conventional causticizing and lime kiln system. This process is based on the fact that certain amphoteric oxides react with sodium carbonate liberating the alkali bound carbon dioxide from the mixture at high temperatures and forming mixed oxide compounds (smelt) which will give a strong base on dissolution in water.

The oxides proposed in the literature as agents for the autocausticizing reaction can be divided into two main groups according to their behaviour in the smelt dissolving stage. The first group of compounds consists of chemicals which form alkaline solutions in which the amphoteric oxide is in a soluble form, so that it is carried through the whole cycle of the process, and increase the inorganic load in the system. In this group of compounds are mainly borates,

phosphates, silicates and aluminates (18). The second group of compounds are precipitated from the sodium hydroxide solutions during the dissolution step. Examples of compounds in this group are titanium dioxide, ilmenite ($FeTiO_2$) and iron oxide (Fe_2O_3) (18).

Titanium dioxide was studied as a catalyst by Kiiskila (20,21). Although it gave very good causticizing efficiency it didn't appear promising because of the high cost of this chemical. A pilot plant study was performed using iron oxide by Australian Paper Manufacturers Ltd. using a fluidized bed reactor, and promising results were reported (4). The behaviour of the sodium borates as causticizing agents has been studied by J. Janson (8). According to the results of this work, borates seems to be the best agent for autocausticizing reactions. Although sodium borates were studied as an autocausticizing agent there has been no literature available on the chemistry and kinetics of the process which uses calcium borate (colemanite) as an autocausticizing agent.

Colemanite is a cheap unrefined rock which is found in California and Turkey. Since it is partially soluble, it has certain advantages over sodium borates and it is expected to be compatible with the other autocausticizing agents studied previously.

2. LITERATURE REVIEW

2.1 Kraft Pulping

The Kraft process is the most widely used method of pulping in North America and in the world. The following figure shows this process diagrammatically. The cooking liquor (white liquor) which consists of sodium hydroxide and sodium sulfide is sent to a digester where delignification of the wood takes place according to the reactions

$$Na_2S + H_2O \rightarrow NaSH(aq) + NaOH \qquad (2.1)$$

$$NaOH(aq) + NaSH(aq) + HOrg \rightarrow NaSH(aq) + NaOrg(aq) \qquad (2.2)$$

where HOrg stands for the alkali consuming wood components. In the recovery cycle, spent cooking chemicals (black liquor), a mixture of many sodium-sulfur-carbon compounds are converted to sodium sulphide (Na_2S) and sodium carbonate (Na_2CO_3) in the recovery furnace following the reactions

$$NaOrg + xO_2 \rightarrow 1/2\ Na_2CO_3 + yH_2O + zCO_2 \qquad (2.3)$$

and

$$NaSH + NaOrg + xO_2 \rightarrow Na_2S + yH_2O + zCO_2 \qquad (2.4)$$
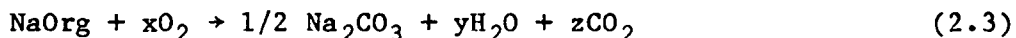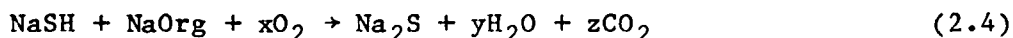
The product (smelt) is dissolved in water to give the so called green liquor. The remainder of the cycle is concerned with converting Na_2CO_3 to sodium hydroxide which will be reused in the pulping
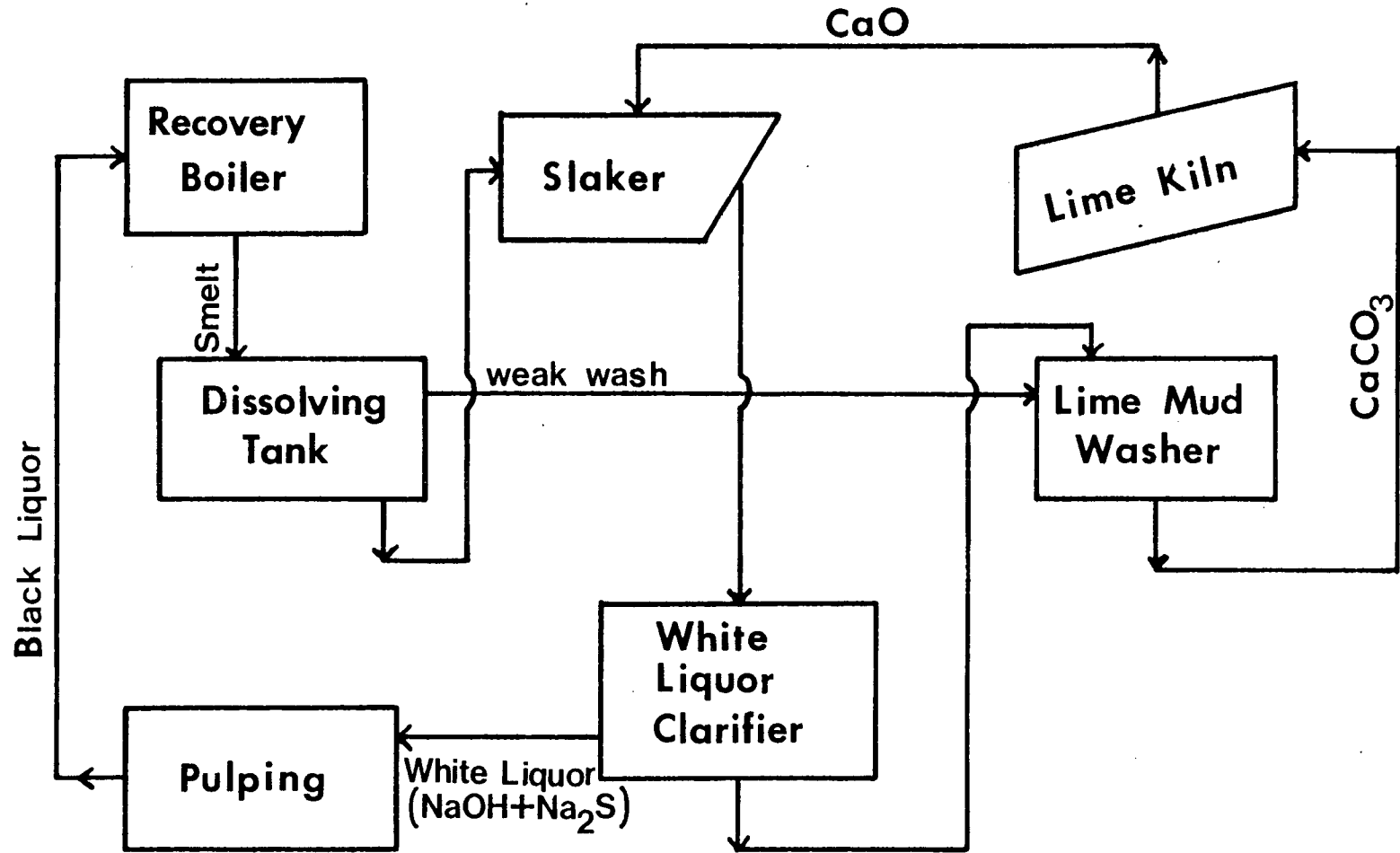
Figure 1: Schematic diagram of Kraft Process.

process. This causticization process uses calcium hydroxide which is obtained by calcining calcium carbonate in a lime kiln via the reaction

$$CaCO_3 \rightarrow CaO + CO_2 \qquad (2.5)$$

The final stage of the recovery takes place in the slaker where soluble sodium hydroxide is formed via the overall reaction

$$CaO + H_2O + Na_2CO_3 \rightarrow 2NaOH + CaCO_3 \qquad (2.6)$$
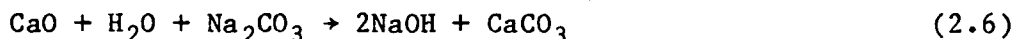
The insoluble calcium carbonate is separated from the solution and is sent back to the lime kiln.

2.1.1 Problems of Kraft Recovery System.

Although the Kraft process has found worldwide use in pulping there are some problems especially associated with the present recovery system.

The Kraft Recovery Process is capital intensive, and it is often difficult to get an adequate return on this investment. The capital cost structure (18) of a Kraft pulp mill is given in Table 1. The share of chemical recovery in the departmental capital cost distribution is about 27.5% and the machinery costs are about 48% of the total investment (18). It is also seen from this table that the lime kiln and causticizing make up 20% of the total investment of the recovery system.

Table 1: Capital cost structure of a new Kraft pulp mill. (18)

Total capital cost distribution (%) Ref. Ehrnrooth (1)		Department capital cost distribution (%) Ref. Harris (25)		Capital investment cost distribution of recovery (%) Ref. Kiiskila (23)	
Building	18	Wood preparation	6.2	Recovery furnace	60
Machinery	48	Pulping	16.3	Evaporation	20
Piping	8	Bleaching	11.8	Lime kiln	16
Electrification	9	Drying and baling	15.6	Causticizing	4
Instrumentation	4	Chemical recovery	27.5		
Project administration	13	Effluent treatment	5.8		
		Power generation	16.8		
Total	100		100		100

The net amount of usable energy obtained from the organic substances in the black liquor by burning in the recovery boiler is low. At present, less than 40% of the fuel input to the recovery process is available as steam or power outside the recovery process itself (6). Much of the energy potentially available is now used for evaporating water. In addition a substantial amount of fuel, usually fossil fuels, is burned in the lime kiln. A modern fuel efficient kiln requires 8×10^6 Btu/Ton of product. As the cost of energy continues to increase, the potential for a simplified recovery systems is increasing.

Environmental pressures have also had a major impact on recovery technology. Odors which are the largest single environmental problem of the Kraft Recovery Process are inherent in the process if sulfide is used for pulping, due to the very low odor thresholds of the compounds involved. Sulfur dioxide emissions can also be a problem in some areas.

There are some potential safety problems in the present Kraft recovery technology. The most pervasive is the potential for smelt-water explosions when water comes in contact with molten smelt. Another potential hazard involves the collection and incineration process for odorous gases, since these are toxic and can form explosive mixtures with air.

Another disadvantage of the present recovery system is its low causticizing efficiency, resulting in low sodium hydroxide concentrations in the white liquor. As a result of incomplete causticizing about 15% of the alkali circulates as sodium carbonate

through the whole pulping and chemical recovery system as a dead load. Since the sodium hydroxide concentration in the white liquor is limited, because of its influence on the causticizing equilibrium, it also influences the total evaporation demand on a mill (13).

The status of current Kraft recovery technology might be characterized as "mature" but certainly not stagnant. None of the problems of the present technology are severe enough to render it obsolete. Rather, they represent opportunities for further improvement. There are two directions that evolving Kraft recovery technology might take, continued improvement of the existing technology and the development of alternative processes.

2.1.2 Alternatives to Conventional Kraft Pulping.

A number of new chemical recovery methods have been patented and published in recent years. These new methods can be divided, according to their principal aims, into two main groups (18);

1. The methods intended to replace the conventional recovery furnace and, as far as possible, eliminate the smelt explosion danger. Examples of these methods are wet combustion (18), fluidized bed (4), hydropyrolysis (18) and the SCA Billerud (18) methods.

2. The methods intended to replace the conventional wet causticizing and lime reburning system. The drawbacks of wet causticizing could be avoided by performing the causticizing in a dry state so that the smelt would be decarbonized by adding an auxiliary compound to the smelt or by using an unconventional alkali in pulping.

These methods are called autocausticizing and will be discussed in the following section.

The air and water pollution caused by sulfur compounds has led to the development of non-sulfur pulping methods. The most promising non-sulfur pulping method seems to be two-stage soda-oxygen pulping (18). The latest results on the use of anthraquinone type compounds (18) in soda pulping suggest new and interesting possibilities for modifying the conventional alkaline pulping methods. However the changeover from Kraft pulping to a new pulping system must be motivated not only environmentally but also economically. So most of the present research is concentrated on finding the autocausticizing agent which will reduce considerably the cost of the process.

2.2 Autocausticizing Processes

Autocausticizing is a new method to regenerate sodium hydroxide or another strong base from the sodium carbonate and seems to be the most promising alternative for the conventional Kraft Recovery System.

Autocausticizing is defined as the self-induced expulsion of the carbon dioxide bound in the smelt or in ash formed during the burning of spent liquor, without the use of causticizing chemicals such as calcium oxide. This method depends on the fact that certain amphoteric oxides react with sodium carbonate, liberating the alkali bound carbond dioxide from the mixture at high temperatures and form mixed oxide compounds. The principle of the autocausticizing method can be illustrated by the following general reaction

$$a\ Na_2CO_3 + b\ M_xO_y \rightarrow a\ Na_2O \cdot b\ M_xO_y + a\ CO_2 \uparrow \qquad (2.7)$$
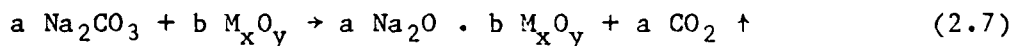
Autocausticizing processes are divided into two main groups depending on the behaviour of the amphoteric oxide used during the smelt dissolution step. This step can be represented by the following reaction

$$a\ Na_2O \cdot b\ M_xO_y + a\ H_2O \rightarrow 2a\ NaOH + b\ M_xO_y \qquad (2.8)$$
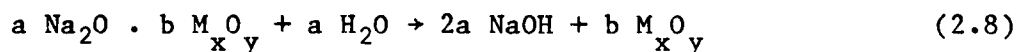
if the amphoteric oxide is insoluble, it precipitates and can easily be separated from the white liquor and recycled without entering into the digestion loop as shown in Figure 2. This is called smelt causticizing or the DARS method. If the amphoteric oxide is soluble, it circulates through the whole pulping cycle. So it should not only be autocausticizible under reasonable conditions, but also be sufficiently alkaline to function as a delignification agent.

The research on both types of autocausticizing methods was started in 1974 in Finland. Since most of the work is patented, not much is known about the process. However, during the past two years, pilot plant work has been started; one study by J. Janson (9) in Finland and the other by an Australian company under the supervision of G. Covey (4). A plant is to go on stream using autocausticization in 1984 at the Kotka Mill, Finland.

Figure 2 shows the comparison of an autocausticizing method with the Kraft recovery process. The advantages and disadvantages of autocausticizing will be discussed in detail in section 2.2.3 for the specific autocausticizing agents.
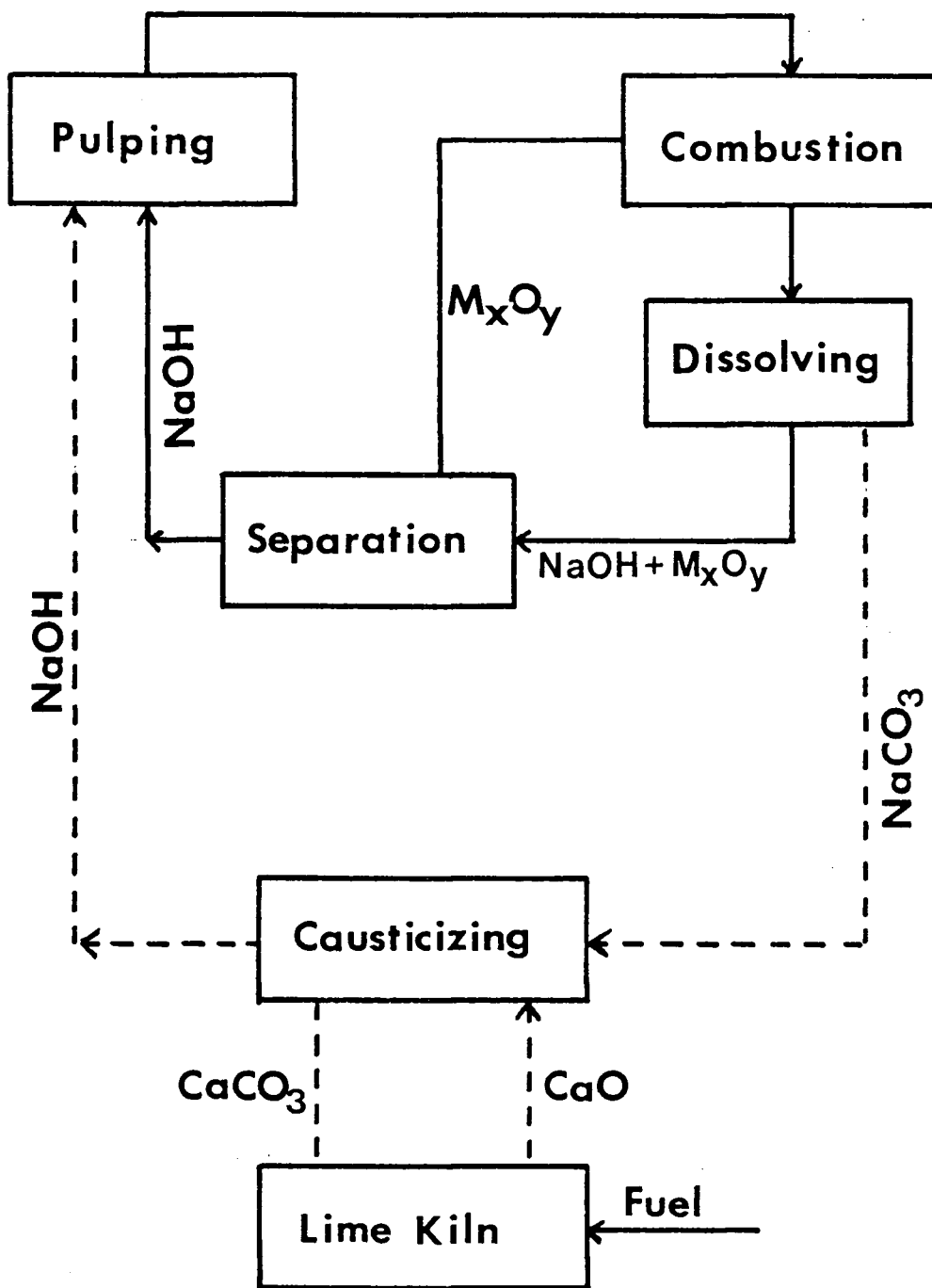
Figure 2:   Comparison of autocausticizing with conventional
            causticizing.

2.2.1 Decomposition of Sodium Carbonate Without an Autocausticizing Agent.

Sodium carbonate is thermally unstable above its melting point and can be slowly decomposed at low carbon dioxide partial pressure even without adding amphoteric oxides (23), according to the reaction

$$Na_2CO_3 \rightleftharpoons Na_2O + CO_2 \qquad (2.9)$$
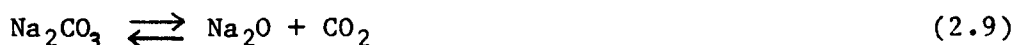
However, this reaction is hindered by the high partial pressures of carbon dioxide in the recovery furnace. Besides, sodium oxide is volatilized from the smelt if there is no stabilizing auxiliary compound present in the smelt (23).

Thermal decomposition of sodium carbonate by itself will be studied in section 6.2 and illustrated in Figure (22). This reaction most likely doesn't take place below 850°C and its rate is very slow even at 1000°C.

2.2.2 Autocausticizing Reactions.

Autocausticizing reactions will be examined in two parts.

1. Decomposition

2. Hydrolysis

The decomposition reaction takes place at high temperatures. The optimum temperature for the reaction is strongly dependent on the type of agent choosen. This reaction is generally illustrated as

$$a\ Na_2CO_3 + b\ M_xO_y \rightarrow a\ Na_2O \cdot b\ M_xO_y + a\ CO_2 \uparrow \qquad (2.10)$$
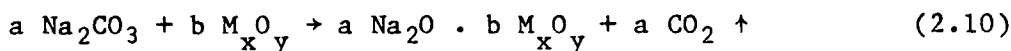
The causticizing agent which is an amphoteric oxide, either soluble or insoluble, acts in a two-fold manner in the decarbonization:

(i) It accelerates the decomposition of sodium carbonate.

(ii) It stabilizes the sodium oxide in the smelt.

There are many factors to be analyzed, depending on the choice of the autocausticizing agent, whether it is soluble or insoluble. If it is soluble it should either replace the sodium hydroxide and act as a cooking agent or circulate through the system as a dead load. In this case its effects on the efficiency of the delignification of the wood during cooking and the properties of the pulp must be considered.

For both types of agents the effect of the following factors which exist in the drying and burning zones of Kraft furnace should be analyzed, as well as the reaction itself.

1. Effect of presence of sulfur on the reaction.

2. Effect of carbon dioxide pressure.

3. Effect of the presence of organics.

The experiments which were performed by J. Janson (9) and Kiiskila (23) showed that the presence of sulfur and the organics did not have a significant effect on the reaction. However it was found that in the absence of gaseous CO_2, the decarbonization of the smelt can be more effective.

The hydrolysis step is more important in the cases where insoluble amphoteric oxides are used. The studies on the hydrolysis of causticized smelt showed that the mixed oxides formed as product of the autocausticizing reaction can be effectively decomposed to

sodium hydroxide at a sufficiently high dissolving temperature (90°C) with low washing losses (23). The insoluble fraction of sodium oxide influences the causticizing efficiency after several repeated runs. This was also studied by Kiiskila (23) using different kinds of autocausticizing agents.

2.2.3 Agents Proposed for Autocausticizing.

The agents which are proposed in the literature for autocausticizing reactions are listed in Table 2, including the desired reaction products. These are divided into two main groups according to their behaviour in the smelt dissolving step. The oxides listed in group one are chemicals which form ionized alkaline solutions in which the amphoteric oxide is at least partially soluble. The compounds in the second group are insoluble and can be precipitated from the sodium hydroxide solutions formed in the dissolving stage.

2.2.3.1 Titanium Dioxide.

Titanium dioxide is the compound which is found to be most promising among the group two compounds, according to the literature (18). It is a stable but very expensive chemical. It is practically insoluble in alkaline solutions and can be easily separated from the white liquor formed. According to the patent literature (19), the process is based on the formation of sodium metatitanate in mixtures of sodium carbonate and titanium dioxide and is represented by the following chemical formulas

Table 2: Proposed autocausticizing agents.

	M_xO_y	$Na_{2a}M_{bx}O_{a+by}$
Group (1)	B_2O_3	$Na_4B_2O_5$, $NaBO_2$
	P_2O_5	Na_3PO_4
	SiO_2	Na_2SiO_3
	Al_2O_3	$NaAlO_2$
Group (2)	TiO_2	Na_2TiO_3
	$FeTiO_3$	$2\ Na_2O:FeO_3:TiO_2$
	Fe_2O_3	$NaFeO_2$

$$Na_2CO_3 + TiO_2 \quad \rightarrow \quad Na_2O \cdot TiO_2 + CO_2 \quad\quad (2.11)$$

$$Na_2O \cdot TiO_2 + H_2O \quad\quad 2NaOH + TiO_2 \quad\quad (2.12)$$

reuse

(ppt)
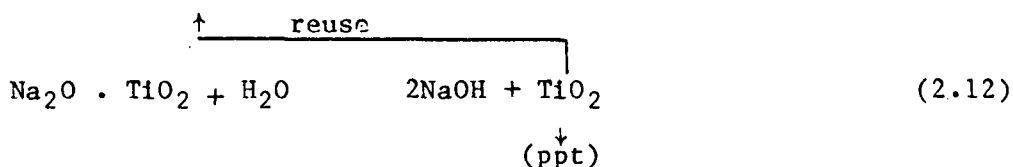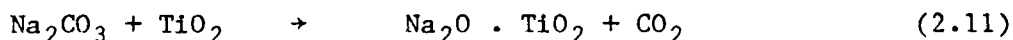
The carbon dioxide bound in the alkali during black liquor combustion is liberated from the smelt when the mixed oxide is formed. Because of the weak coordination of the alkaline oxide with the titanium, the compound decomposes when it is dissolved in water.

Decarbonization of sodium carbonate by titanium dioxide was studied by Erkki Kiiskila (18,20,21). The thermogravimetric curves for the mixture of sodium carbonate and titanium dioxide at a molar ratio of 1.1:1.0 showed that the decomposition of sodium carbonate caused by titanium dioxide starts in the solid phase at 500°C (19), but this reaction is very slow until the melting point of sodium carbonate is reached. Above 850°C the rate of the reaction between melted sodium carbonate and solid titanium dioxide is fast if the molar ratio of Na_2O/TiO_2 of the reaction product is 1.0 (19). The rapid decomposition of sodium carbonate at 850-950°C is due to the formation of $4Na_2O \cdot 5TiO_2$ which reacts further with sodium carbonate to yield $Na_2O \cdot TiO_2$ at low CO_2 partial pressure. According to the final weight loss of samples at 980°C, 79% of the CO_2 was removed from the mixture for a sodium carbonate to titanium dioxide ratio of 1.0 (19). Some isothermal experiments were also carried out. It was found that complete decomposition of sodium carbonate is possible by lengthening the reaction time, provided that the temperature is high enough (1100°C) (19) (Fig. 3). It was also found that the presence of

titanium dioxide decreases the sodium losses in the flue gases.

Volatilization of the Na_2O becomes significant only above 1100°C (20).
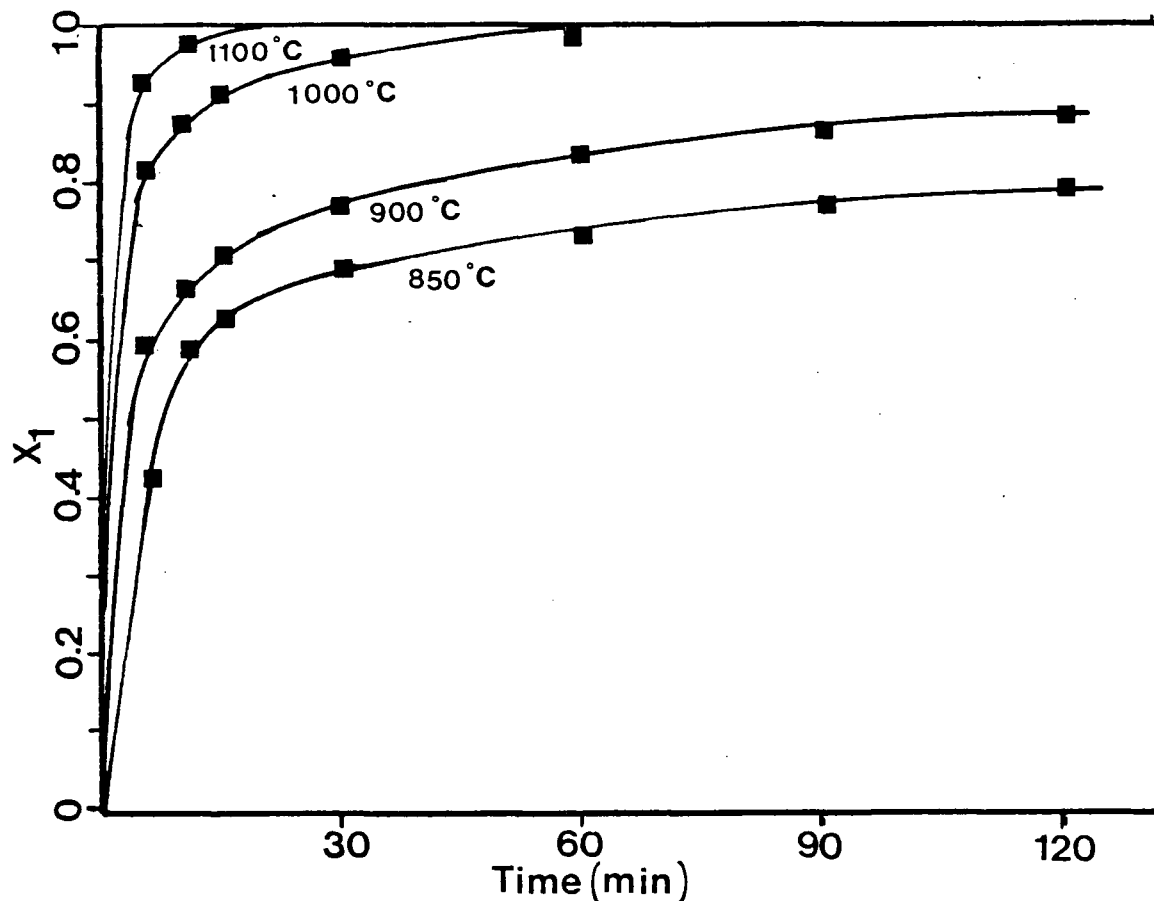
Figure 3: Fraction of the Decomposed Sodium Carbonate as a Function of the Reaction Time with the use of TiO_2

Studies on the hydrolysis of the causticized smelt were also made and it was found that the degree of sodium hydroxide formation from bound sodium oxide (Na_2O) was dependent on the Na_2O/TiO_2 ratio of the titanates in the smelt. The degree of hydrolysis decreased with an increase in the titanium dioxide content of these compounds. The sodium hydroxide formed from $Na_2O \cdot TiO_2$ corresponded to 65.8% of the

total sodium, which was the highest recovery; compared to the values
for the other titanates such as $4Na_2O.5TiO_2$, $Na_2O.3TiO_2$ (20). So in
all cases studied, the hydrolysis was not complete, and the insoluble
titanium dioxide residue contained about 0.33 moles of sodium oxide
per mole of titanium dioxide (20). For this reason the sodium
hydroxide yield is dependent not only on the degree of sodium
carbonate decomposition but also on the Na_2O/TiO_2 ratio of the smelt.

The effect of time and temperature on the hydrolysis of the
smelt was studied as well as the effect of the amount of water used in
the extraction (20). The rate of hydrolysis increased when the
temperature was raised from 30°C to 60°C, but a further rise in
temperature did not improve the efficiency significantly. Experiments
were performed at 90° with the retention time of three hours and it
was found that even after three hours the insoluble residue still
contained insoluble Na_2O in the hydrolyzed compounds (20). This
evidently reduces the efficiency of titanium dioxide in causticizing.
Because this undissolved residue is nearly constant per mole of
titanium dioxide, it causes a constant reduction in the causticizing
efficiency when titanium dioxide is reused.

On the whole, it seems that sodium carbonate can be efficiently
causticized by using titanium dioxide. Although it is theoretically
suitable for this purpose, it is too expensive to use on a commercial
scale. For this reason investigations were concentrated on finding
cheaper chemicals like Fe_2O_3 and ilmenite.

2.2.3.2 Ferric Oxide.

The use of ferric oxide for the causticization of sodium carbonate has been studied by Kiiskila (21). The chemistry can be represented as follows

$$Na_2CO_3 + Fe_2O_3 \quad \rightarrow \quad 2NaFeO_2 + CO_2 \uparrow \qquad (2.13)$$

$$2NaFeO_2 + H_2O \quad \rightarrow \quad 2NaOH + Fe_2O_3 \downarrow \qquad (2.14)$$
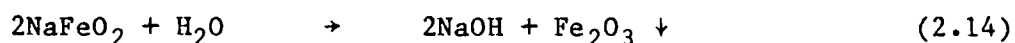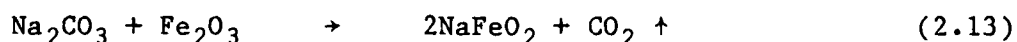
Experiments were performed at 900°C and 1000°C and it was found that it is possible to obtain a causticizing efficiency as high as 95 percent. The chemical load is lower than in the titanium dioxide case due to the more complete hydrolysis of sodium ferrites which results in more effective causticizing of the smelt to sodium hydroxide. Use of ferric oxide has the disadvantage that the ferric oxide suspended in the aqueous solution is not easily precipitated and is hard to separate. In addition to this, its use in Kraft recovery is restricted because of the reduction of ferric oxide and its reactions with sodium sulfide. However, it could be applied to the soda or soda-oxygen processes which are sulfur free.

The work on the utilization of ferric oxide as an autocausticizing agent gained importance during 1977 and since then work has been done to commercialize it. A process which uses a fluidized bed type furnace was developed by G. Covey (4). This process has been operated since early 1980 at a pilot plant at the Maryvale Mill of Australian Paper Manufacturers. The simplified flow diagram of the process is shown in Figure 4. The pilot plant operation has been reported to be successful (4).
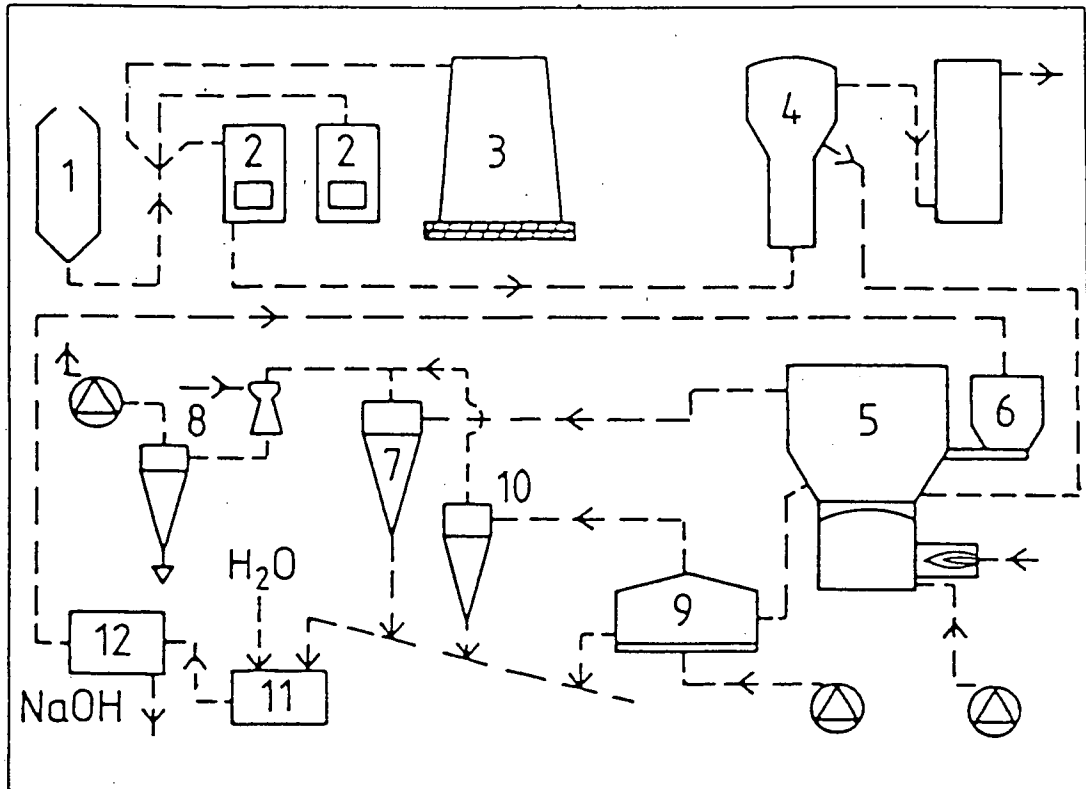
Figure 4: Simplified flow sheet of the DARS research plant (4).

1. Digester
2. Batch diffusers
3. Live-bottom blow tank
4. Evaporator
5. Fluidized bed
6. Ferric oxide silo
7. Main cyclone
8. Venturi scrubber
9. Product cooler
10. Cooler cyclone
11. Ferrite leacher
12. Filter

2.2.3.3 Ilmenite.

Ilmenite is a double oxide which consists of iron (II) oxide and titanium dioxide. Therefore both components can be expected to react with molten sodium carbonate, if iron (II) oxide is oxidized to iron (III) oxide. Table 3 shows the composition of this ore.

Laboratory experiments showed that sodium carbonate can be decomposed by adding ilmenite to the smelt. The titanium dioxide part of the ilmenite reacted to sodium titanates while the ferrous iron reacted to sodium ferrites after being oxidized to ferric iron. The reaction was found to be most effective at 940°C (22). The causticizing efficiency was found to be lower than that for titanium dioxide and ferric oxide. This is due to the fact that the ilmenite lattice is only partially broken in the absence of oxygen. The hydrolysis of the smelt was not complete due to the incomplete hydrolysis of sodium titanates (31). In addition to these problems high volatilization losses of sodium oxide were reported with ilmenite (22).

2.2.3.4 Silicates, Aluminates and Phosphates.

These compounds are among those classified as the first group of autocausticizing agents which are soluble in alkaline solutions and circulate throughout the process. They must not only be autocausticizible but also must be strongly alkaline in order to function as delignification agents. Among these, phosphates and aluminates were preferred because of their high melting point at 1340°C and 1150°C respectively. The reaction products were also solid. This has the

Table 3:   Composition of ilmenite (17).

Composition	Titanium ore (Ilmenite) weight %	Titanium ore after 10 times repeated use weight %
TiO_2	52.2%	53.4%
Fe_2O_3	46.8%	46.3%
Al_2O_3	0.6%	0.2%
SiO_2	0.1%	–
Others	0.3%	0.1%

advantage of easy handling, transport and easier dissolution in water compared to the glassy, slowly dissolving smelts. The problem with the phosphates is that their alkalinity is not strong enough to match sodium hydroxide. Therefore it can not be used in the normal Kraft process but it is suitable to be used together with other delignifying agents such as oxygen. Aluminates are not suitable for this reaction because sodium aluminates are rather unstable and aluminum hydroxide precipitates even in strongly alkaline solutions and can cause scaling (13). Besides, the temperature of the autocausticizing reaction was found to be 1150°C which is much higher than the one found for all other agents.

Silicates can also act as a decarbonizing agent. However in the case of silica, when the compound oxide thus formed is dissolved in water, the silica is partly dissolved in the form of sodium silicate into the solution of caustic soda, so that when a regenerated white liquor is used for pulp digestion, silicate compounds are deposited on the inner surfaces of the digester and heat exchangers thus causing scale trouble.

2.2.3.5 Borates.

Borates are one of the alternatives which may be used in autocausticizing processes. It has been found that borate compounds fulfill the requirements as regard both the alkalinity during cooking and the desired reaction during regeneration. Research has been done by the Finnish Pulp and Paper Research Institute in Helsinki and by J. Janson, and very promising results including some pilot

plant data have been reported on the use of sodium borates.

Laboratory experiments were performed using mixtures of monosodium borate and sodium carbonate at a molar ratio of Na:B of 2.0. In this case the following reactions can be expected.

$$2NaB(OH)_4 \rightarrow 2NaBO_2 + 4H_2O \qquad (2.15)$$

$$2NaBO_2 + Na_2CO_3 \rightarrow Na_4B_2O_5 + CO_2 \qquad (2.16)$$
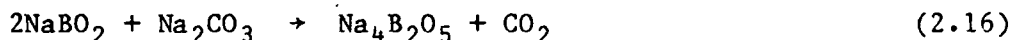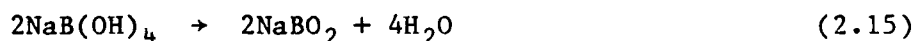
In the recovery furnace monosodium borate is dehydrated to sodium metaborate which reacts with the carbonate with the expulsion of carbon dioxide, to form tetrasodium diborate. On dissolution in water the tetrasodium diborate yields sodium borate which will take the place of sodium hydroxide as a cooking alkali. Table 4 summarizes the differences between the chemical systems in conventional and borate-based pulping. These laboratory experiments showed that about two hours at 875°C was needed to give an 80 percent removal of CO_2 (10). This is shown in Figure 5. The data fitted the kinetics of a second order reaction better than first and third order reaction. The activation energy was found to be 148 kJ/mol and the frequency factor was found to be -0.304 for these specific conditions (10). Seventy percent of the weight loss occurred before levelling off at 800-1000°C (10).

In the case of the borate reactions the ratio of sodium to boron is a very important parameter to be considered. The alkalinity of borates and thus their delignifying ability in water solution increases with increasing ratio of Na:B. On the other hand their

Table 4: Main constituents of cooking chemical system (9).

Chemical system	White liquor	Black liquor	Smelt	Green liquor
Normal	NaOH (Na$_2$S)	NaOrg (NaSH)	Na$_2$CO$_3$ (Na$_2$S)	Na$_2$CO$_3$ (Na$_2$S)
Borate-based	Na$_2$HBO$_3$ (Na$_2$S)	NaOrg (NaSH) NaH$_2$BO$_3$	Na$_4$B$_2$O$_5$ (Na$_2$S)	Na$_2$HBO$_3$ (Na$_2$S)

REMAINING CO$_2$
FRACTION OF ORIGINAL
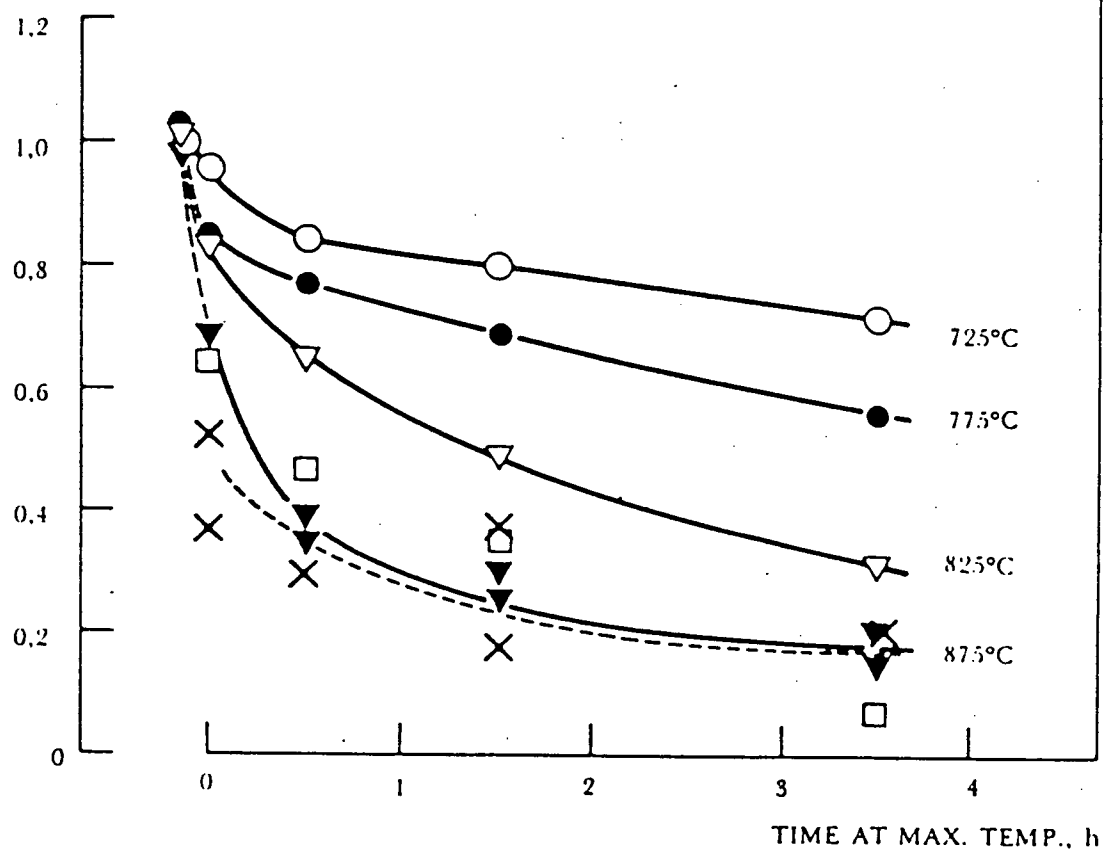
Figure 5:   Autocausticizing reaction in air:
$2 \ NaH_2BO_3 + Na_2CO_3 \rightarrow Na_4B_2O_5 + 2 \ H_2O + CO_2$ (8)

acidity decreases which would result in a decrease in the efficiency of carbon dioxide expulsion from the carbonate. Various Na:B ratios were tried by J. Janson and the optimum ratio was reported as 2.0 (10) for the Kraft process. Figure 6 shows the areas of application for different ratios of sodium to borate.

Experiments have also been made on the pulping characteristics of sodium borates. It was found that one mole of sodium hydroxide can be replaced by one mole of disodium borate without essentially changing any other conditions (11). There was very little difference in the pulp yields from hydroxide and borate based pulping, nor were there any differences in pulp properties. Black liquor from the borate cooks contained relatively more inorganic matter and therefore had a correspondingly lower heat value on a dry basis. Thus it will be necessary to burn auxiliary fuel in the recovery furnace.

According to the results of a 9 hour mill trial it was found that the melting point of the smelt was lowered by roughly 50°C. This would be advantageous from the standpoint of smelt dissolution with a lowered risk of explosion. It was also found that the amount of fly ash was reduced by half when the borate-based liquors were used.

Among the disadvantages of using borate-based liquors are: the probable decrease in evaporator performance, probable difficulties during burning in the recovery furnace due to the increased viscosity of the borate liquor which would cause a larger drop size when sprayed into the furnace, and inferior heat economy due to the higher inorganic content of the black liquor.
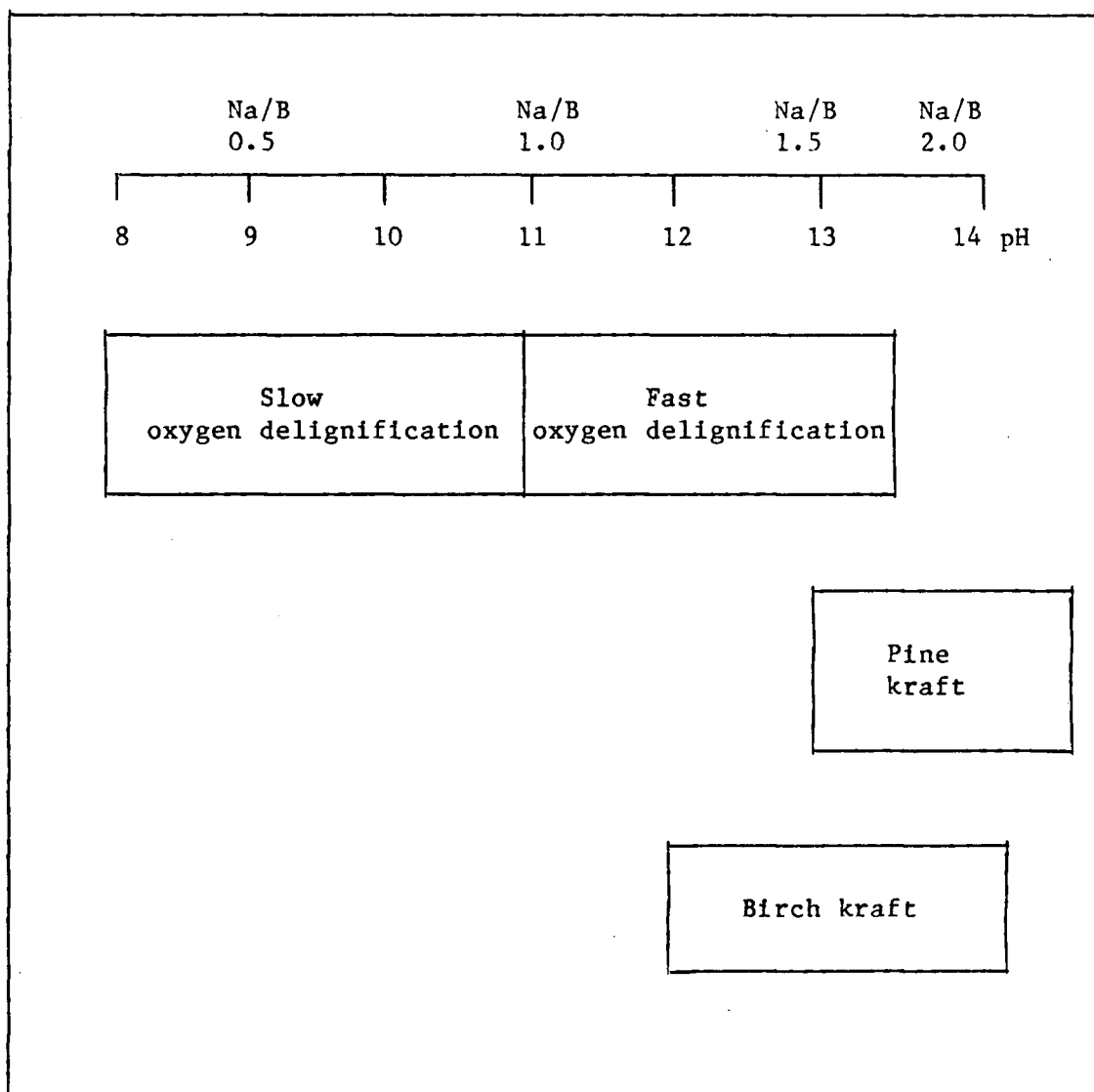
Figure 6: Areas of application for different kinds of
autocausticizable alkali (9).

J. Janson has also performed some calculations to evaluate the economic aspects of using borates in Kraft pulping. Preliminary calculations were made on the changes in investment costs and operation costs of a new Kraft mill (15) assuming a pulp production of 600 ton/day. Table 5 shows his conclusions. The investment cost will be lower when autocausticizing is employed, with the largest difference being in the lime kiln costs. Regarding the operation costs, it was noted that the make-up chemicals are more expensive in the borate alternative while somewhat less manpower will be needed and energy will be saved. Table 6 shows the changes in consumption and cost of energy by a borate-based system.

2.2.3.6 Colemanite (calcium borates).

Borate deposits are formed when one or more of the hydrated borates of sodium, calcium and magnesium are crystallized by the evaporation and probable cooling of surface water in a desert basin. Colemanite is one type of borate deposit which can be represented by the formula $2CaO \cdot 3B_2O_3 \cdot 5H_2O$.

The main colemanite deposits of the world are located in Southeastern California, Southern Nevada and Turkey.

Colemanite has been crystallized from aqueous solution as have other forms of crystalline calcium borate hydrates. Often the precipitate first formed is amorphous and crystallizes after standing in contact with the mother liquor for several days (25). Some studies have shown that the crystal structure of the borate ions of colemanite can be represented as

Table 5: Change in costs by choice of borate-based system (600 t/d) (15).

```
Investment:

-30 . 10^6 FIM* (-7.5 . 10^6 USD)

Operation:
        Energy: -23 FIM ptp
     Chemicals:  14 FIM ptp
        Labour:  -1 FIM ptp
 Total change: -10 FIM ptp
           or:  -2.5 USD ptp

*FIM: Finish money
```

Table 6: Consumption and costs of energy (15).

Change in energy costs by choice of
a borate-based system (600 t/d)

Prices: Oil: 750 FIM/t = 20 FIM/GJ
         HP steam: 24 FIM/GJ
         LP steam: 12 FIM/GJ
         El. power: 120 FIM/MWh

Change in consumption/generation ptp (per ton dry pulp):

	Oil		Heat		El. power	
	MJ	FIM	MJ	FIM	kWh	FIM
Consumption						
Evaporation	–		-380		–	
Combustion	1400		–		–	
Causticizing	–		-100		-12	
Lime reburning	-2000		–		- 8	
Σ	-600	-11.3	-480	-5.8	-20	-2.4
Generation						
HP steam	–	–	130	3.1	–	–
Net change	-600	-11.3	-610	-8.9	-20	-2.4

Total change in energy costs: -22.6 FIM ptp
                          or: - 5.7 USD ptp

$$\left[\begin{array}{c} \text{OH} \\ | \\ \text{B} \\ \text{O} \quad \quad \text{O} \\ \text{HO} \quad \quad \quad \text{OH} \\ \text{B} \quad \text{O} \quad \text{B} \\ \text{HO} \quad \quad \quad \text{OH} \end{array} \right]^{-2}$$
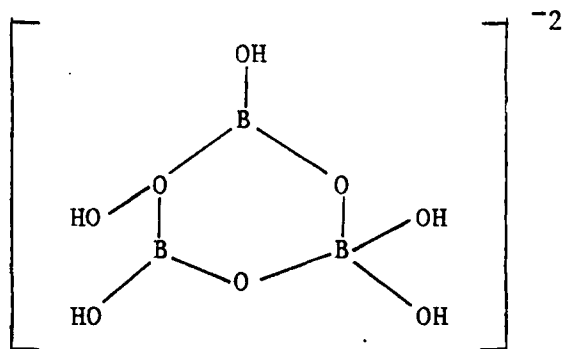
These ions have been polymerized by the elimination of water between them to form long chains at high temperatures to form colemanite (25).

Since colemanite comes from natural rocks it may contain impurities such as silicates, ferric oxides and aluminates. Pure colemanite contains 50.8 percent boric oxide (B_2O_3) (25). Although it is reported to be insoluble, it was found to be soluble to a certain degree due to the impurities in it (26). The composition and physical properties of Turkish colemanite determined by the American Borate Company is shown in Appendix III.

An examination of the thermal characteristics of colemanite indicates that the thermal changes fall into four groups (25).

a) irreversible endothermic peaks associated with dehydration

b) reversible endothermic peaks associated with polymorphic transitions

c) reversible endothermic effects associated with melting

d) irreversible exothermic effects associated with solid-state transformations.

Table 7 shows the temperatures associated with each of the thermal
changes in colemanite.

Table 7: Thermal characteristics of colemanite (3).

Mineral	Endothermic Peaks				Exothermic Peaks	
	1	2	3	4	1	2
Colemanite	320-380	380-400	410	-	710-770	-

The idea of using colemanite as an autocausticizing agent
is very recent and there is no literature available on this subject.
The results reported by J. Janson on the autocausticizing effect of
sodium borates indicated that colemanite which is an insoluble borate
compound, might act in the same manner. If it would be possible to
use colemanite as an autocausticizing agent, the disadvantages
resulting from the soluble character of the sodium borates such as the
increased inorganic load, complexities due to the change of
conventional cooking chemical etc. would be eliminated or reduced.
Since it is only partially soluble the majority can be recycled
without passing throughout the pulping system. Besides this,
colemanite is a cheap chemical which costs 21 cents/kg, compared to

sodium borates at $1.20/kg. This would make a considerable difference from the economic feasibility point of view of the process if equal quantities are used. It was for this reason that research on the autocausticizing properties of colemanite was undertaken as the subject of this thesis.

2.3 Study of Reaction Kinetics by Thermogravimetry.

Thermogravimetry can be used to study the kinetics of a chemical reaction and determine the basic kinetic constants such as the rate constant, activation energy, order of the reaction and frequency factor.

When the kinetic study is based on the observation of the weight change, two approaches are possible in principle, the isothermal and the dynamic heating methods. The isothermal method is the conventional method for studying the kinetics of the thermal decomposition of solids and is based on the determination of the degree of transformation, which is the fraction of material reacted, as a function of time at constant temperature. The dynamic method is the determination of the degree of transformation as a function of time during a linear increase of temperature. Ideally, a single thermogram is equivalent to a very large family of comparable isothermal curves and, as such, constitutes a rich source of kinetic data. It was in 1932 that Skramousky (29) pointed out the advantages of this method. Since the method demands strict experimental conditions and a high accuracy in the measurement, development took

place only after 1960 when the equipment reached a sufficiently high
standard (30).

Compared with the static method, this method has certain
advantages. It requires a far smaller number of experimental data
because the kinetic values can be determined from a single
thermogravimetric curve for the whole temperature range and one sample
suffices for the whole kinetic analysis. This also gives a better
indication of the state of the sample at any moment with respect to
temperature and degree of reaction. In the case of isothermal methods
the greatest experimental difficulty is the introduction of the sample
into the preheated furnace. Time elapses before the sample attains
the required temperature, and during this time the reaction occurs to
a certain extent. Thus, instead of a correct value of the weight loss
corresponding to the termination of the reaction, a value is obtained
which is decreased by an amount corresponding to the reaction which
took place before the required temperature was attained. This causes
an appreciable amount of error, especially in the case of rapid
reactions and can be eliminated with dynamic thermogravimetric
methods.

However, in order to obtain dependable results with
thermogravimetry it should be remembered that the measured values such
as temperature and the weight change of the sample should be obtained
with the maximum possible accuracy. The factors effecting the
accuracy of obtained kinetic data will be discussed in the following
section.

2.3.1 Accuracy of Thermogravimetric Data.

The accuracy of the kinetic data is influenced by the following factors:

1. The accuracy of maintaining under strict control during the reaction, the linearity of temperature increase, consistency of aerodynamic conditions and composition of the gaseous medium.

2. The accuracy of mathematical evaluation of experimental curves.

Maintenance of the predefined conditions can be disturbed by the two important transfer mechanisms which are heat and mass transfer.

When the heat transfer rate is disturbed, non linear temperature increase occurs (29). Linearity of temperature increase depends on the heat capacity of the furnace, heat inertia of the crucible which depends on its weight, heat capacity and thermal conductivity, and most importantly the amount of sample and the heating rate. The amount of sample influences the enthalpy change during the reaction in the sample and is able to slow down (or speed up) the temperature increase with respect to the original programme (29). Large amounts of sample also cause temperature gradients within the sample and appreciable differences between the temperature of the sample and that of the sample holder. If the heating rate is chosen as small as possible the above stated factors might be removed. The proper heating rate should be chosen not only for this purpose but also considering its influence on the temperature range over which the reaction will be accomplished. There is a chance of missing a fast

reaction or causing an overlapping of the associated weight losses due to two reactions which follow rapidly one after the other.

When the mass transfer phenomena is important the most common disturbing effect is the removal of gaseous reaction product from the reaction interface (29). The factors effecting the diffusion mechanism could be the shape, size and size distribution of the sample and the consistency of the gaseous environment composition. The amount of sample also has an effect on the mass transfer phenomena, because if the sample layer becomes too thick the problem of internal diffusion arises. The appropriate experimental conditions may be found by means of semi-empirical tests in the apparatus intended for kinetic analysis. For example, it is possible to decide whether a stream of inert gas may influence a reverse reaction or whether the use of vacuum is necessary (29).

There has been a lot of work done by several authors on the effects of all these factors on the accuracy of the thermogravimetric data (29).

The accuracy of the mathematical evaluation of experimental curves will be discussed in section 2.4.1.

2.3.2 The Thermogravimetric (TG) Curve.

As noted earlier the weight losses or gains due to each decomposition step or reaction is detected as a function of temperature in thermogravimetric experiments. The record of percent weight losses versus temperature is called a TG curve. A typical TG curve is shown in Figure 7.
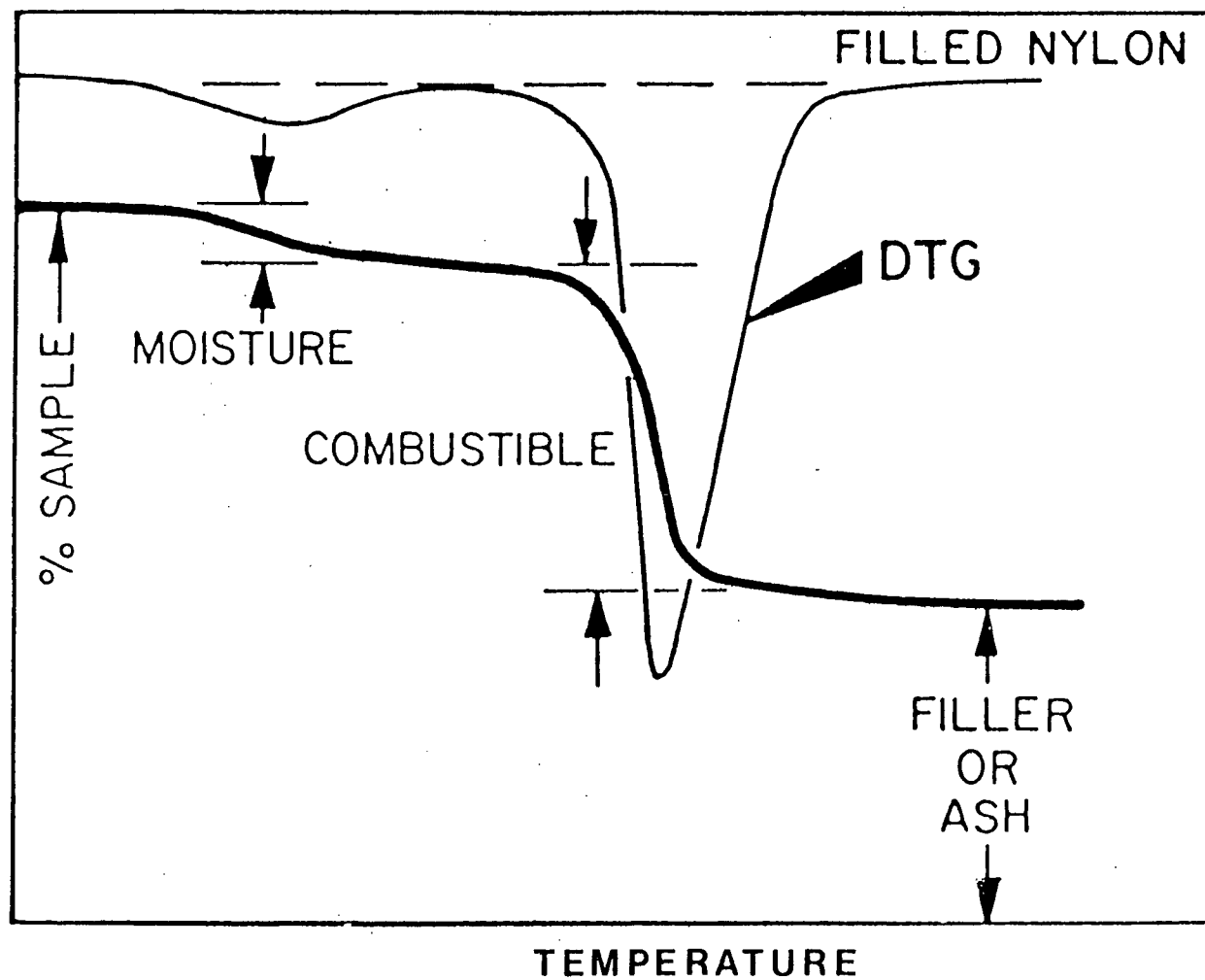
Figure 7: A typical TG curve.

In this figure the dark thick line shows the change in the weight with temperature. The curve above this is the derivative curve which gives additional information such as a change in the mechanism, namely a change of a slope represented by different peaks in the derivative curve.

2.3.3 Mathematical Evaluation of Experimental Parameters.

Mathematical methods used for the evaluation of TG data are more complicated than the isothermal methods because of the continuous increase of the temperature. One method is based on the assumption that the thermal decomposition of a solid may be expressed by

$$\frac{d\alpha}{dt} = kf(\alpha) \tag{2.17}$$

where $f(\alpha)$ depends on the reaction mechanism and k is the rate constant. The temperature dependence can be expressed by the Arrhenius equation

$$k = Z \exp (-E_a/RT) \tag{2.18}$$

where E_a is the activation energy and Z is the frequency factor.

Under the conditions of TG analysis the temperature of the system increases linearly:

$$dT = q \ dt \tag{2.19}$$

where q is the constant rate of heating. The following equation is obtained by combining equations (2.17), (2.18), (2.19)

$$\frac{d\alpha}{f(\alpha)} = \frac{Z}{q} \exp (- E_a/RT)dT \qquad (2.20)$$

Integration of this equation results in the model of the TG curve (27). The integral of the left hand side can be evaluated when the analytical form of the function $f(\alpha)$ is known and leads to a new function $g(\alpha)$.

$$g(\alpha) = \int_o^\alpha \frac{d\alpha}{f(\alpha)} \qquad (2.21)$$

The right hand side can be integrated if E_a is known (27). Doyle (5) showed that the following form is obtained by the integration of equation (2.20):

$$g(\alpha) = \frac{ZE_a}{Rq} p(x) \qquad (2.22)$$

The function $p(x)$ is defined by

$$p(x) = \frac{e^{-x}}{x} - \int_x^\infty \frac{e^{-u}}{u} du \qquad (2.23)$$

where $u = E_a/RT$ and $x = E_a/RT_\alpha$. This function was tabulated by Doyle (5), Akahira (2) and Zsako (31).

The main difficulty in applying eq. (2.22) is the dependence of $P(x)$ on both temperature and activation energy. Doyle (5) has suggested a trial and error curve fitting method for the determination of activation energy. He discussed reactions for which the function $f(\alpha)$ was known, and thus $g(\alpha)$ values could be computed from thermogravimetric data. Under such conditions he obtained the

approximate value of E_a from the slope of the thermogram and calculated the theoretical curve by means of eq. (2.22). By modifying the presumed E_a value, agreement between the theoretical and experimental curves can be achieved. The activation energy value which ensures the best fit will be the required one.

Zsako (31) has simplified Doyle's trial and error method. Taking the logarithm of each side of equation (2.22) gets

$$\log g(\alpha) - \log p(x) = \log \frac{ZE}{Rq} = \bar{B} \tag{2.24}$$

where $\bar{B}$ depends only upon the nature of the compound studied, upon the heating rate, but not upon the temperature. The value of $g(\alpha)$ for a given temperature can be calculated from the experimental data if $f(\alpha)$ is known. Similarly $p(x)$ for the same temperature can be found if the activation energy is known. Constancy of $\log g(\alpha) - \log p(x)$ enables the determination of the activation energy, consistent with a given function $f(\alpha)$. This procedure is explained in more detail in section 5.1. The agreement between experimental data and assumed activation energy E_a can be characterized quantitatively by the standard deviation of individual B_i values for each estimated E_{a_i} from their arithmetical mean $\bar{B}$. This will be defined as

$$\delta = \frac{(B_i - \bar{B})^2}{r} \tag{2.25}$$

where r is the number of experimental data points used for the calculation of $\bar{B}$. The minimum of δ indicates the best E_a value. At the same time, this δ_{min} is a measure of the consistency of the

decomposition process with the function $f(\alpha)$. By presuming other kinetic equations and by calculating the corresponding δ_{min} values, the minimum of δ_{min} values will indicate the function $f(\alpha)$, among those tested which ensures the maximum consistency with experimental data. If the minimum value, δ_{min}, is small enough, the validity of a kinetic equation with the corresponding $f(\alpha)$ and the determined E_a value as the apparent activation energy is concluded.

The best $\bar{B}$ value can be used for the calculation of the frequency factor, Z, by the following equation

$$\log Z = \bar{B} + \log Rq - \log E_a \qquad (2.26)$$

By knowing the best E_a value and Z the rate constant of the reaction, k, can be calculated as a function of temperature.

Satava and Skvara (27) brought a further simplification to the method of Zsako by suggesting a graphical comparison of $\log g(\alpha)$ and $\log p(x)$. The $\log g(\alpha)$ values for various rate processes are plotted vs. the corresponding T_α values on a transparent paper. The plot of $-\log p(x)$ vs. T_α values is also prepared. The plot of $\log g(\alpha)$ is placed on top of the $\log p(x)$ diagram so that the temperature scales coincide and it is then shifted along the ordinate until one of the $\log g(\alpha)$ curves fits one of the $\log p(x)$ curves. From this $\log p(x)$ curve the activation energy can be read. The best fitting $\log g(\alpha)$ curve determines the most probable kinetic equation. For this method to be accurate the experimental TG data must fit for the whole range of α.

2.3.4 Comparison of the Accuracy of Mathematical Methods for the Evaluation of the TG Curve.

Each mathematical method is subject to some inexactness that influences the accuracy of the results to a greater or lesser extent.

Doyle's method seems to be very simple because kinetic data may be obtained from a single point on the decomposition curve. The necessity to know the value of the reaction order beforehand appears to be a disadvantage. When the right value of reaction order is assumed the error from the application of this method is around 4% (29).

Zsako's method is almost free from errors if the real value of the integral p(x) is used. Since the standard deviation is a quantitative measure of the consistency between experimental data and the presumed kinetic equation, the minimization of the standard deviation ensures the accuracy of the estimations.

Although the Satava's method seems simple there is always a question mark as to whether there is only one function p(x) which fits eq. (2.22) when g(α) is given. If the mechanism of the reaction is known, the accuracy of the estimated activation energy is $\mp 5\%$ (27).

2.3.5 Theoretical Considerations for the Evaluation of an Equation for Function f(α).

The mathematical expressions derived in section 2.3.3 were based on the assumption that the reaction can be expressed by the equation

$$\frac{d\alpha}{dt} = k(1-\alpha)^m \qquad (2.27)$$

But in solid state reactions, the concepts of concentration and order of reaction generally have no significance. A rate constant cannot be defined in the same way as for reactions in gases or solutions. It was reported that a simple rate expression like that from which all the derivations quoted are ultimately derived, will not be applicable to all solid state decomposition reactions (1).

Coats and Redfern (1) have pointed out that for certain exponents (m=0, 0.5, 0.67, 1.0), equation (2.27) corresponds to certain kinetic equations, as follows:

when $\qquad$ m = 0 $\qquad$ $\alpha = kt$ $\qquad\qquad\qquad\qquad$ (2.28)

when $\qquad$ m = 0.5 $\qquad$ $R_2(\alpha) = 1 - (1-\alpha)^{1/2} = kt$ $\qquad\qquad$ (2.29)

when $\qquad$ m = 0.67 $\qquad$ $R_3(\alpha) = 1 - (1-\alpha)^{1/3} = kt$ $\qquad\qquad$ (2.30)

when $\qquad$ m = 1.0 $\qquad$ $F_1(\alpha) = - \ln (1 - \alpha) = kt$ $\qquad\qquad$ (2.31)

Equation (2.28) holds for reactions involving a high degree of surface adsorption. Equations (2.29) and (2.30) describe reactions proceeding by the movement of an interface in two and three dimensions respectively. Equation (2.31) is the integrated form of the equation for a reaction controlled by random nucleation. Random nucleation has been studied by Avrami (1) and Erofe'ev (1) and the following equations have been given

$$A_2(\alpha) = \sqrt{-\ln (1-\alpha)} = kt \qquad\qquad (2.32)$$

$$A_3(\alpha) = \sqrt[3]{-\ln (1-\alpha)} = kt \qquad\qquad (2.33)$$

On the other hand many solid state reactions are controlled by diffusional processes and these reactions cannot be expressed in the form of equation (2.27). For example, the simplest equation for a diffusion-controlled reaction takes the form $\alpha^2 = kt$ which gives

$$- \frac{dc}{dt} = (k/2) \ (1+c+c^2+ \ ...)$$ (2.34)

For a diffusion-controlled reaction in a spherical particle the equation is

$$1 - 2\alpha/3 - (1-\alpha)^{2/3} = kt$$ (2.35)

which gives

$$- \frac{dc}{dt} = (3k/2) \ c^{1/3} \ (1+c^{1/3}+c^{2/3}+ \ ...)$$ (2.36)

For diffusion controlled reactions the general equation can be written

$$\frac{d\alpha}{dt} = k \ f(\alpha)$$ (2.37)

where k is given by the Arrhenius equation and $f(\alpha)$ depends on the form of the diffusion mechanism. If the rise of temperature is linear, $T = t_0 + qt$, then

$$\frac{d\alpha}{dT} = (k/q) \ f(\alpha)$$ (2.38)

and

$$(1/f(\alpha))(d\alpha/dT) = (Z/q) \ \exp \ (-E_a/RT)$$ (2.39)

The form of $f(\alpha)$ depends on the nature of the reaction.

For one-dimensional diffusion-controlled reactions in platelike particles

$$D_1(\alpha) = \alpha^2 \qquad\qquad (2.40)$$

and

$$f_1(\alpha) = 1/2\alpha \qquad\qquad (2.41)$$

For two-dimensional diffusion-controlled reaction in a circular disc

$$D_2(\alpha) = (1-\alpha) \ln (1-\alpha) + \alpha \qquad\qquad (2.42)$$

hence

$$f_2(\alpha) = 1/[-\ln (1-\alpha)] \qquad\qquad (2.43)$$

The equation for a diffusion controlled reaction in a sphere

$$D_3(\alpha) = [1 - (1-\alpha)^{1/3}]^2 \qquad\qquad (2.44)$$

which gives

$$f_3(\alpha) = (3/2)[(1-\alpha)^{-1/3}-1] \qquad\qquad (2.45)$$

The relevant form of $f(\alpha)$ should be determined from an initial measurement of α versus t for controlled conditions of T, P and other variables (particle size, etc.). Then equation (2.39) can be used to determine values of Z and E_a from TG data.

2.3.6 Influence of Variation of Kinetic Constants on Shape and Position of Theoretical Thermogravimetric Curves.

In contrast to isothermal decomposition curves, the shape of which depends only on the reaction mechanism, the shape of the TG curve is influenced by the variations in the values of E_a and Z as well as the reaction order. Figure 8 shows how different rate controlling processes affect the shape of the theoretical TG curves.

Changes in the frequency factor Z and the activation energy E_a induce either a change in the multiplying constant or a change in the $[\int]$ term of the right hand side of the eq. 2.21. A decrease in frequency factor shifts the decomposition of substances to the high temperature region as shown in Figure 9.

If the value of the activation energy is increased by 10% and the original value of Z is maintained, the change in the value of the multiplying constant is small but with respect to the change of integral limits, the value of $(\int)$ decreases considerably. This may be compensated for by an increase in the value of the temperature. The compensation will reshift the curves to the region of high temperatures characterising the increase in decomposition temperature due to a higher activation energy (29). This effect is also shown in Figure 9.

False determination of directly measured quantities due to errors caused by the experimental arrangement has also an effect on the shape and position of the curves. A theoretical analysis of errors proves that faulty measurements of temperature must distort the value of activation energy while non-linearity of heating rate distorts the value of the reaction order (29).
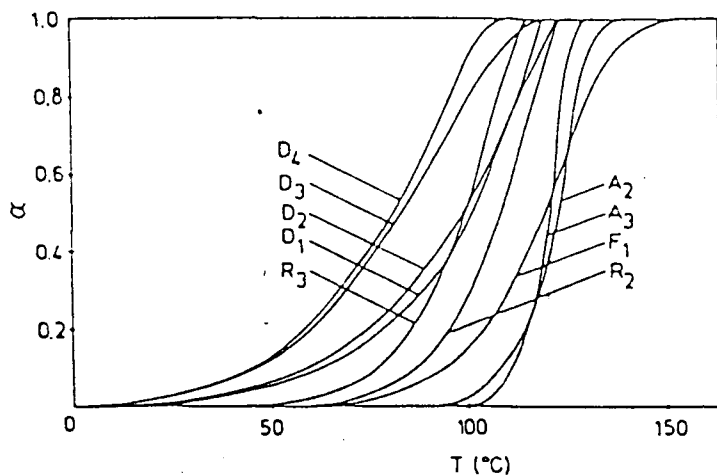
Figure 8: Theoretical TG curves calculated for r characterised by
E = 20 kcal/mol, Z = 10^6, q = 1°C/n by different rate-
controlling processes. (27)
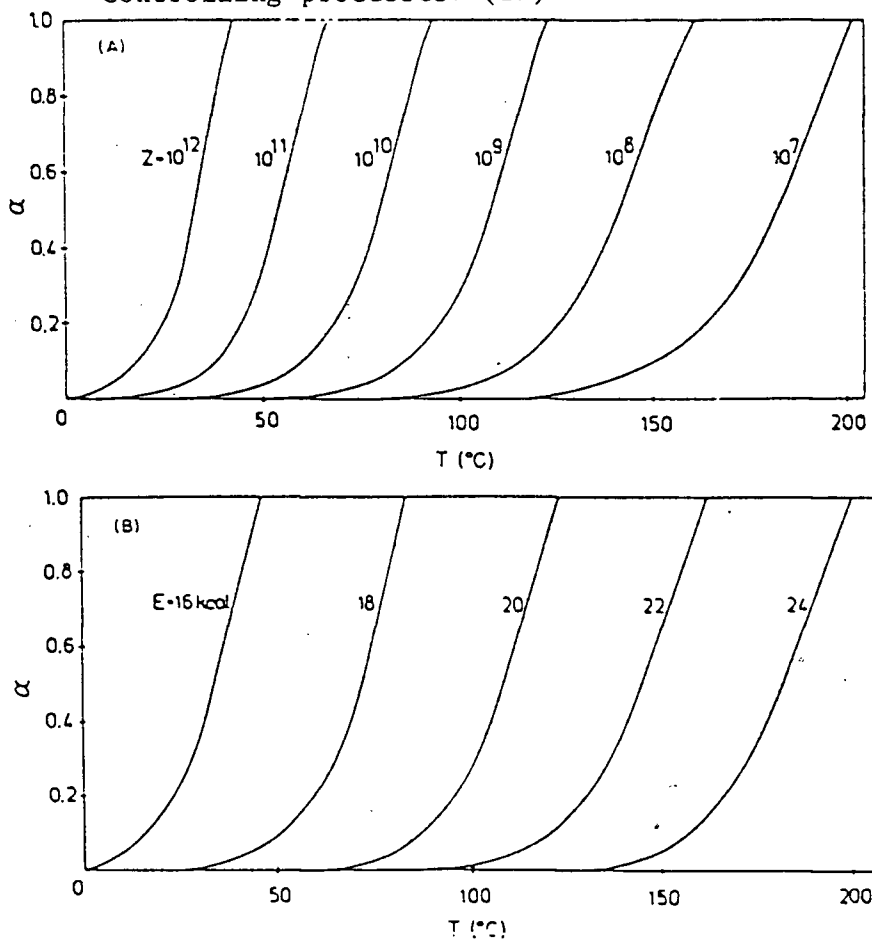
Figure 9: Theoretical TG curves (fraction reacted, α, vs T)
calculated for reaction fitting function R_2
with q = 1°/min. (A) E = 20 kcal/mol at various
values of Z and (B) Z = 10^9 s^{-1} $mol^{1/2}$
at various values of E. (27)

3. MODELLING

In this section mathematical expressions which will give fractional conversions and the rate of the reaction as a function of temperature will be developed for the reaction between sodium carbonate and colemanite. In a thermogravimetric analysis, the residual weight fraction versus temperature for a sample heated at a fixed rate is recorded. Since the temperature is not constant throughout the experiment a new procedure must be developed to interpret the kinetic data from the thermogram.

3.1 Development of a Rate Expression

In this study colemanite is used as an autocausticizing agent, and takes part directly in the reaction. So the following expression can be written to symbolize the reaction

$$aA(s) + bB(s) \rightarrow cC(s) + dD(g) \tag{3.1}$$

In general the rate expression for such a solid phase reaction can be written as follows

$$-\frac{dW_A}{dt} = k_1 W_A{}^m W_B{}^n \tag{3.2}$$

where m and n are the orders of the reaction with respect to compounds A and B respectively. W_A and W_B are the weights of the reacting compounds and k is the rate constant.

In terms of the fractional conversions W_A and W_B can be expressed as

$$W_A = W_{A_o} (1-\alpha_A) \qquad (3.3)$$

$$W_B = W_{B_o} (1-\alpha_B) \qquad (3.4)$$

where α_A and α_B are the weight fractions of the initial compounds reacted. Weight fractions were used instead of mole fractions because the molecular weight of the active part of colemanite was not known exactly. The reacted fraction of compound B can be expressed in terms of the reacted fraction of compound A as follows

$$\alpha_B = \frac{W_{A_o} \alpha_A}{MW_A} \cdot \frac{b}{a} \cdot \frac{MW_B}{W_{B_o}} \qquad (3.5)$$

where MW_A and MW_B are molecular weights of compounds A and B respectively. By substituting eq. (3.5) into (3.4)

$$W_B = W_{B_o} (1 - \frac{b}{a} \frac{MW_B}{MW_A} \frac{W_{A_o}}{W_{B_o}} \alpha_A) \qquad (3.6)$$

Substitution of eq. (3.3) and (3.6) into eq. (3.2) gives

$$- \frac{d[W_{A_o} (1-\alpha_A)]}{dt} = k_1 W_{A_o}^{\,m} W_{B_o}^{\,n} (1-\alpha_A)^m (1 - \frac{b}{a} \frac{MW_B}{MW_A} \frac{W_{A_o}}{W_{B_o}} \alpha_A)^n \qquad (3.7)$$

this equation can be rewritten as

$$\frac{d\alpha_A}{(1-\alpha_A)^m(1 - \frac{b}{a} \frac{MW_B}{MW_A} \frac{W_{A_o}}{W_{B_o}} \alpha_A)^n} = k_1 W_{A_o}^{m-1} W_{B_o}^{n} dt \qquad (3.8)$$

Introducing

$$f(\alpha_A) = (1-\alpha_A)^m(1 - \frac{b}{a} \frac{MW_B}{MW_A} \frac{W_{A_o}}{W_{B_o}} \alpha_A)^n \qquad (3.8A)$$

the final form of the equation (3.8) becomes

$$\frac{d\alpha_A}{f(\alpha_A)} = k_1 W_{A_o}^{m-1} W_{B_o}^{n} dt \qquad (3.9)$$

where function $f(\alpha)$ depends on the reaction mechanism.

In eq. (3.9) k_1, which is the rate constant, cannot remain constant under the conditions of thermogravimetric analysis and will depend upon temperature. The temperature dependence of k_1 can be expressed by the Arrhenius equation

$$k_1 = Z_1 \exp (-E_1/RT) \qquad (3.10)$$

where E_1 is the activation energy and Z_1 is the frequency factor.

Under the conditions of thermogravimetric analysis, the temperature of the system increases linearly, in other words thermogravimetric analysis is carried out with a constant heating rate q, where

$$q = dT/dt \tag{3.11}$$

Substituting dt = dT/q and combining eq. (3.10) and eq. (3.11) with eq. (3.9) gives

$$\frac{d\alpha}{f(\alpha_A)} = \frac{Z_1}{q} W_{A_o}{}^{m-1} W_{B_o}{}^{n} \exp\left(-\frac{E_1}{RT}\right) dt \tag{3.12}$$

Integration of equation (3.12) results in the equation of the thermogravimetric curves. To perform this integration the method which was developed by Doyle (5) and described in the literature part of this thesis was used. The following equation is obtained by the integration of equation (3.12)

$$g(\alpha_A) = \frac{Z_1 E_1}{Rq} (W_{A_o}{}^{m-1} W_{B_o}{}^{n}) p(x), \tag{3.13}$$

where p(x) is defined by equation (2.23). This equation can further be simplified by introducing the notation

$$k* = \frac{Z_1 E_1}{Rq} W_{A_o}{}^{m-1} W_{B_o}{}^{n} \tag{3.14}$$

and the equation of the thermogravimetric curves can be written as

$$g(\alpha) = k*p(x) \tag{3.15}$$

3.2 Expressions for Fractional Conversions and Function f(α) for the Reaction of Sodium Carbonate and Colemanite.

Reaction between sodium carbonate and colemanite is very complex. There are many factors affecting it and the unknown structure of colemanite which comes naturally from the rocks mixed with impurities makes the problem more complicated.

In order to be able to apply the rate expression derived in the previous section the stoichiometric constants of the reaction should be known. The formula of pure colemanite is given as $2CaO \cdot 3B_2O_3 \cdot 5H_2O$ and contains 50.8 percent B_2O_3. The phase diagram for the $Na_2O-B_2O_3$ system shown in Fig. 10 indicates that for a sodium to boron molar ratio greater than 0.995 which is satisfied for all the colemanite percentages analyzed in this study (Appendix II), the reaction product would be $Na_2OB_2O_3$ regardless of temperature (7). Hence the proposed form of reaction equation is

$$3Na_2O_3 + [2CaO \cdot 3B_2O_3 \cdot 5H_2O] \rightarrow 3Na_2OB_2O_3 + 3CO_2 \uparrow$$
$$+ 2CaO + 5H_2O \qquad (3.16)$$
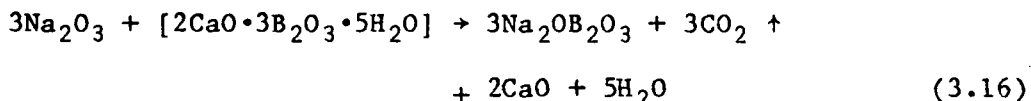
giving the stoichiometric constants a and b in eq. 3.1 as a = 3 and b = 1.

3.2.1 Expression of the Fractional Conversion of Sodium Carbonate.

The following assumptions can be made to simplify the mechanism of this reaction.

1. There is no loss of sodium or sodium oxide at elevated temperatures. Hence all the weight loss comes from the expulsion of carbon dioxide which is a reaction product.
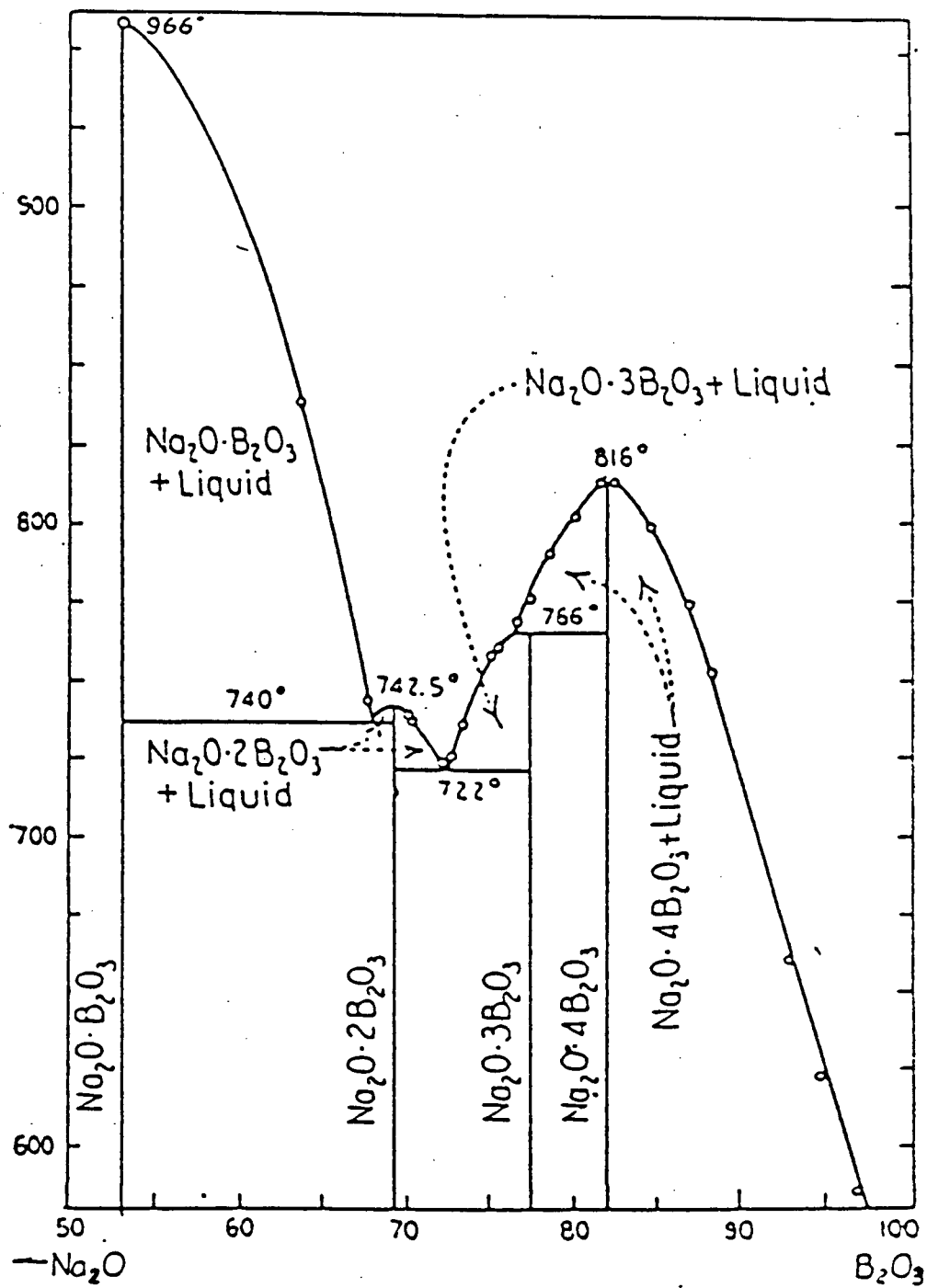
Figure 10: Phase diagram for the system
$B_2O_3-Na_2O \cdot B_2O_3$. (7)

2. There is only one reaction that takes place within the analyzed temperature range (190-700°C).

Since the only source of weight loss is the evolution of carbon dioxide which is formed by the decomposition of sodium carbonate the following expression can be written

$$W_{s_o} \alpha_s = \frac{W_{s_o} - W}{MW_{CO_2}} \ MW_s \tag{3.17}$$

and subsequently

$$\alpha_s = \frac{W_{s_o} - W}{W_{s_o}} \cdot \frac{MW_s}{MW_{CO_2}} \tag{3.18}$$

where W is the weight at any time during the reaction and can be read from TG curve for the corresponding temperature.

3.2.2 Expression for the Fractional Conversion of Colemanite.

Substitution of a and b values in eq. (3.5) gives the following expression for α_B which will be denoted as α_c specifically for colemanite

$$\alpha_c = \frac{1}{3} \frac{MW_c}{MW_s} \frac{W_{s_o}}{W_{c_o}} \alpha_s \tag{3.19}$$

However, the colemanite used in this study was not pure and an independent study which was performed by using the same colemanite stock showed that it contained 25.24 percent impurity (26). Colemanite is also very hydroscopic and TG analysis showed that it contained 9 percent humidity (see Fig. 30). When the necessary corrections have been made equation (3.19) becomes

$$\alpha_c = \frac{1}{3} \frac{MW_c}{MW_s} \frac{W_{s_o}}{W_{c_o}} \frac{(100 - H_c)}{(100 - I_c)} \alpha_s \qquad (3.20)$$

where H_c = percent humidity in colemanite

I_c = percent impurity in colemanite

The ratio of $\frac{W_{s_o}}{W_{c_o}}$ will be different for each colemanite-Na_2CO_3 mixture analyzed. Therefore, this ratio must be represented by a general expression which will apply to all colemanite percentages. The initial weight of colemanite in a sample can be written as follows

$$W_{c_o} = W_{s_o} \left(\frac{Y_c}{100 - Y_c}\right) \left(\frac{100 - H_c}{100}\right) \qquad (3.21)$$

where Y_c is the colemanite percentage in the samples. Equation (3.21) can also be written in terms of the weight fraction of colemanite and the following equation is obtained after making the necessary simplifications

$$\frac{W_{c_o}}{W_{s_o}} = \frac{X_c(100 - H_c)}{(1 - X_c)} \qquad (3.22)$$

If equation (3.22) is substituted in equation (3.20) the final

expression for the fractional conversion of colemanite is

obtained.

$$\alpha_c = \frac{1}{3} \frac{MW_c}{MW_s} \frac{(1 - X_c)}{X_c (100 - H_c)} \alpha_s \qquad (3.23)$$

3.2.3 Analytical Forms of Function $f(\alpha)$ and Function $g(\alpha)$ For the Reaction of Sodium Carbonate and Colemanite.

As can be seen from eq. (3.23), all the terms are constant in

that expression except α_s. Introducing constant N

$$N = \frac{1}{3} \frac{MW_c}{MW_s} \frac{(1 - X_c)}{X_c (100 - H_c)} \qquad (3.24)$$

eq. (3.20) can be written in the following form:

$$\alpha_c = N\alpha_s \qquad (3.25.)$$

Then eq. (3.8A) becomes

$$f(\alpha) = (1-\alpha_s)^m (1-N\alpha_s)^n \qquad (3.26)$$

and the corresponding forms of the function $g(\alpha)$ can be evaluated by

integrating this function between the limits of 0 to α.

In Table 8 analytical forms of the function $f(\alpha)$ and function

$g(\alpha)$ for the most probable mechanisms for the thermal decomposition of

solid substances are tabulated. This table also shows the expressions

for k* which will be used in the calculation of the frequency factor,

Z, and the rate constant, k, corresponding to these proposed

mechanisms.

Table 8: Analytical forms of function $f(\alpha)$ and $g(\alpha)$ for the most probable mechanisms.

mechanism	$f(\alpha) = (1-\alpha_s)^m(1-N\alpha_s)^n$	$g(\alpha) = \int_0^\alpha \frac{d\alpha}{f(\alpha)}$	$k^* = \frac{z_1E_1}{Rq} W_{s_o}^{m-1} W_{c_o}^{n}$
$m = 0$ $n = 1/3$	$f(\alpha) = (1-N\alpha_s)^{1/3}$	$g(\alpha) = \frac{3}{2}\left[\frac{1 - 3(1-\alpha_s)^{2/3}}{N}\right]$	$\frac{z_1E_1}{Rq} \frac{(W_{c_o})^{1/3}}{W_{s_o}}$
$m = 0$ $n = 1/2$	$f(\alpha) = (1-N\alpha_s)^{1/2}$	$g(\alpha) = 2\left[\frac{1 - \sqrt{1-\alpha_s}}{N}\right]$	$\frac{z_1E_1}{Rq} \frac{(W_{c_o})^{1/2}}{W_{s_o}}$
$m = 0$ $n = 2/3$	$f(\alpha) = (1-N\alpha_s)^{2/3}$	$g(\alpha) = 3\left[\frac{1 - \sqrt{(1-\alpha_s)^{1/3}}}{N}\right]$	$\frac{z_1E_1}{Rq} \frac{(W_{c_o})^{1/3}}{W_s}$
$m = 1/3$ $n = 0$	$f(\alpha) = (1-\alpha_s)^{1/3}$	$g(\alpha) = \frac{3}{2}\left[1 - 3(1-\alpha_s)^{2/3}\right]$	$\frac{z_1E_1}{Rq} W_{s_o}^{-2/3}$
$m = 1/2$ $n = 0$	$f(\alpha) = (1-\alpha_s)^{1/2}$	$g(\alpha) = 2[1 - \sqrt{1-\alpha_s}]$	$\frac{z_1E_1}{Rq} W_{s_o}^{-1/2}$
$m = 0$ $n = 0$	$f(\alpha) = 1$	$g(\alpha) = \alpha_s$	$\frac{z_1E_1}{Rq} W_{s_o}^{-1}$

3.3 Expressions for the Decomposition of Sodium Carbonate.

3.3.1 Development of a Rate Expression.

Besides the colemanite reaction, sodium carbonate may decompose directly at high temperatures. The following reaction can represent the decarbonization reaction of sodium carbonate

$$Na_2CO_3 \rightarrow NaO + CO_2 \qquad (3.27)$$

or

$$A(s) \rightarrow B(s) + C(g) \qquad (3.27A)$$

The rate of reaction for such a reaction can be written as

$$-\frac{dW_A}{dt} = k_2 W_A^{\nu} \qquad (3.28)$$

where ν is the order of the reaction and k_2 is the rate constant.

In terms of the fractional conversion W_A can be written as follows

$$W_A = W_{A_o}(1 - \alpha_A) \qquad (3.29)$$

Substituting equation (3.29) into equation (3.28) gives

$$-\frac{d[W_{A_o}(1-\alpha_A)]}{dt} = k_2 W_{A_o}^{\nu}(1-\alpha_A)^{\nu} \qquad (3.30)$$

After making the necessary simplifications the following equation is obtained.

$$\frac{d\alpha_A}{(1-\alpha_A)^\nu} = k_2 W_{A_o}^{\nu-1} dt \qquad (3.31)$$

Introducing

$$f(\alpha_A) = (1-\alpha_A)^\nu \qquad (3.32)$$

and

$$k_2 = Z_2 \exp(-E_2/RT) \qquad (3.33)$$

equation (3.31) becomes

$$\frac{d\alpha_A}{f(\alpha_A)} = Z_2 \exp(-E_2/RT) W_{A_o}^{\nu-1} dt \qquad (3.34)$$

Since the thermogravimetric analysis is carried out with a constant

heating rate, q

$$dt = \frac{dT}{q} \qquad (3.35)$$

Substitution of equation (3.35) into the equation (3.34) gives the

final form of the rate equation as such

$$\frac{d\alpha_A}{f(\alpha_A)} = \frac{Z_2}{q} W_{A_o}^{\nu-1} \exp(-E_2/RT) dT \qquad (3.36)$$

Integration of equation (3.36) results in the equation of the

thermogravimetric curves which is given in equation (3.37) by applying

the same procedure described in section 3.1

$$g(\alpha) = \frac{Z_2 E_2}{Rq} W_{A_o}^{\nu-1} p(x) \qquad (3.37)$$

3.4 Analytical Forms of Functions f(α) and g(α).

The analytical forms of function $f(\alpha)$ and function $g(\alpha)$ are summarized in Table 9 including the mechanisms for diffusion control and random nucleation for which the equations were given in section 2.3.5.

Table 9: Analytical forms of function $f(\alpha)$ and $g(\alpha)$ for the probable mechanisms for the decomposition of Na_2CO_3.

mechanism	$f(\alpha) = (1-\alpha_A)^{\nu}$	$g(\alpha) = \int_o^{\alpha} \dfrac{d\alpha_A}{f(\alpha_A)}$
$m = 0$	1	α_A
$m = 1/2$	$(1-\alpha_A)^{1/3}$	$3/2\,[1 - (1-\alpha_A)^{2/3}]$
$m = 2/3$	$(1 - \alpha_A)^{1/2}$	$2[1 - \sqrt{1-\alpha_A}]$
$m = 1/3$	$(1-\alpha_A)^{2/3}$	$3[1 - (1-\alpha_A)^{1/3}]$
$m = 1$	$(1-\alpha_A)$	$-\ln(1-\alpha_A)$
$m = 2$	$(1-\alpha_A)^2$	$\dfrac{\alpha_A}{1-\alpha_A}$
One dimensional diffusion	D_1	$\alpha_A{}^2$
Two dimensional diffusion	D_2	$(1-\alpha_A)\ln(1-\alpha_A) + \alpha_A$
Three dimensional diffusion	D_3	$[1 - (1-\alpha_A)^{1/3}]^2$
Aurami eq.	A_2	$[\,\ln(1-\alpha_A)]^{1/2}$
Aurami eq.	A_3	$[\,\ln(1-\alpha_A)]^{1/3}$

4. EXPERIMENTAL STUDIES

The experimental work in this study consists of two major parts:

1. Experiments performed to determine the most suitable agent for the decarbonization of sodium carbonate by evaluating the efficiencies of a number of proposed autocausticizing agents. These experiments were performed under isothermal conditions.

2. Experiments performed to evaluate the kinetic constants of the reaction of sodium carbonate with the agent chosen from the results of experiments performed in part one. Reaction mixtures were analyzed in a thermogravimetric analyzer under the constant heating rate condition.

4.1 Isothermal Experiments

These experiments were based on the measurement of the reacted fraction of the sodium carbonate as a function of time at constant temperature and pressure.

The experimental set-up used in these experiments is shown in Figure 11. The desired temperature for the reaction was maintained in an electric furnace (Thermolyne, model F-A1730) which can operate as high as 2000°F (1093°C). The constancy of the temperature in the reaction chamber was maintained by a digital temperature controller (Sybron/Thermolyne, model LT310X2). The controller held the furnace temperature at the desired level within ∓5%.
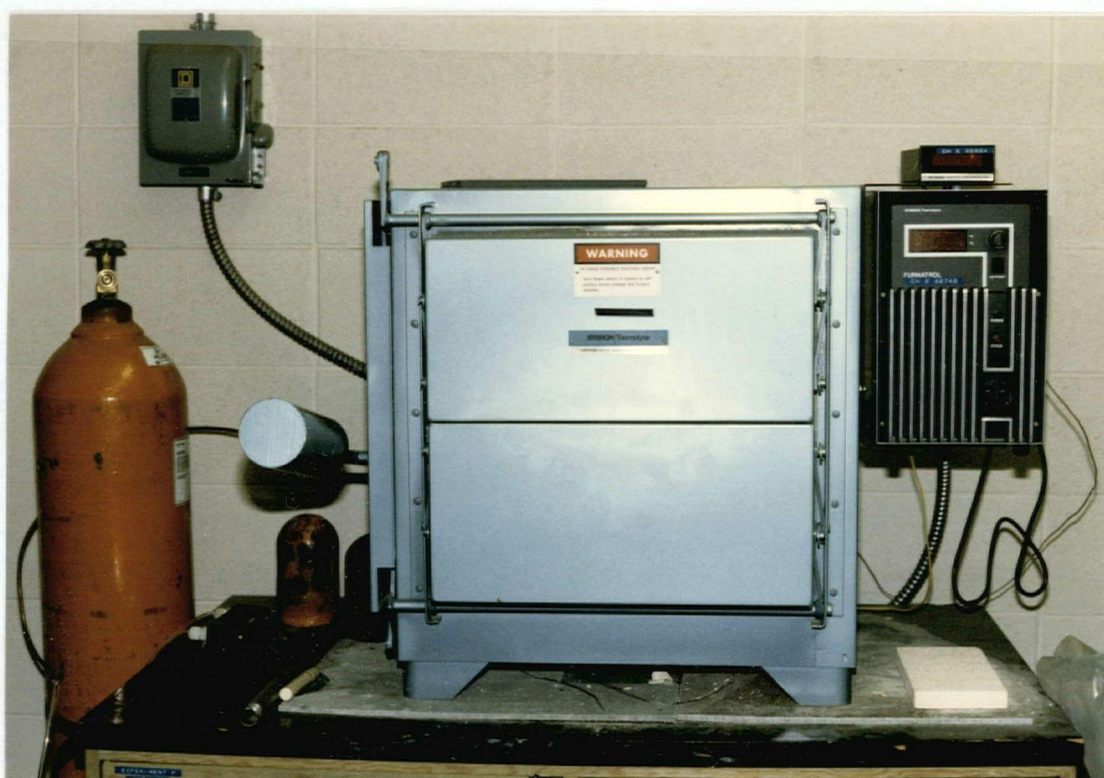
Figure 11: Experimental Set-up for Isothermal Runs

The temperature of the furnace was measured with a Chromel/Alumel thermocouple which was installed in a protective tube at the back of the furnace.

Samples were introduced in 10 ml zirconium crucibles. Zirconium was used because of the extremely corrosive nature of high temperature molten caustic. The crucibles stood up well. After 10 runs of about one hour each only two crucibles out of ten had corroded, although most of them had deformed slightly. For efficient heating the crucibles were placed away from the sides of the furnace and from the tube in which the thermocouple was inserted. They were also placed about 1.5 cm apart to allow the circulation of gas around them.

Helium was supplied at a rate enough to maintain an inert atmosphere in the furnace. The aim of this was to prevent the crucibles from corroding and to sweep the carbon dioxide from the chamber.

4.1.1 System Variables.

The chosen variables in this project were temperature, time and composition of the reaction mixture. For a wide range of independent variables, decomposition of sodium carbonate was tested for the causticizing agents titanium dioxide, alumina and colemanite.

Temperature: Temperatures ranging from 800°C to 1100°C were tested, as was suggested by the literature.

Time: Reaction time was between 5 min. and 80 min. The maximum time was determined by preliminary runs which showed that after 60 minutes the reaction proceded very slowly and was almost complete at

the end of 80 minutes. Reaction times were chosen according to the
nature of the autocausticizing agent and varied slightly.

Composition of the reaction mixture: As was proposed in the
literature, 10 and 20 weight percent of autocausticizing agent in the
mixture were tested for titanium dioxide and alumina. Because of the
high molecular weight of colemanite it was necessary to test higher
concentrations, in the range from 10 to 60 weight percent.

4.1.2 Preparation of Samples.

In these experiments, as in all the tests made a homogeneous
mixture was very important. For this reason special attention was paid
to obtain well mixed samples.

The reagents used in the preparation of samples were anhydrous
sodium carbonate which was 99.5% pure and supplied by WEB, titanium
dioxide (supplied by Coast Ceramics Ltd.), alumina, colemanite
(supplied by Coast Ceramics Ltd., Nevada colemanite). The purity of
the titanium dioxide and the alumina was greater than 99 percent.
Since colemanite comes from an unrefined rock there was no information
available about its purity and composition.

The reagents were weighed on an analytical balance (Mettler
H10T) and placed in the crucibles. Two sets of six samples were
weighed out, one set at ten percent and one set at twenty percent agent
concentration. Total weight of samples was chosen as one gram because
if the thickness of sample layer is too great the diffusion of carbon
dioxide could be impeded resulting in a considerable decrease in the
reaction rate. After weighing, the reagents in each crucible were

mixed thoroughly with a scoopula to obtain a homogeneous mixture. Then they were slurried with distilled water which was just sufficient to wet the mixture. In order to prevent flashing off the samples from the crucibles when they were placed into the hot furnace they were dried in an oven at 110°C for approximately one hour. They were then stored until the furnace test in a desiccator filled with silicagel. In the case of colemanite, in addition to the samples prepared at ten and twenty percent colemanite concentrations, samples containing thirty, fourty, fifty and sixty percent colemanite in sodium carbonate were prepared as well.

The experiments performed under the isothermal conditions are summarized in Table 10 which shows the type of agent and the conditions used with each sample. Each run was repeated in order to minimize the errors. Consistency of the titration results were checked and found to be accurate to ∓ 1%.

4.1.3 Experimental Procedure.

Experimental procedure can be divided into three parts:

    1. Reaction of the sample

    2. Dissolution of the sample

    3. Analysis of products

    1. Reaction of sample: Reaction takes place in the furnace. The furnace was preheated to the desired temperature and kept at this temperature for about one hour to assure a stable operating temperature when the runs were started. Stable temperature was assumed when the temperature controller was cycling frequently. The oven was also

Table 10: Conditions tested in the isothermal experiments.*

Run #	Agent type	Agent concentration	Temperature (°C)	Reaction time (min)
1	TiO_2	10	800	5
2	TiO_2	20	800	5
3	TiO_2	10	800	15
4	TiO_2	20	800	15
5	TiO_2	10	800	25
6	TiO_2	20	800	25
7	TiO_2	10	800	35
8	TiO_2	20	800	35
9	TiO_2	10	800	50
10	TiO_2	20	800	50
11	TiO_2	10	900	5
12	TiO_2	20	900	5
13	TiO_2	10	900	15
14	TiO_2	20	900	15
15	TiO_2	10	900	25
16	TiO_2	20	900	25
17	TiO_2	10	900	35
18	TiO_2	20	900	35
19	TiO_2	10	900	50
20	TiO_2	20	900	50
21	Al_2O_3	10	800	10
22	Al_2O_3	20	800	10
23	Al_2O_3	10	800	20
24	Al_2O_3	20	800	20
25	Al_2O_3	10	800	30
26	Al_2O_3	20	800	30
27	Al_2O_3	10	800	40
28	Al_2O_3	20	800	40
29	Al_2O_3	10	800	50
30	Al_2O_3	20	800	50
31	Al_2O_3	10	900	10
32	Al_2O_3	20	900	10
33	Al_2O_3	10	900	20
34	Al_2O_3	20	900	20
35	Al_2O_3	10	900	30
36	Al_2O_3	20	900	30
37	Al_2O_3	10	900	40
38	Al_2O_3	20	900	40
39	Al_2O_3	10	900	50
40	Al_2O_3	20	900	50

Table 10:   Conditions tested in the isothermal experiments.*
            Continued

Run #	Agent type	Agent concentration	Temperature (°C)	Reaction time (min)
41	Colemanite	40	800	10
42	Colemanite	40	800	20
43	Colemanite	40	800	30
44	Colemanite	40	800	40
45	Colemanite	40	800	50
46	Colemanite	40	800	60
47	Colemanite	10	900	10
48	Colemanite	20	900	10
49	Colemanite	30	900	10
50	Colemanite	40	900	10
51	Colemanite	50	900	10
52	Colemanite	60	900	10
53	Colemanite	10	900	20
54	Colemanite	20	900	20
55	Colemanite	30	900	20
56	Colemanite	40	900	20
57	Colemanite	50	900	20
58	Colemanite	60	900	20
59	Colemanite	10	900	30
60	Colemanite	20	900	30
61	Colemanite	30	900	30
62	Colemanite	40	900	30
63	Colemanite	50	900	30
64	Colemanite	60	900	30
65	Colemanite	10	900	40
66	Colemanite	20	900	40
67	Colemanite	30	900	40
68	Colemanite	40	900	40
69	Colemanite	50	900	40
70	Colemanite	60	900	40
71	Colemanite	10	900	50
72	Colemanite	20	900	50
73	Colemanite	30	900	50
74	Colemanite	40	900	50
75	Colemanite	50	900	50
76	Colemanite	60	900	50

*   All runs in this table were repeated.

flushed with helium for about 15 minutes before the start of each run

and it flowed continuously throughout the run at a slower rate.

At the start of each run, all twelve crucibles were placed into

the oven. At elapse times of 10, 20, 30, 40, 50 and 80 minutes, two

crucibles were removed from the oven. One contained 10 and the other

contained 20 percent autocausticizing agent. Samples were immediately

placed into the desiccator which contained ascarite and silicagel. The

function of the ascarite was to prevent carbon dioxide in the air from

recombining with sodium oxide to form sodium carbonate. Then the

samples were weighed to determine the weight loss due to the reaction.

This was done as quickly as possible to decrease the chance of the

samples reacting with carbon dioxide of the air. Each crucible was

immediately put back into the desiccator after weighing. For the

colemanite runs two autocausticizing agent concentrations would be

reacted at the same time until all the samples had been tested.

2. Dissolution of samples: The next step was the removal of

products from the crucibles. This was done by filling the crucibles

with distilled water, covering them with a watchglass and letting them

boil for about 15 minutes on a hot plate. It was assumed that the

water vapor leaving the crucible would prevent carbon dioxide from

diffusing to the basic solution. The crucibles were then scraped out

with a scoopula. Since the products were fused at high temperatures,

they stuck to the sides of the crucibles in the form of a thin film and

this made their removal from the crucibles very difficult even after

they were boiled. The samples were then dissolved in 100 ml of

distilled water at 90°C with vigorous swirling. This temperature was

reported (20) as the optimum to obtain almost complete dissolution of the product. The erlenmeyers which contained dissolved samples were placed into a desiccator that was filled with ascarite.

3. Analysis of products: The samples were analyzed for sodium carbonate and sodium hydroxide. This was done by two sets of titrations for each sample solution; one for the determination of total alkali and the other for the determination of sodium hydroxide alone. Methyl orange was chosen as an indicator rather than phenolphthalein, which is usual for the determination of total alkali, because at the sodium bicarbonate stage the pH of half-neutralized sodium carbonate is about 8.3, but the pH changes comparatively slowly in the neighbourhood of the equivalence point, consequently the indicator colour-change with phenolphthalein (pH range 8.3-10.0) is not too sharp. Phenolphthalein was used as an indicator for the determination of sodium hydroxide. The procedure can be summarized as follows.

1. A 25 ml aliquot of sample was taken from each erlenmeyer with a pipette. Care was taken not to withdraw solids with the sample because of the possibility that solids could cause errors in the measurement. It was later proven that the solids contributed no alkali to the mixture. Each aliquot was then poured into a separate 125 ml stoppered flask. Two samples were taken from each solution.

2. Five drops of methyl orange were added to each solution of the first sample and these were titrated with 0.998 N sulphuric acid to the end point; colour change of orange to yellow. To obtain satisfactory results with this indicator, the solutions were kept in an ice bath before titration and the loss of carbon dioxide was prevented

as far as possible by keeping the tip of the burette immersed in the liquid. The volume of sulfuric acid used in this titration was recorded and used to calculate the total carbonate.

3. One percent barium chloride solution was added slowly to each flask in the second set from a burette in slight excess, i.e. until no further precipitate was produced. This precipitated the unreacted sodium carbonate. Then five drops of phenolphthalein was added to each sample and they were titrated with 0.998 N sulfuric acid to the end point; pink to clear colour change. The barium carbonate precipitate was not removed since it is stable in acid and made the end point easier to see.

4.1.4 Experimental data.

The experimental data taken in this part of the study are summarized in Tables 11, 12, 13 and 14 for titanium dioxide, alumina and colemanite respectively. Fractional conversions of sodium carbonate were calculated from the titration results. (See Appendix II).

Table 11:   Conversion time data for TiO_2

Temp. (°C)	% TiO_2	Time (min.)	% Conversion
800	10	5	2.0
		15	7.3
		25	9.3
		35	9.6
		50	14.1
800	20	5	2.6
		15	5.7
		25	10.1
		35	13.9
		50	14.9
900	10	5	13.0
		15	18.8
		25	20.8
		35	25.4
		50	32.8
900	20	5	20.3
		15	26.9
		25	32.6
		35	38.5
		50	43.6
1000	10	5	29.6
		15	33.1
		25	27.3
		35	33.4
		50	34.7
1000	20	5	32.9
		15	36.0
		25	39.3
		35	43.5
		50	51.2

Table 12: Conversion time data for alumina

Temp. (°C)	% Alumina	Time (min.)	% Conversion
800	10	10	1.3
		20	1.3
		30	2.5
		40	2.8
		50	4.7
	20	10	1.2
		20	2.2
		30	3.3
		40	4.8
		50	5.0
900	10	10	13.1
		20	34.8
		30	41.4
		40	19.9
		50	31.3
	20	10	16.3
		20	23.8
		30	17.7
		40	25.1
		50	34.2
1000	10	5	20.7
		15	42.6
		25	86.6
		30	—
		35	74.3
	20	5	20.4
		15	26.8
		25	45.3
		30	49.5
		35	54.8
1000	10	5	20.9
		15	27.1
		25	23.8
		30	25.4
		35	28.3
	20	5	32.1
		10	25.6
		20	35.4
		30	51.9
		35	36.1

Table 13: Conversion time data for colemanite

Temp. (°C)	% Colemanite	Time (min.)	% Conversion
900	10	10	18.5
		30	18.8
		50	23.9
		70	28.3
900	20	10	32.1
		20	36.4
		30	36.5
		40	38.3
		50	38.7
900	30	10	39.2
		20	46.3
		30	48.1
		40	50.9
		50	51.4
900	40	10	56.5
		20	63.0
		30	62.1
		40	67.3
		50	68.5
900	50	10	58.4
		20	67.6
		30	70.9
		40	72.6
		50	73.4
900	60	10	69.7
		20	73.0
		30	79.5
		40	71.1
		50	84.1

Table 14: Conversion time data for colemanite
at different temperatures.

Agent: Colemanite (40%)

Temp. (°C)	Time (min.)	% Conversion
800	10	34.4
	20	46.7
	30	48.8
	40	53.9
	50	56.8
900	10	56.5
	20	60.0
	30	62.1
	40	67.3
	50	68.5

4.2 Thermogravimetric Analysis

These experiments were only performed for colemanite which was chosen as the best autocausticizing agent according to the results from the isothermal experiments. The basic measurement in this method is the weight change of the sample as a function of a linearly increasing temperature. This was done in a Perkin-Elmer thermogravimetric analyzer (model TGS-2) along with the thermal analysis data station (TADS).

4.2.1 Apparatus.

The complete TGS-2 system which is shown in Figure 12 consists of the following units: the thermobalance, the electronic balance control, the temperature control and the heater control unit.

The analyzer is the main part of this system. Figure 13 shows the furnace which is made of a thin-walled alumina mandril wound with a platinum filament which acts as a platinium resistance thermometer and resistance heater. The temperature range for this sytem is from 300 to 1273 K and heating rates of 0.3 to 160°K/min. can be employed. The sample is contained in a platinium pan supported by a platinum stirrup which hangs inside the furnace on a wire which is connected to one arm of the microbalance. The sample pans are 5.8 mm ID and 1.8 mm deep and hang about 2 mm above the thermocouple inside the furnace. The furnace is surrounded by a pyrex tube and purged with an inert gas which is preferably nitrogen. The normal flow rate for the purge gas is 45 cc/min.
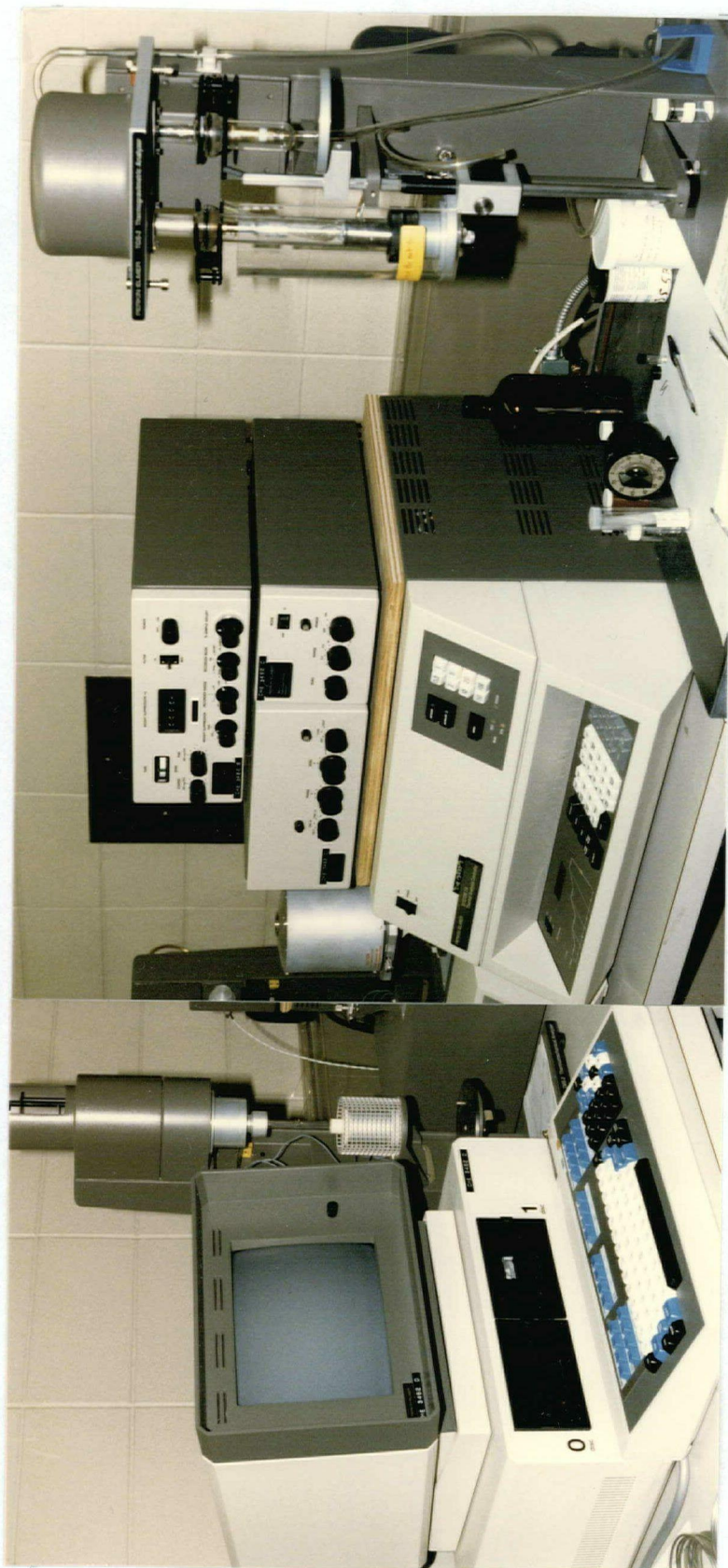
Figure 12: The TGS-2 System
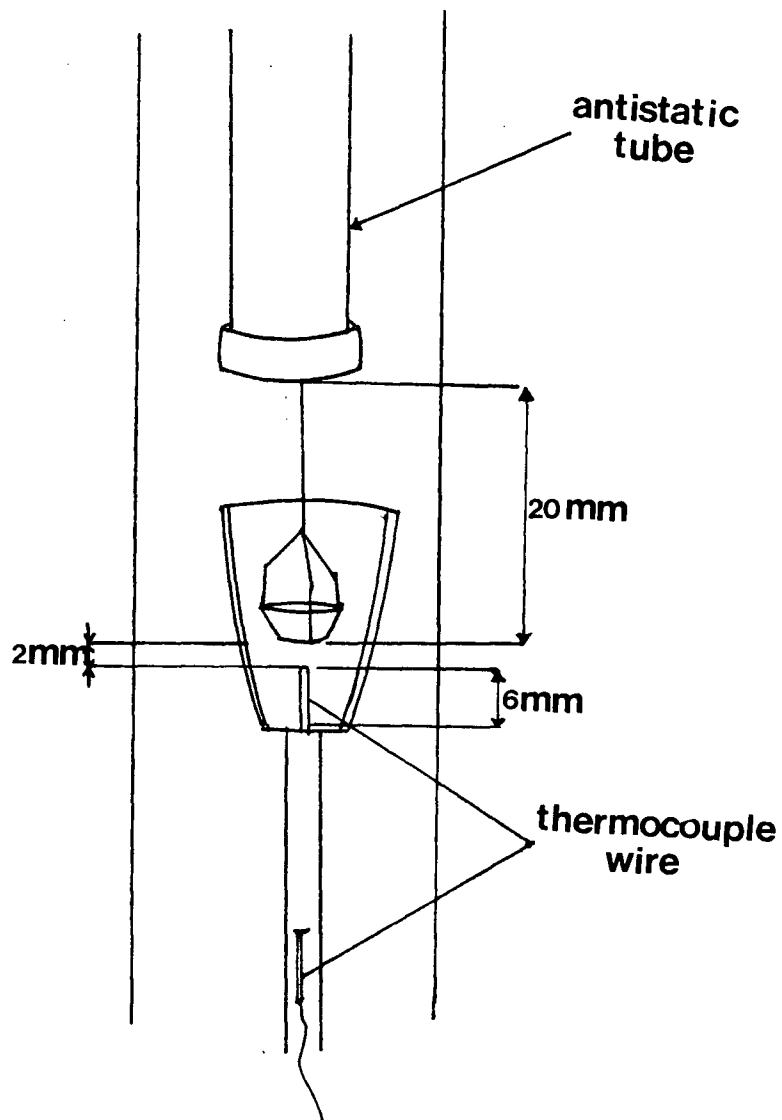
Fig. 13: Cutaway Furnace
Showing Relative Position of Sample,
Furnace, Baffle and Thermocouple

The other units in the system measure the weight by means of the microbalance and control the temperature inside the furnace adequately. The microbalance measured the weight of the samples within an accuracy of ∓ 1 percent.

The temperature controller is the unit which provides for operator control over the temperature with its controls, the reaction starting temperature, heating rate, stopping temperature etc. are specified.

The heater control provides the controls for calibrating the furnace so that the sample temperature is the same as that indicated on the programmer readout within a 2 percent accuracy. It also provides the thermocouple circuitry for monitoring the temperature of the sample environment.

The results are recorded on a 5 inch floppy disc and analyzed with a software program supplied by the manufacturer. They are also plotted using a Hewlet-Packard digital plotter.

For more specific information on the description and operation of the TGS-2 and TADS system, the reader should consult the operating manuals for these systems (32).

4.2.2 Preparation of the Samples.

Sample preparation for these experiments is very similar to the procedure described in the isothermal experiment section. One gram mixtures of 10, 20, 30, 40, 50, 60, 70, 80 percent colemanite in sodium carbonate were slurry mixed and dried on watch glasses overnight in an oven at 110°C. The mixtures were then scraped off the watch glasses

and ground to a diameter of approximately 0.05 millimetres, using a glass rod. They were then stored in vials in a desiccator which was filled with silicagel to prevent their hydration.

In addition to these colemanite-sodium carbonate mixtures, samples containing 20, 40, 50, and 60 percent calcium borate, which was prepared in the laboratory by mixing the hot solutions of calcium hydroxide and 20% excess boric acid, were prepared in the same way as stated above.

Samples of 100 percent colemanite, 100 percent sodium carbonate and 100 percent calcium borate were also prepared. In each case the reagent was slurried with distilled water, dried overnight in an oven and ground in the same manner as the mixtures.

Table 15 summarizes the experiments performed by using TG.

4.2.3 Selection of Experimental Conditions.

Experimental conditions were set by running some preliminary tests on colemanite-sodium carbonate mixtures as well as by considering some of the theoretical aspects discussed in the literature part of this thesis which were needed to obtain accurate results.

Sample size was between 10 and 30 milligrams. Use of small samples usually results in the best temperature accuracy and repeatability while large sample sizes often favour better weight change accuracy. For most applications the range from 5-40 milligrams is given as optimum for this TG system.

Table 15:   List of the experiments performed using TG.*

Sample #	Agent type	Agent conc. (% weight)	Temp. span (°C)	Heating Rate
1	Colemanite	10	40-1000	10°C/min.
2	Colemanite	20	40-1000	10°C/min.
3	Colemanite	30	40-1000	10°C/min.
4	Colemanite	40	40-1000	10°C/min.
5	Colemanite	50	40-1000	10°C/min.
6	Colemanite	60	40-1000	10°C/min.
7	Colemanite	70	40-1000	10°C/min.
8	Colemanite	80	40-1000	10°C/min.
9	Colemanite	100	40-1000	10°C/min.
10	Sodium carbonate	100	40-1000	10°C/min.
11	Calcium borate	20	40-1000	10°C/min.
12	Calcium borate	40	40-1000	10°C/min.
13	Calcium borate	50	40-1000	10°C/min.
14	Calcium borate	60	40-1000	10°C/min.
15	Calcium borate	100	40-1000	10°C/min.
16	Boron trioxide	100	40-1000	10°C/min.

* Each run was repeated three times except the run for boron trioxide.

The heating rate was chosen as 10°C/min. in order to separate any series reaction. Temperatures of 40°C and 1000°C were set for the minimum and maximum temperatures respectively for this specific reaction system.

The furnace was purged with nitrogen to remove carbon dioxide whose presence in the vicinity of the sample would inhibit further reaction. It also supplied a non-oxidative atmosphere for the sample holders in the temperature range of the investigation.

4.2.4 Experimental Procedure and Recording of the Data.

The simplified procedure can be summarized as:

1. The autobalance and other control units and the computer were switched on with a clean weighing pan in place and the furnace tube in position. Meanwhile the purge gas was started to the furnace.

2. The standard TGS-2 mini-floppy disk was placed into port '0' of the TAD station, while a blank formatted mini-floppy disk was placed into port '1'. After the required information was entered into the TAD station, the TG program was read into the TADS system memory and the system was commanded to proceed to the set-up section of the run. The required parameters and conditions were then entered into the system. These parameters were also entered into the system 7/4 thermal analysis controller.

3. The weight of the empty pan was displayed on the computer when the read weight button was pressed on the keyboard. The balance was zeroed by using coarse and fine zero nobs on the balance control.

Then the sample was placed in the platinum pan.

4. The sample weight was automatically displayed on the computer when the furnace had been set back into position.

5. The start button was pressed after which, the microprocessor proceeded with the heating run and accumulated the data which was also plotted on the computer display. The data were analyzed and the results were used to study the kinetics of the reactions involved.

6. When the maximum temperature was reached the unit automatically started cooling down to the programmed minimum temperature.

The typical TG curves obtained by using this experimental technique are shown in Figures 22 to 30 for 100 percent sodium carbonate, 20, 30, 40, 50, 60, 70, and 80 percent colemanite in sodium carbonate and 100 percent colemanite respectively.

4.2.5 Kinetic Analysis of the TG Data.

It was necessary to recalculate the weight loss data to eliminate the losses that are evident for colemanite when it is heated by itself. This loss would be included in the curves which show the weight loss for mixtures of colemanite and sodium carbonate, in proportion to the colemanite percentage in the samples. This results in higher weight losses than that due to the reaction.

The curves which represent each percentage of colemanite in sodium carbonate were digitized by using the digitizer system which is connected to the U.B.C. main computer. The curve for 100 percent colemanite was also digitized and all data was stored in separate

files. The value of the weight loss at a specific temperature for the 100 percent colemanite was corrected for the weight of colemanite in the mixture and then subtracted from the value of the weight loss for the mixture at the same temperature. This was done for each point on the curve corresponding to the temperature intervals of 5°C. Plots of these corrected data were also obtained by using the Ace:Graph program which is available in the U.B.C. computing centre library.

These plots which are shown in Fig. 14 showed a weight increase at about 380°C on the curves. Since this was impossible it was concluded that the loss seen in the 100 percent colemanite curve at about this temperature should not be included in the subtraction procedure. This loss might be due to the release of a substance which could be bounded by the presence of sodium carbonate. So the digitized data for 100 percent colemanite was corrected excluding the loss from 380-410°C and then the subtruction was repeated. The results were plotted and smoothly decreasing curves which showed the weight loss due to the reaction were obtained for each reaction mixture.

This final form of the thermogravimetric data are shown in Figure 34, 35, 36, 37, and 38 for 20, 30, 40, 50, and 60 percent colemanite mixtures respectively and was used for the evaluation of kinetic constants for this reaction system.
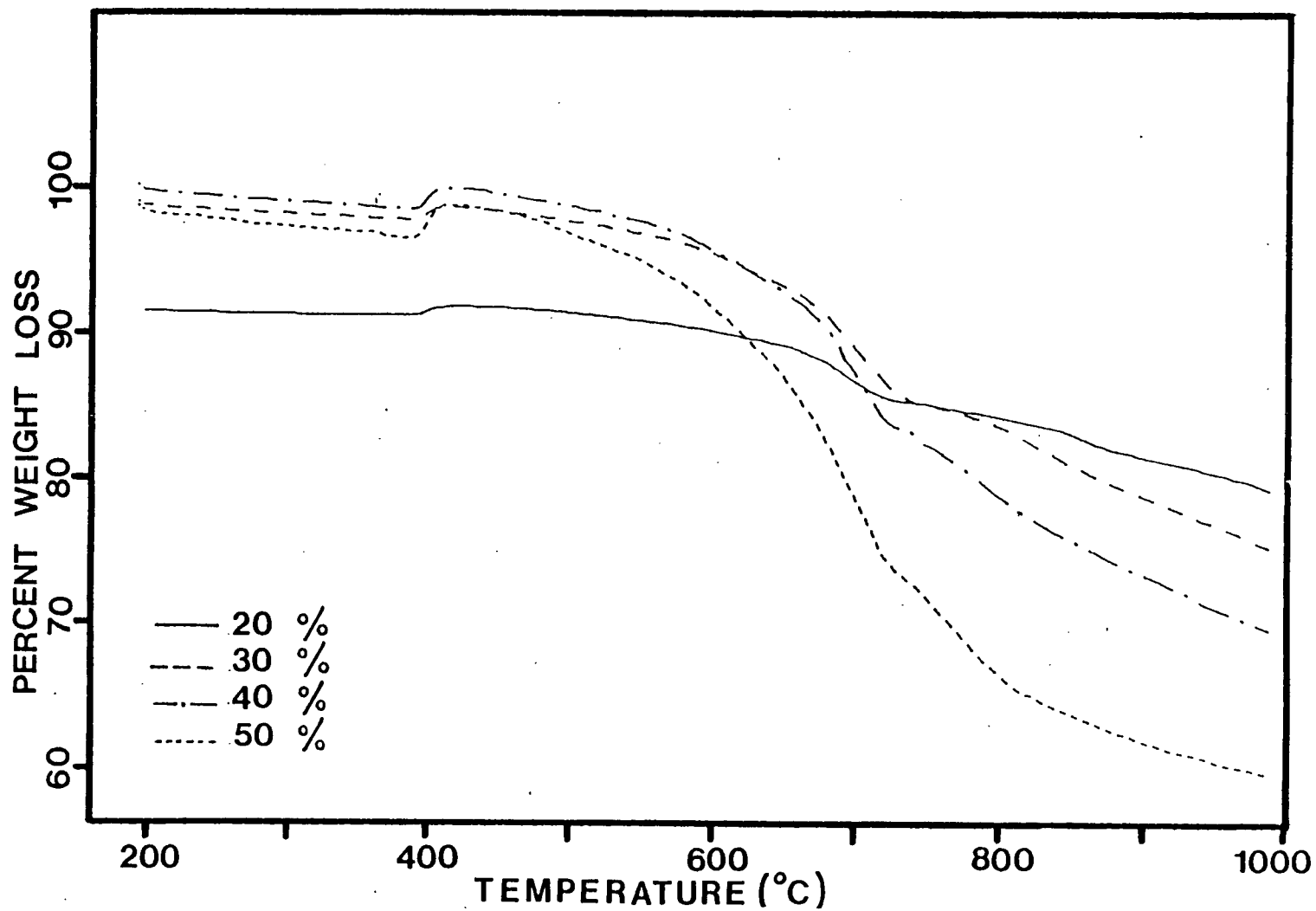
Figure 14: Results after subtraction of the colemanite curve
from the others

4.3 Recycling Experiments

A series of experiments was performed to test the recycling efficiency of colemanite. Tests were made to determine whether there was a decrease in the conversion of sodium carbonate due to the repeated use of colemanite for several runs.

These experiments were done using both the oven and the TGS-2 system. They were performed only for 40 percent colemanite mixtures and the reaction temperature of 900°C. The procedure can be summarized as follows:

1. Five samples, each containing 40 percent colemanite in sodium carbonate, were prepared in the same way as used previously and were reacted in the oven for 80 minutes. They were then dissolved as described in section 4.1.3 and kept in the desiccator until cool.

2. After the solutions had been cooled, carbon dioxide gas was dispersed through each solution for 15 minutes which was found to be sufficient to convert all the sodium oxide in the solution to sodium carbonate. Then the solutions were placed in a vacuum oven and the water was evaporated from the solutions.

3. One of these dried samples was then used in the TG for analysis and the remainder were placed back into the oven for another run.

4. This procedure was continued, each time keeping one sample for the TG analysis after each run.

The TG data are shown in Figures 61, 62 and 63 for the cases of first, second and third recycles respectively.

Some additional experiments were also performed to determine the
boron content and the solubility of the colemanite.

Boron analysis was made by an acid extraction method which is
described in Appendix I. Solubility experiments showed that 60 percent
of the colemanite is insoluble in water at 20°C (26).

5. ANALYSIS OF THERMOGRAVIMETRIC DATA

Thermogravimetric data was analyzed in two parts; reaction between 190-700°C and the reaction between 700-1000°C. (See Figures 23-29.) The temperature 700°C where the derivative curve shows a peak which represent a change in the reaction mechanism was chosen as the temperature at which the first reaction stops and the second reaction starts. This point will be discussed in more detail in section 6.2. These two reactions were not analyzed as simultaneous reactions for two main reasons. The derivative of the weight loss curve showed a sharp break at about 700°C regardless of the colemanite concentration in the mixtures. The digital thermal analyzer (DTA) data also showed a peak which is due to a new heat effect. This peak can not be seen above a concentration of colemanite higher than the stoichiometric amount needed. In addition, the assumption that these two reactions were taking place simultaneously would have made the analysis of the TG data very complex.

5.1 Analysis of the Data for the First Reaction

The method which was developed by Zsako (31) was applied for the analysis of the TG curves which were obtained for the decarbonization reaction of sodium carbonate in the presence of colemanite.

Analytical forms of the functions $f(\alpha)$ and $g(\alpha)$ for the most probable reaction mechanisms are tabulated in Table 8. Utilization of eq. (3.18) enables the calculation of the fractional conversion of sodium carbonate, α_s, throughout the whole temperature range of the

reaction simply by reading the value of W from the TG curve (e.g. Fig. 34) for each corresponding temperature. Substitution of these α_s values into the equations for $g(\alpha)$ tabulated in Table 8 gives the values of function $g(\alpha)$ for each temperature.

The following steps were followed to find the kinetic constants of this reaction:

1. One of the mechanisms listed in Table 8 was presumed. For every temperature starting from 460°K, α_s and the corresponding log $g(\alpha)$ were calculated at temperature intervals of 10°K. At the same time E_1 values were chosen, starting with 1 Kcal/mol and increasing at each step by 1 Kcal/mol, and log $p(x)$ values were evaluated by using the "U.B.C. Integral" program for the same T values used in the calculation of log $g(\alpha)$ values.

2. By taking the differences between the log $g(\alpha)$ and log $p(x)$ values at each temperature, B_i values were found utilizing equation (2.24) in section 2.4. Standard deviation of these B values, δ, were then calculated by using equation (2.25).

3. This procedure was repeated for each mechanism listed in the table and the minimum of the standard deviation values, δ_{min}, were noted for each run, corresponding to a specific E_1, m and n value. The equation with the smallest δ_{min} value among these was taken as the best mechanism that fits this particular reaction and the corresponding E_1 value was given as the activation energy of the reaction.

In addition to this comparison which depends on the standard
deviations, a double check was made by recalculating the α_s values
using the chosen m and n values and best E_1 value. Calculated values
of α_s were then compared with the values of α_s obtained from the
experimental TG curve.

5.2 Analysis of the Data for the Second Reaction

The same method which was used for the evaluation of the kinetic
model for the first reaction was followed for the reaction which took
place within the temperature range from 700-1000°C. All the proposed
mechanisms which were listed in Table 9 were tested by both evaluating
the standard deviations and making the comparison of experimental and
theoretical fractional conversions of sodium carbonate.

The expression which was derived for the fractional conversion
of sodium carbonate eq. (3.18) (see section 3.1.2) applies for this
reaction too. An important point was the substitution of the right
value for the lower limit of the integral in eq. (2.21), which is the
fractional conversion of sodium carbonate at the end of the first
reaction instead of zero, in order to find the value of function $g(\alpha)$.

6. RESULTS AND DISCUSSION

The main aim of this project is to find the best autocausticizing agent for the direct conversion of sodium carbonate to sodium oxide and to study the kinetics of this reaction for the chosen system.

The study was performed in two main parts, as isothermal and as thermogravimetric experiments.

6.1 Isothermal Experiments

Percentage conversion of sodium carbonate as a function of time was calculated for each of the autocausticizing agents which were titanium dioxide, alumina and colemanite, by using the titration data taken in isothermal experiments (Tables 11, 12, 13, and 14).

Conversion calculations were based on the total titrated amount of unreacted and reacted sodium carbonate rather than the initial amount of sodium carbonate at the start of the experiments. The reason for this was the difficulty in recovering the whole sample from the crucibles because the reaction products fused into a solid mass when the samples were cooled. It was assumed that the samples were homogeneous so that the sample which was recovered from the crucible resembled the whole sample. As such it had the same ratio of unreacted to reacted sodium carbonate. Since the samples were prepared by slurry mixing this assumption would be reasonable. A sample calculation of conversion is shown in Appendix II.

Figures 15 and 16 show the results for 10 and 20 percent titanium dioxide respectively. In both cases higher conversions are obtained at higher temperatures for a given time. This is a typical Arrhenius behaviour. It is also seen that higher autocausticizing agent concentration gives higher conversion values. This indicates that reaction rate is proportional to the mass of autocausticizing agent. It was found that 50 percent conversion can be obtained at 1000°C in 50 minutes by using titanium dioxide at a concentration of 20 percent. These results are similar to those obtained by Kiiskila (18).

Figures 17 and 18 show the results for alumina. There is a lot of scatter in this data because of the interference in the titrations due to Al(OH)$_3$ formation (9).

The effect of colemanite as an autocausticizing agent for the direct reduction of sodium carbonate to sodium oxide is shown in Figures 19, 20 and 21. It is seen that colemanite accelerated the reaction as well as titanium dioxide did. It is also noticed that the reaction is faster than the one with titanium dioxide. In the case of colemanite, higher percentages were examined because of the high molecular weight of the colemanite and uncertainty about its purity. For low colemanite concentrations such as 10 and 20 percent the molar ratio of the B$_2$O$_3$, which is believed to be the effective part of the colemanite, to the sodium carbonate is low because of the high molecular weight of the colemanite. Therefore colemanite doesn't seem superior to titanium dioxide when the Figures 15, 16 and 19 are compared for the same agent percentages.
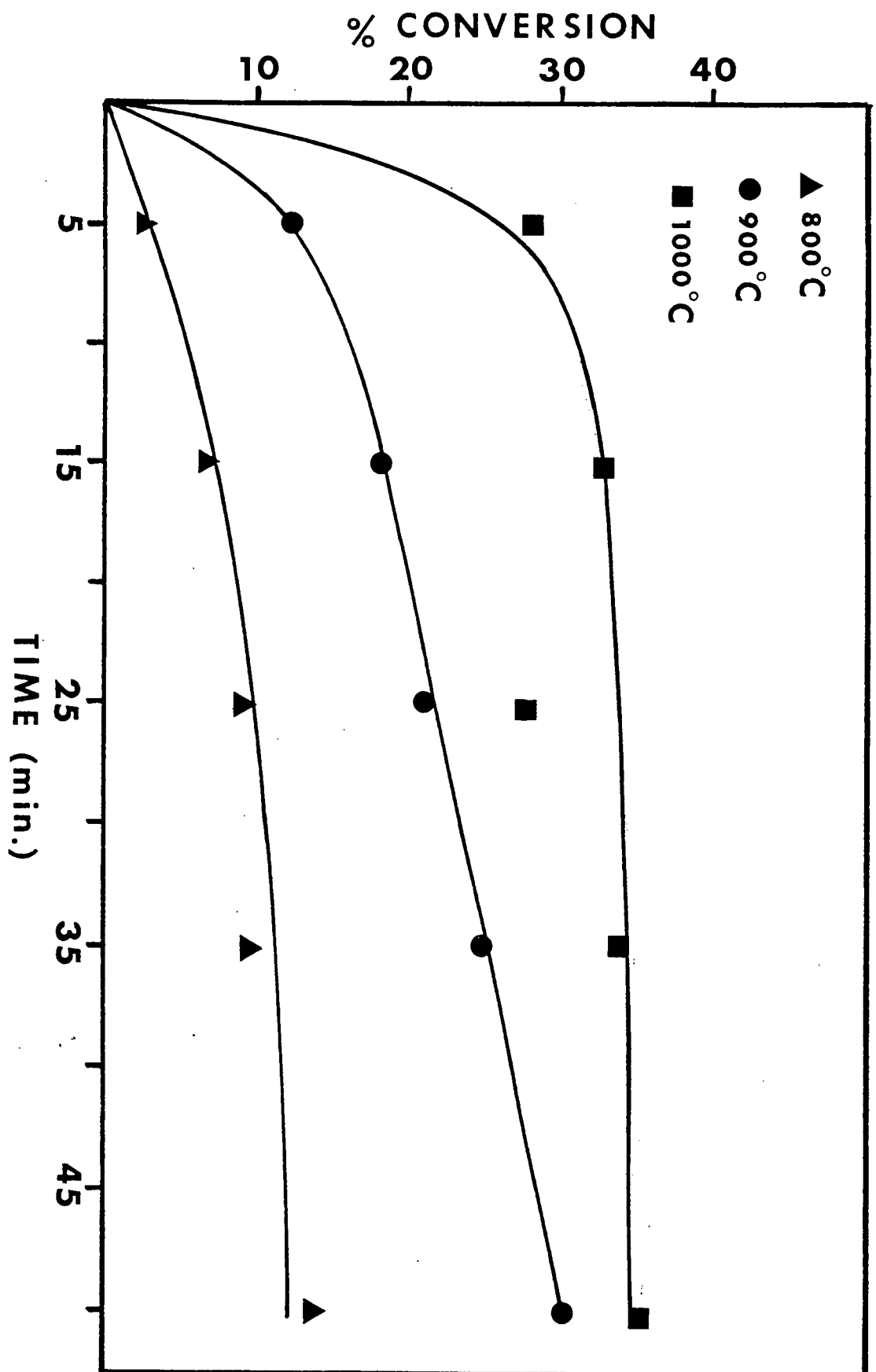
Figure 15: Results of isothermal experiments for 10 percent TiO_2.
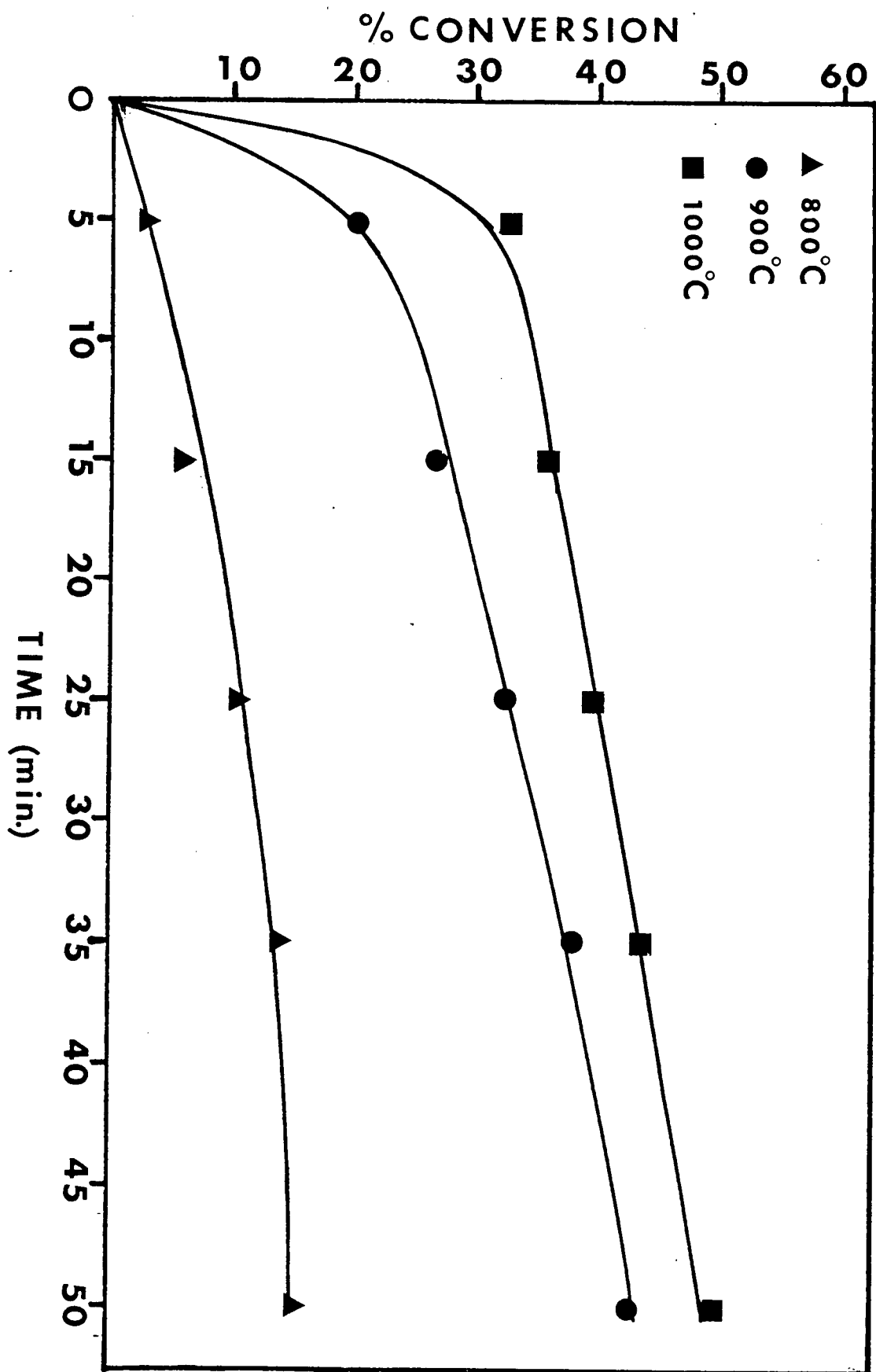
Figure 16: Results of isothermal experiments for 20 percent TiO_2.
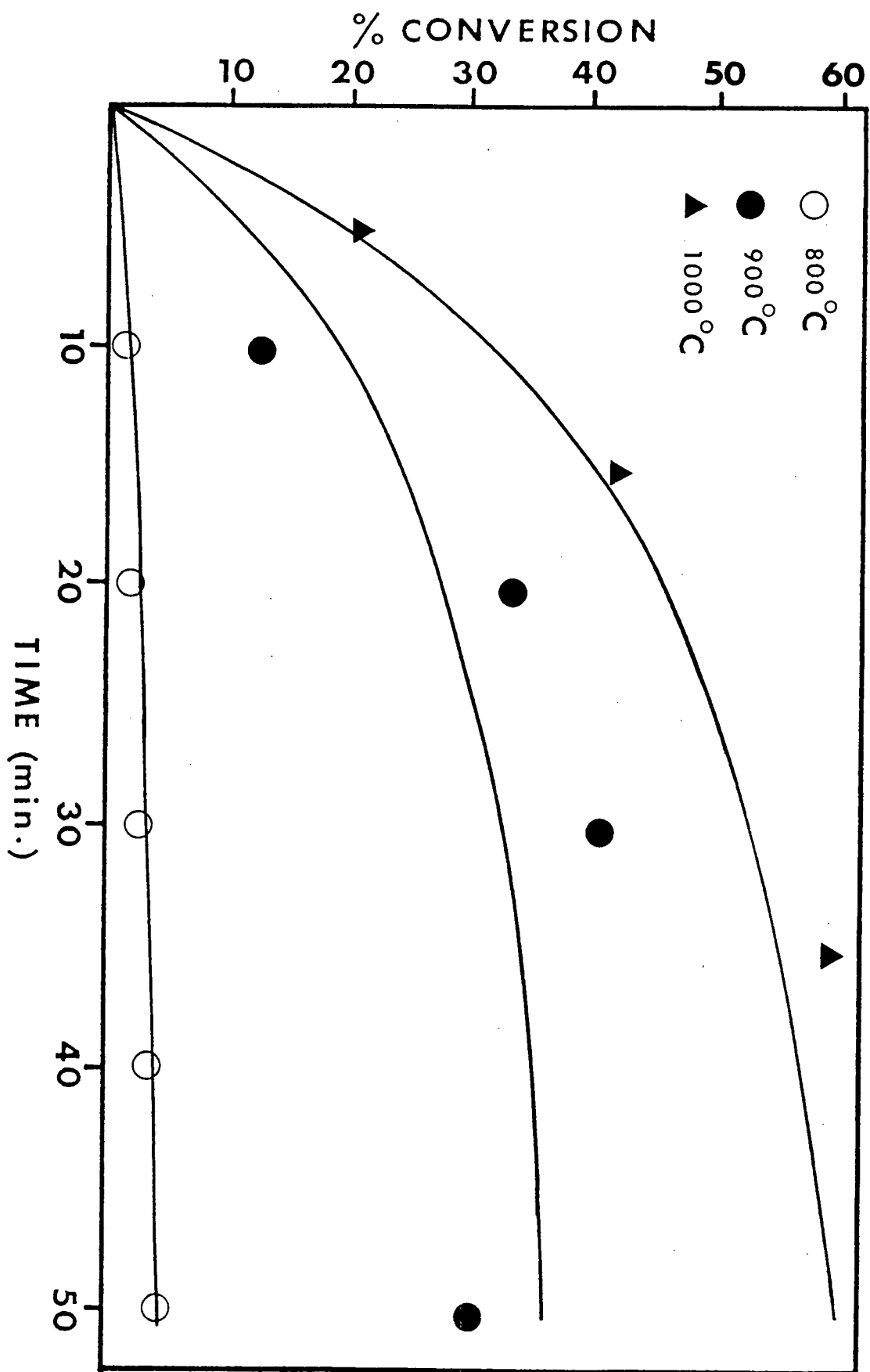
Figure 17: Results of isothermal experiments for 10 percent alumina.
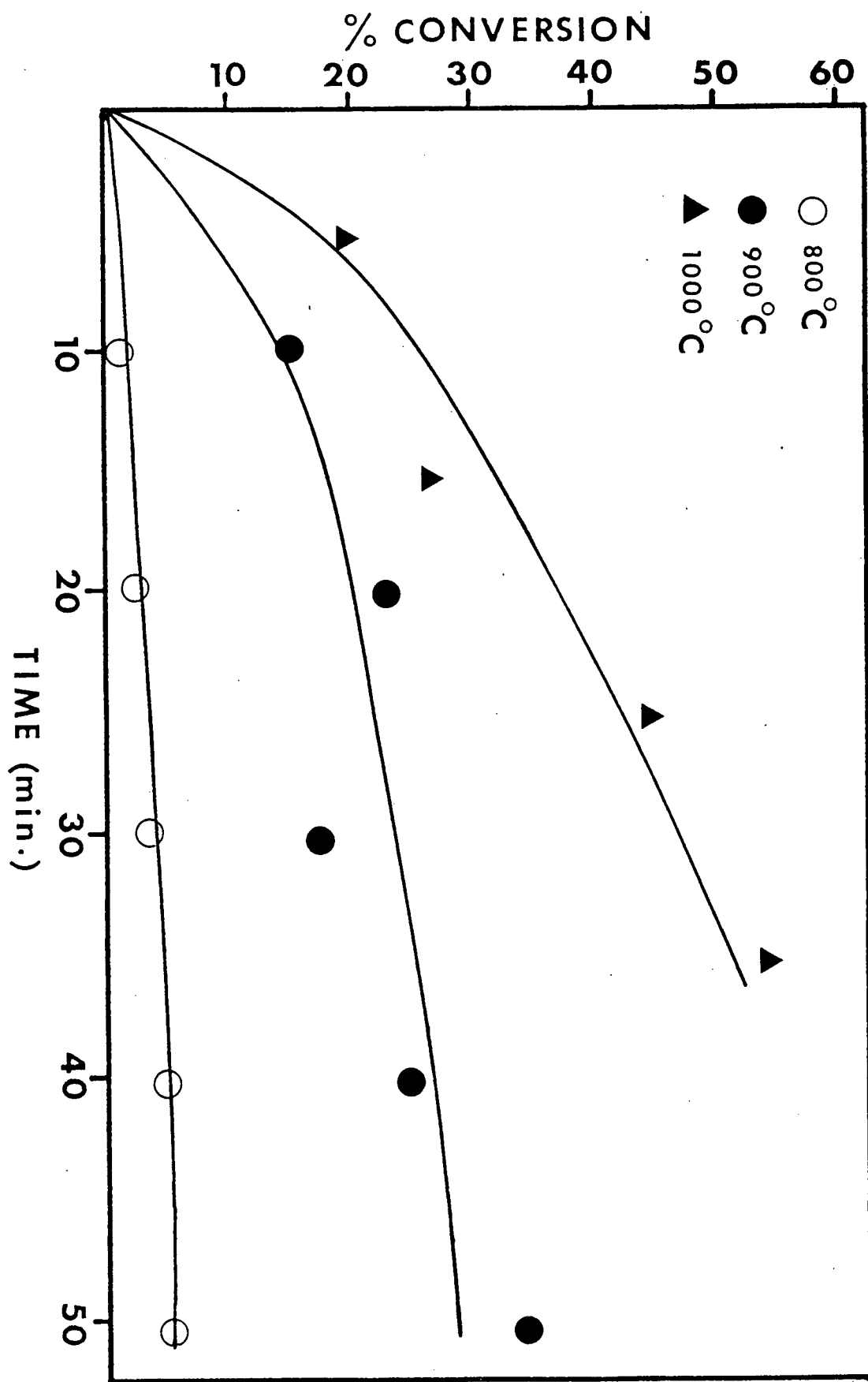
Figure 18: Results of isothermal experiments for 20 percent alumina.
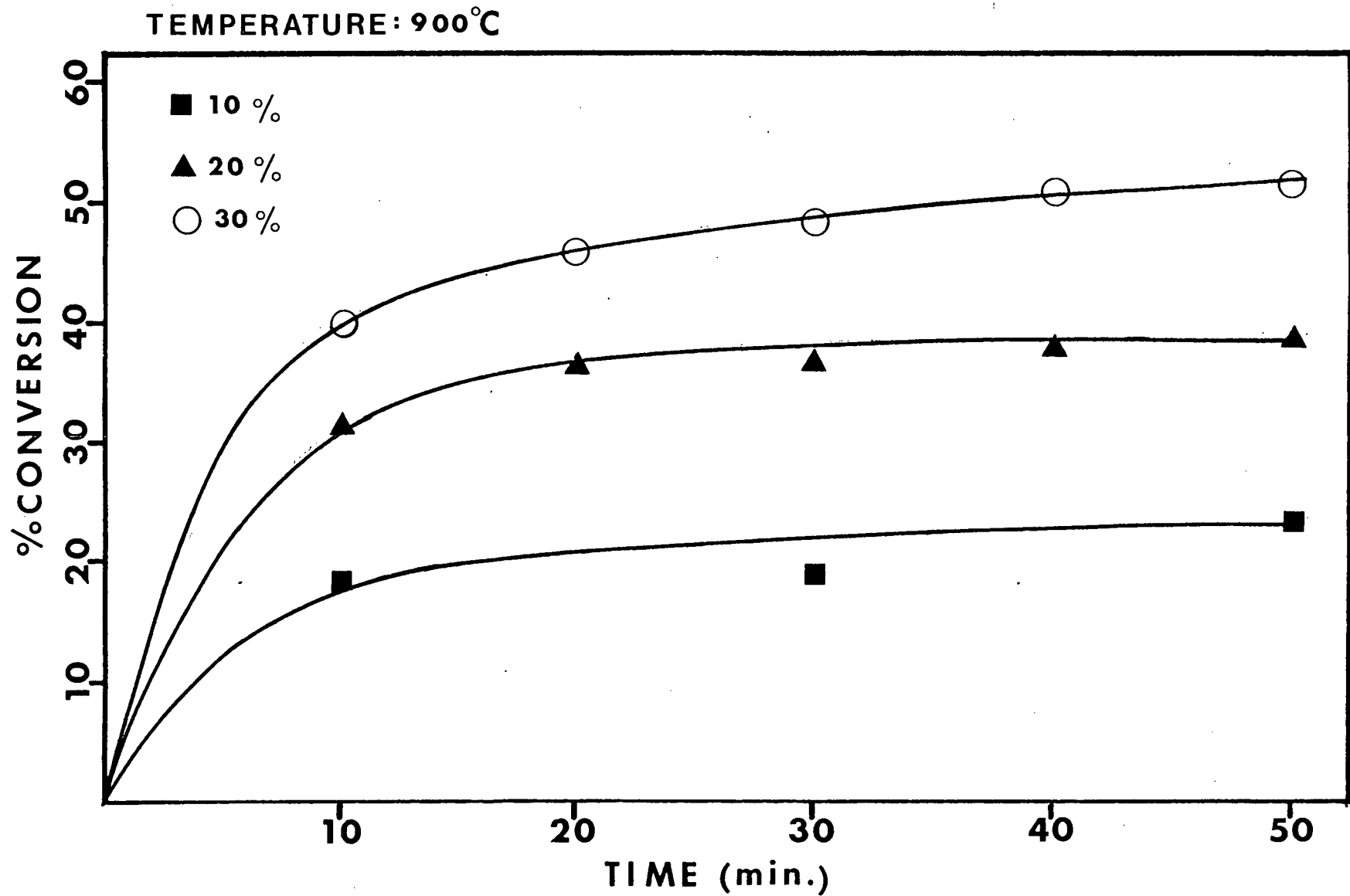
Figure 19: Results of the isothermal runs for 10, 20 and
30 percent colemanite.

In Figure 20 the results of the runs with 40, 50 and 60 percent colemanite in sodium carbonate are plotted. These results show that it is possible to obtain a conversion as high as 80 percent in half an hour at 900°C. Since colemanite is a cheaper material the use of it in large amounts would not be too costly especially since it would most likely be recycled.

Figure 21 shows the effect of the temperature on the reaction. A typical Arrhenius effect is observed as is the case for the other autocausticizing agents studied. Temperatures above 900°C were not studied since the reaction would be too fast above 900°C.

With both agents it is noticed that the reaction rate for all runs is most rapid at first and then falls off with time. This could be explained by the reduction in reactant concentration with time.

In these experiments the major source of error is the time elapsed before the samples attain the required temperature after being introduced into the preheated oven. Reaction occurs to a certain extent during this heat up period so that the measured value of the conversion corresponding to a certain time is decreased due to the occurence of the slow reaction before the desired temperature was attained. This is a common problem associated with the isothermal method. It is greatest for the shorter time periods and is especially important for fast reactions like the one between colemanite and sodium carbonate. Other errors arise from the experimental procedures such as uncertainty in the volumes of acid recorded during the titrations, probability of carbon dioxide absorption by the samples during the
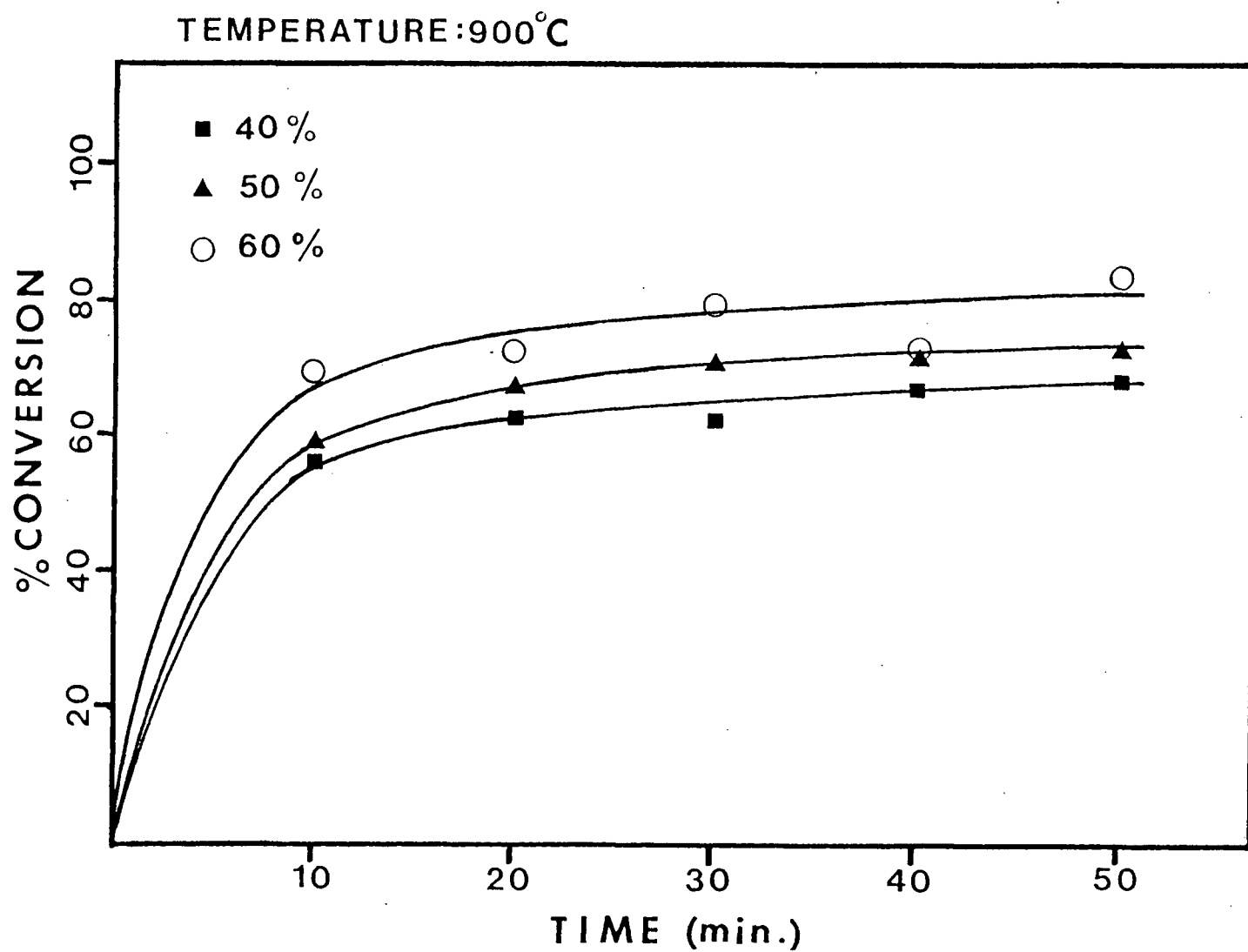
Figure 20: Results of the isothermal runs for 40, 50 and 60 percent colemanite.
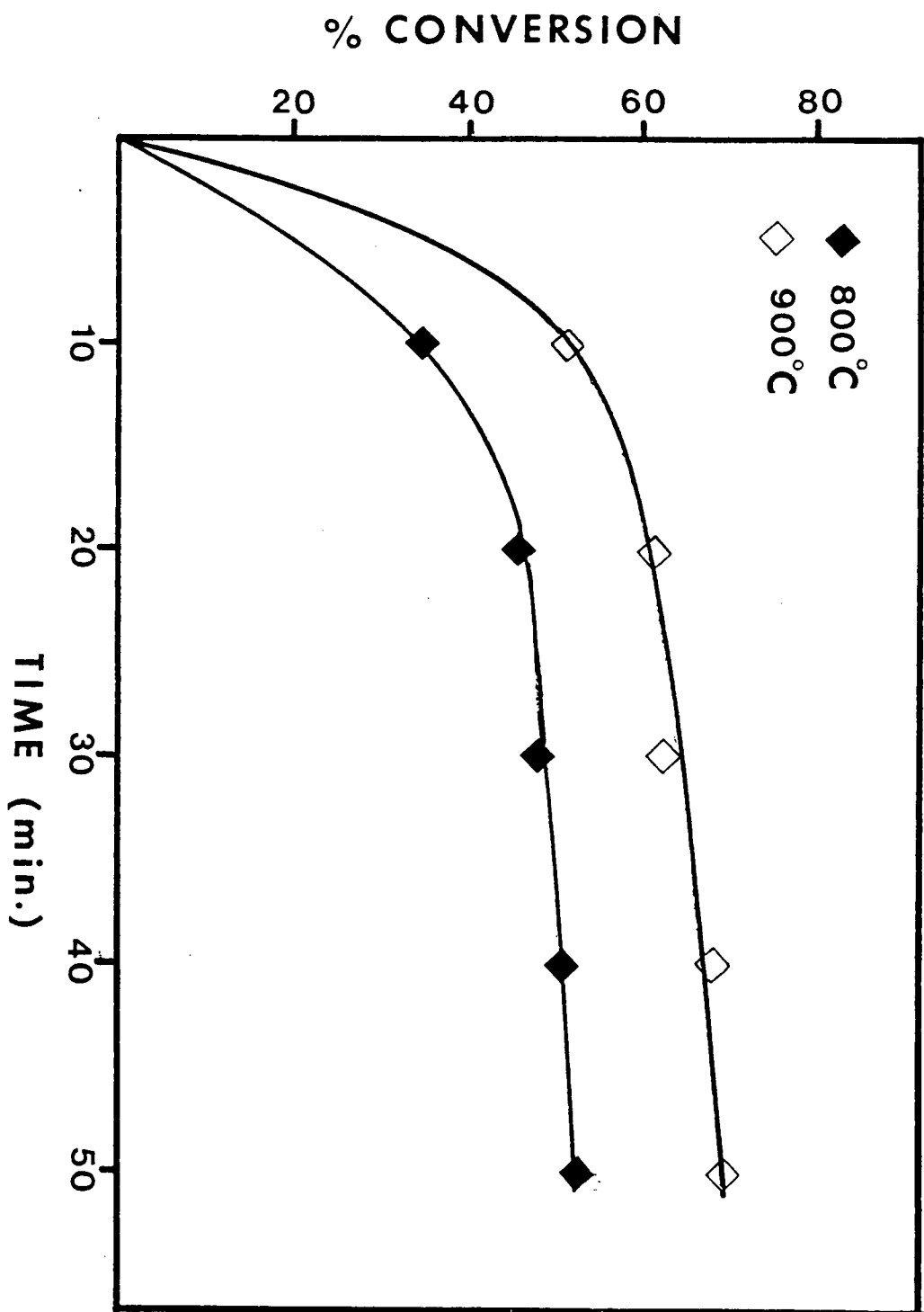
Figure 21: Results of the isothermal runs for colemanite.

transfer of crucibles from oven to desiccator, the weighing and the dissolution steps.

6.2 Differential Thermogravimetric Analysis

At this stage of the study, a new differential thermal analyzer was bought by the department. The thermogravimetric method has many advantages over the isothermal method (see section 2.3). Its use can eliminate most of the errors caused by the other experimental procedures and make possible a better understanding of the reaction mechanism by giving information about the sample at any moment. This added information allows the observation of multiple reactions if they occur. Since colemanite gave the highest rates for this reaction it was chosen as the best autocausticizing agent and further studies are performed on it by using thermogravimetric techniques.

The outputs of the thermogravimetric measurements are shown in Figures 22 to 30 for 0 to 100 percent colemanite concentrations respectively. Sodium carbonate will only begin to dissociate very slowly above 875°C (Figure 22) unless an autocausticizing agent is added. From Figures 23 to 29 it is seen that the reaction has its maximum rate around 640°C for all cases. There are two common points which can be seen when these curves are examined qualitatively. These are the weight losses seen up to 192°C and the inflection point between 650°C and 700°C, which is best shown by the derivative of the weight loss curve. Since the samples were dried at 110°C before use the loss around 190°C would be due to the loss of water of hydration rather than free moisture. The break point between 650-700°C is most likely due to
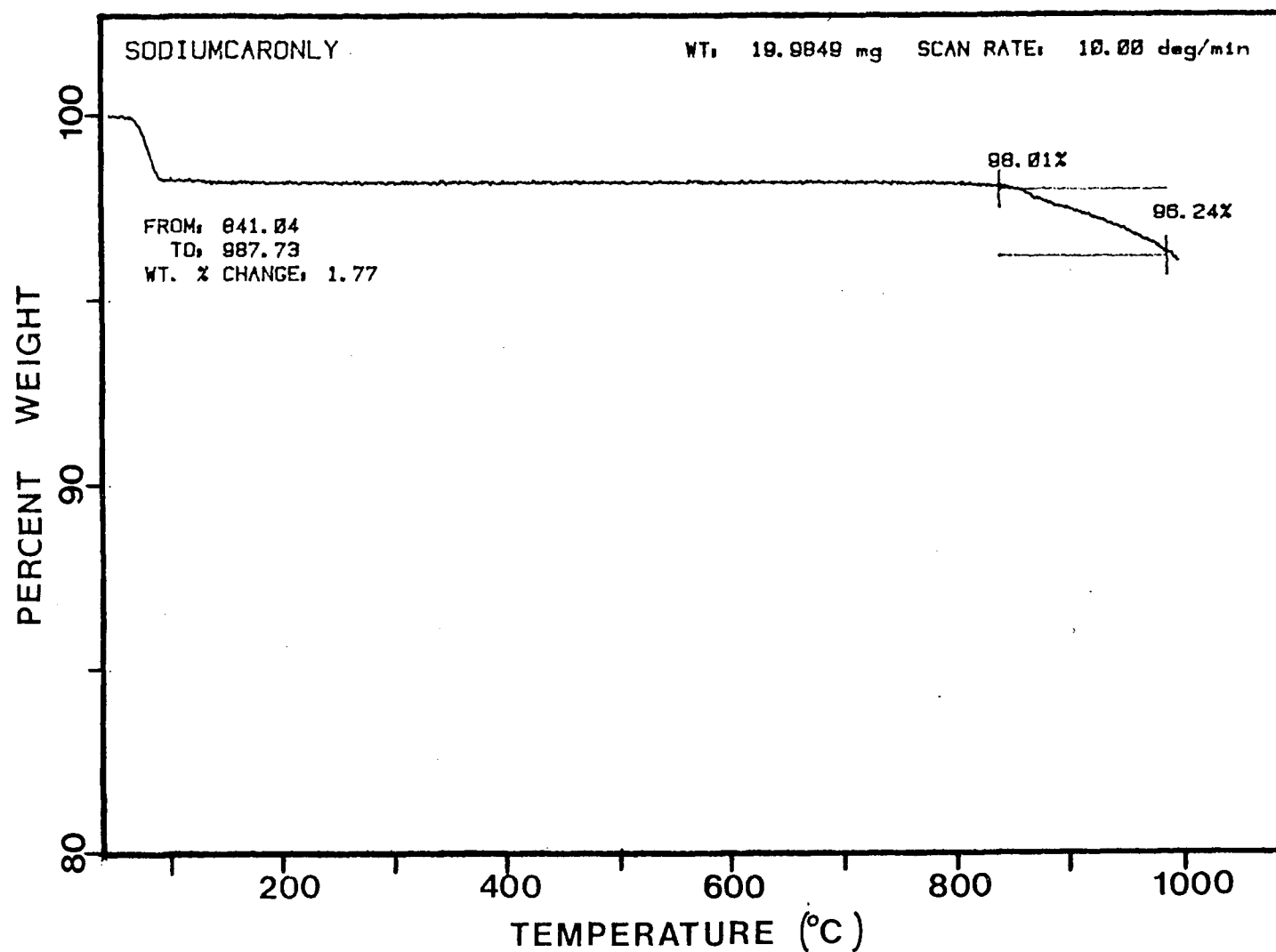
Figure 22: Thermogravimetric data for 100 percent sodium carbonate.
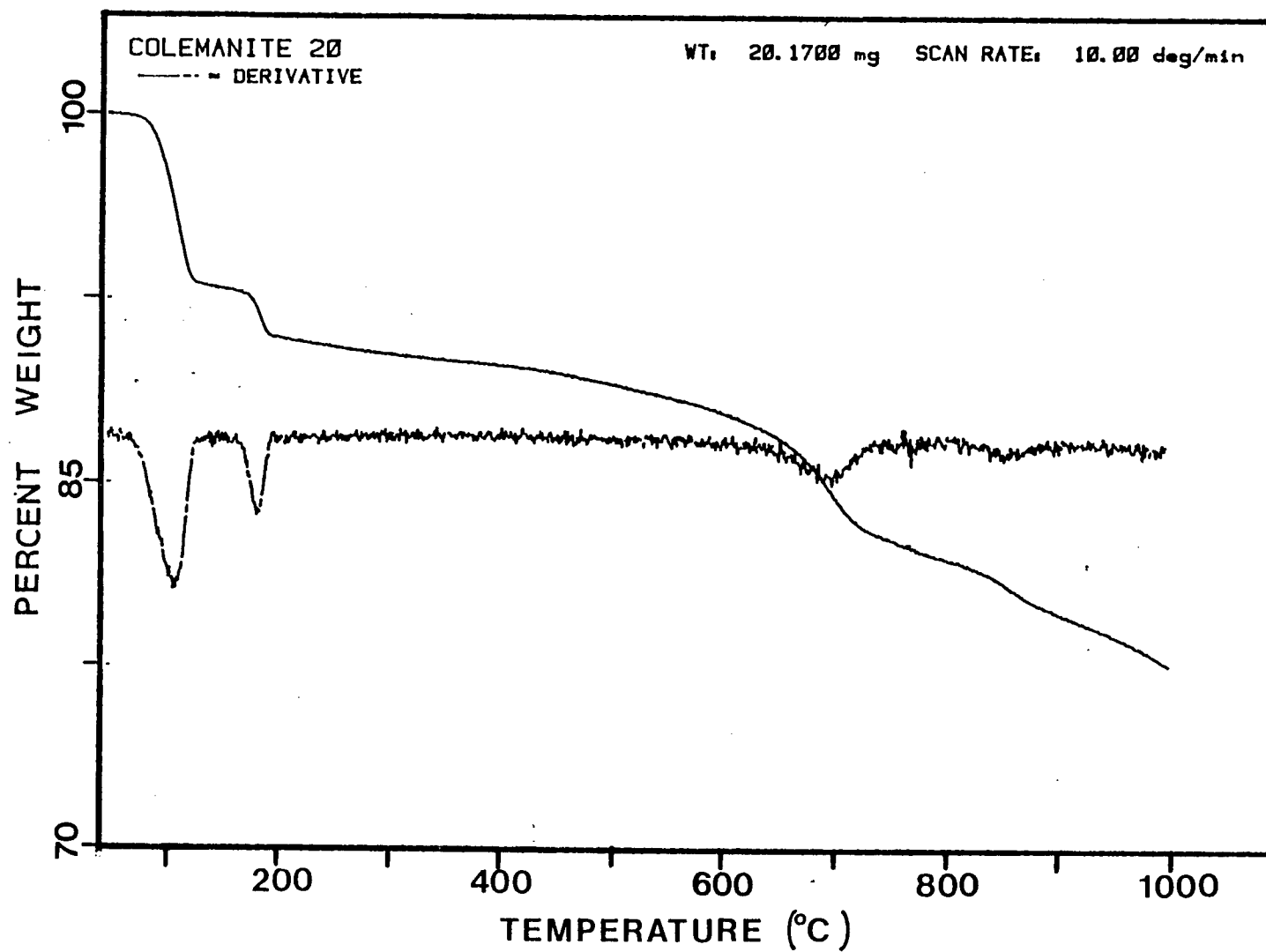
Figure 23: Thermogravimetric data for 20 percent colemanite.
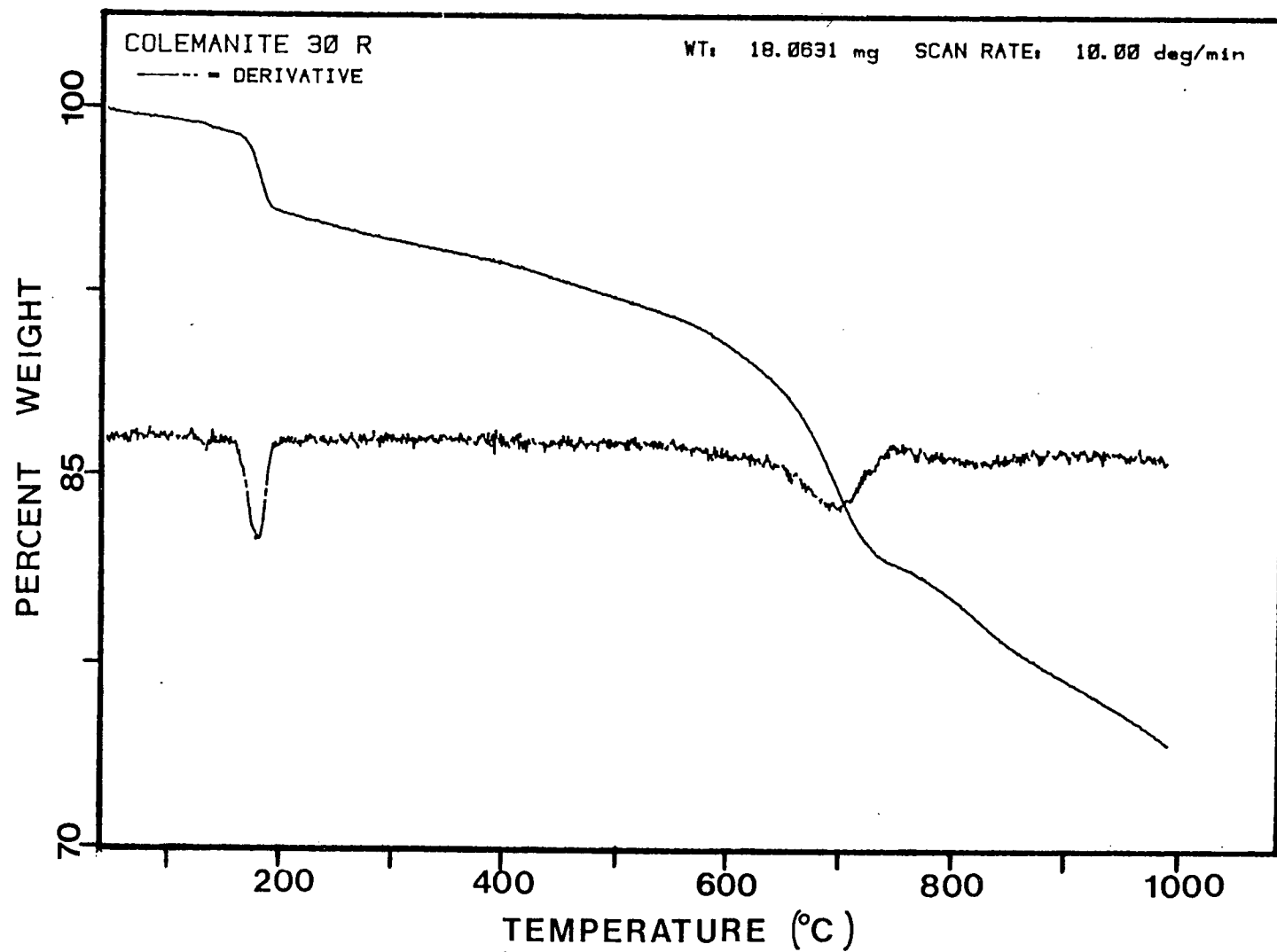
Figure 24:   Thermogravimetric data for 30 percent colemanite.
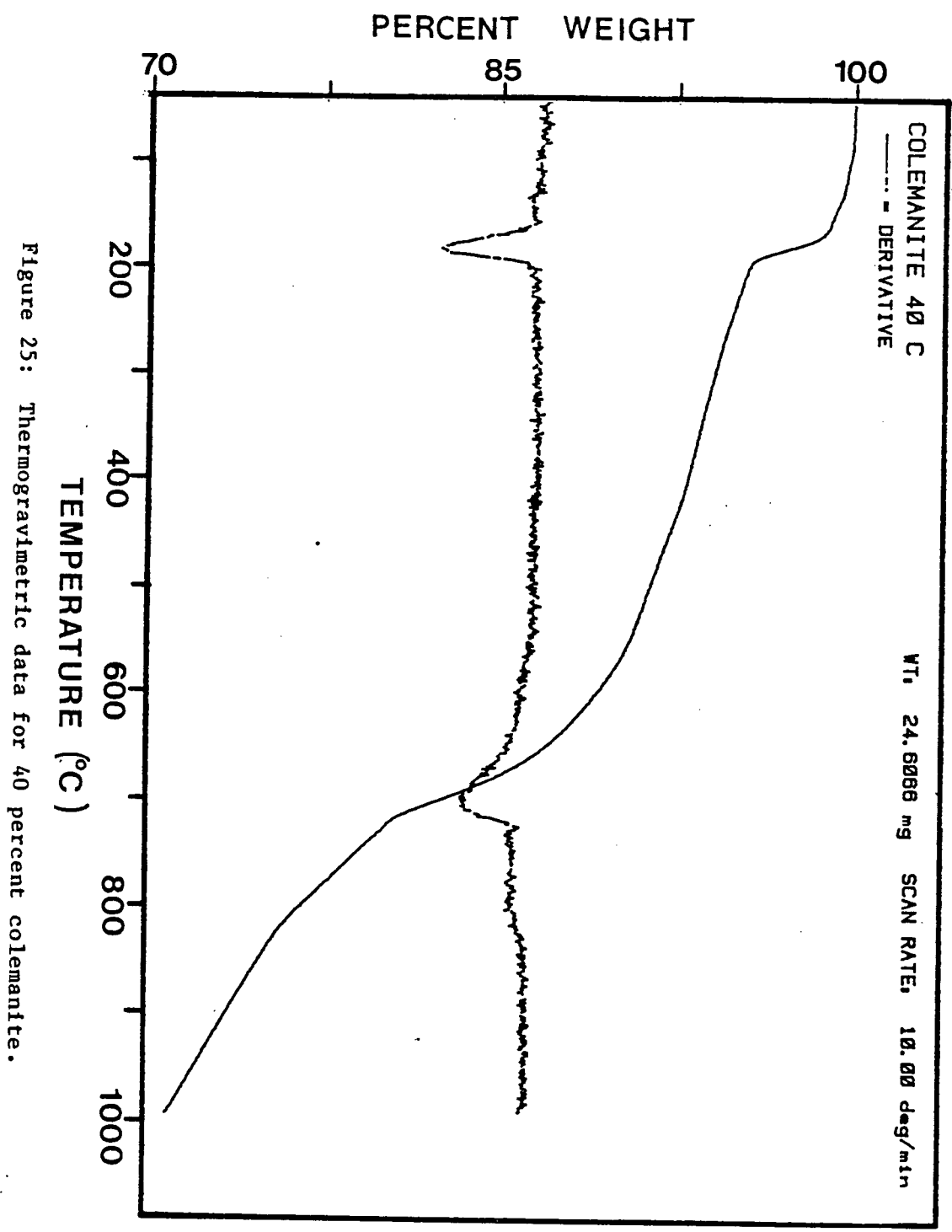
Figure 25: Thermogravimetric data for 40 percent colemanite.

COLEMANITE 50 R
——·· = DERIVATIVE
WT: 17.8384 mg   SCAN RATE: 10.00 deg/min
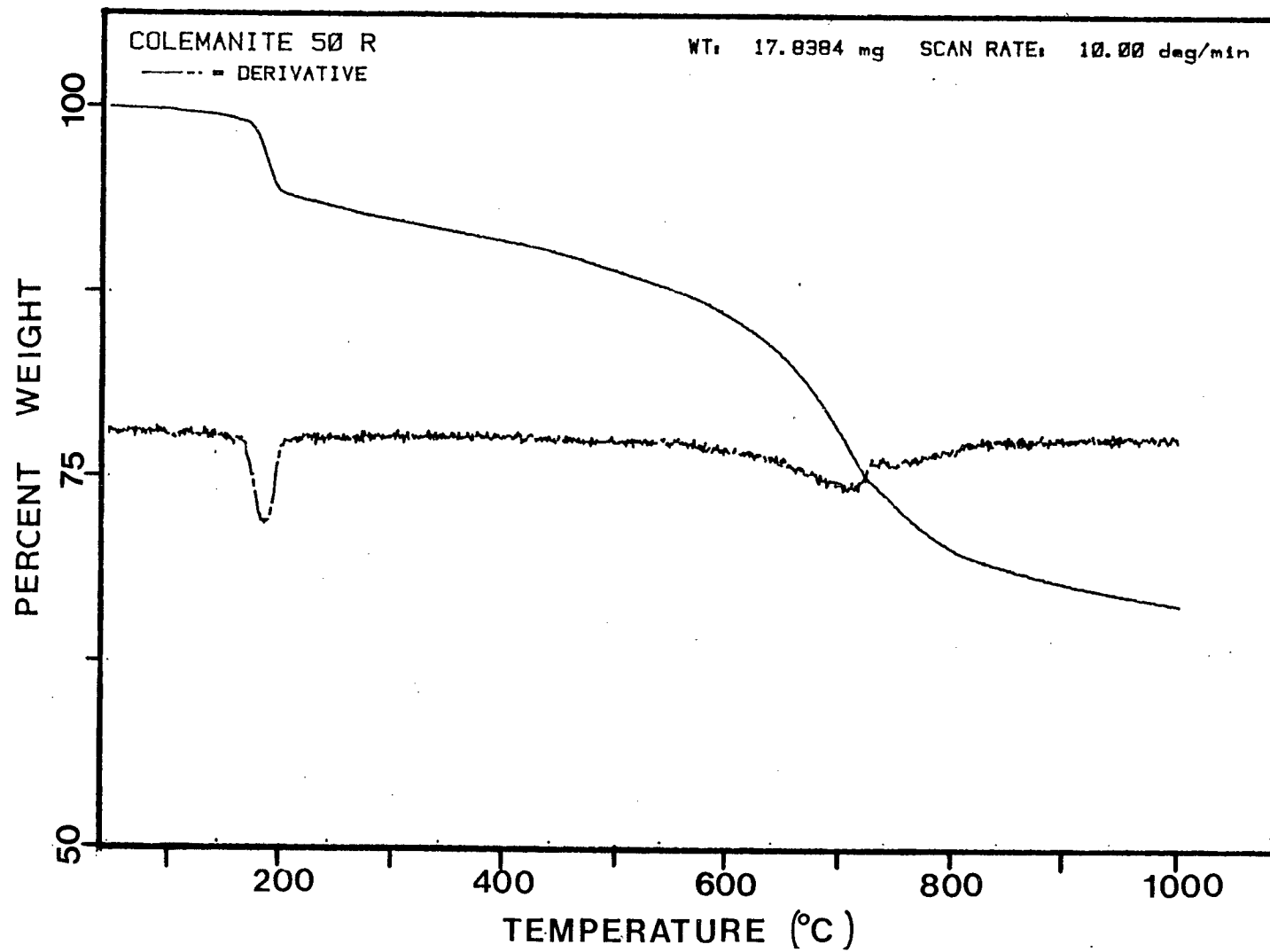
Figure 26:   Thermogravimetric data for 50 percent colemanite.
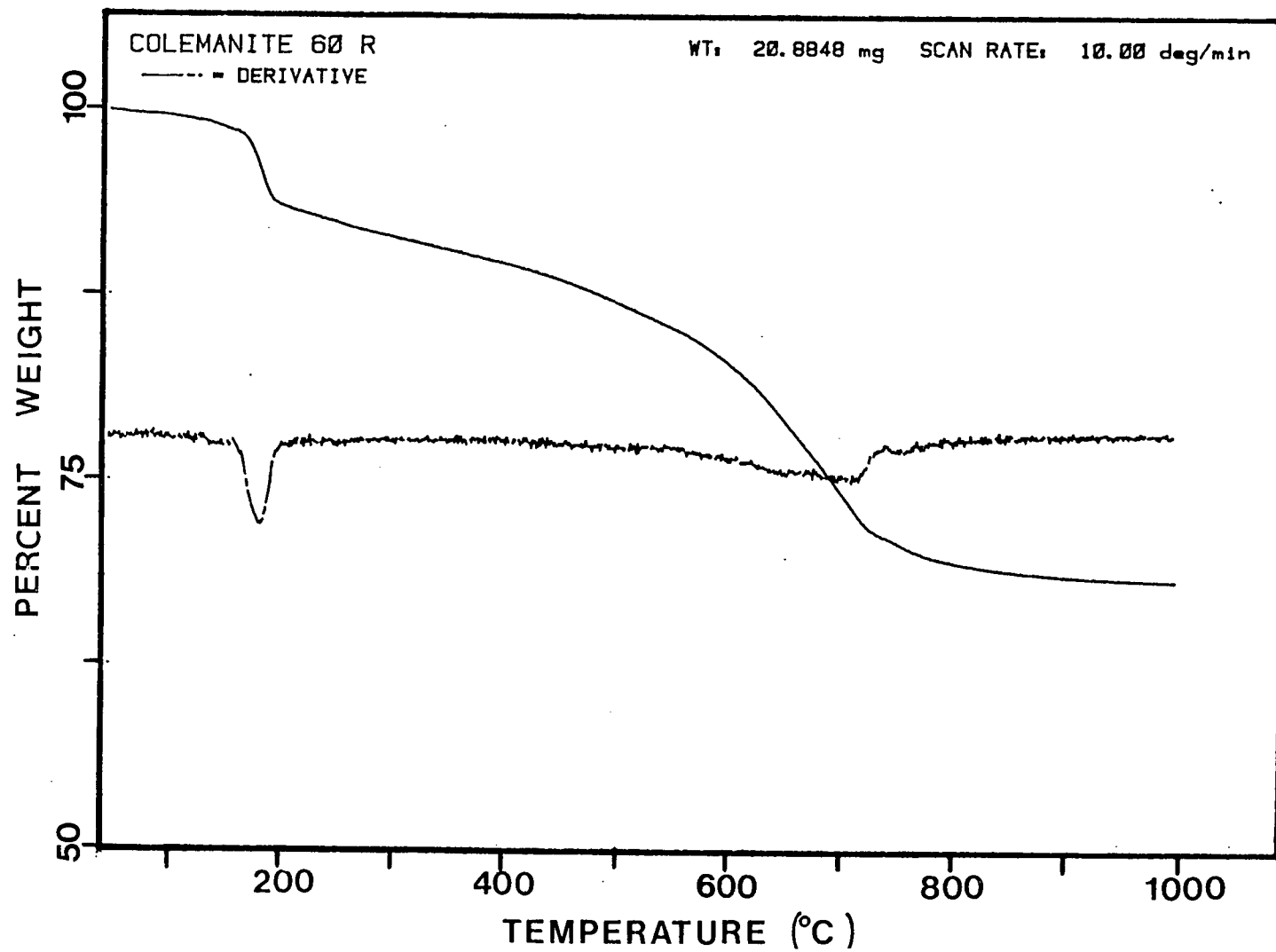
Figure 27: Thermogravimetric data for 60 percent colemanite.
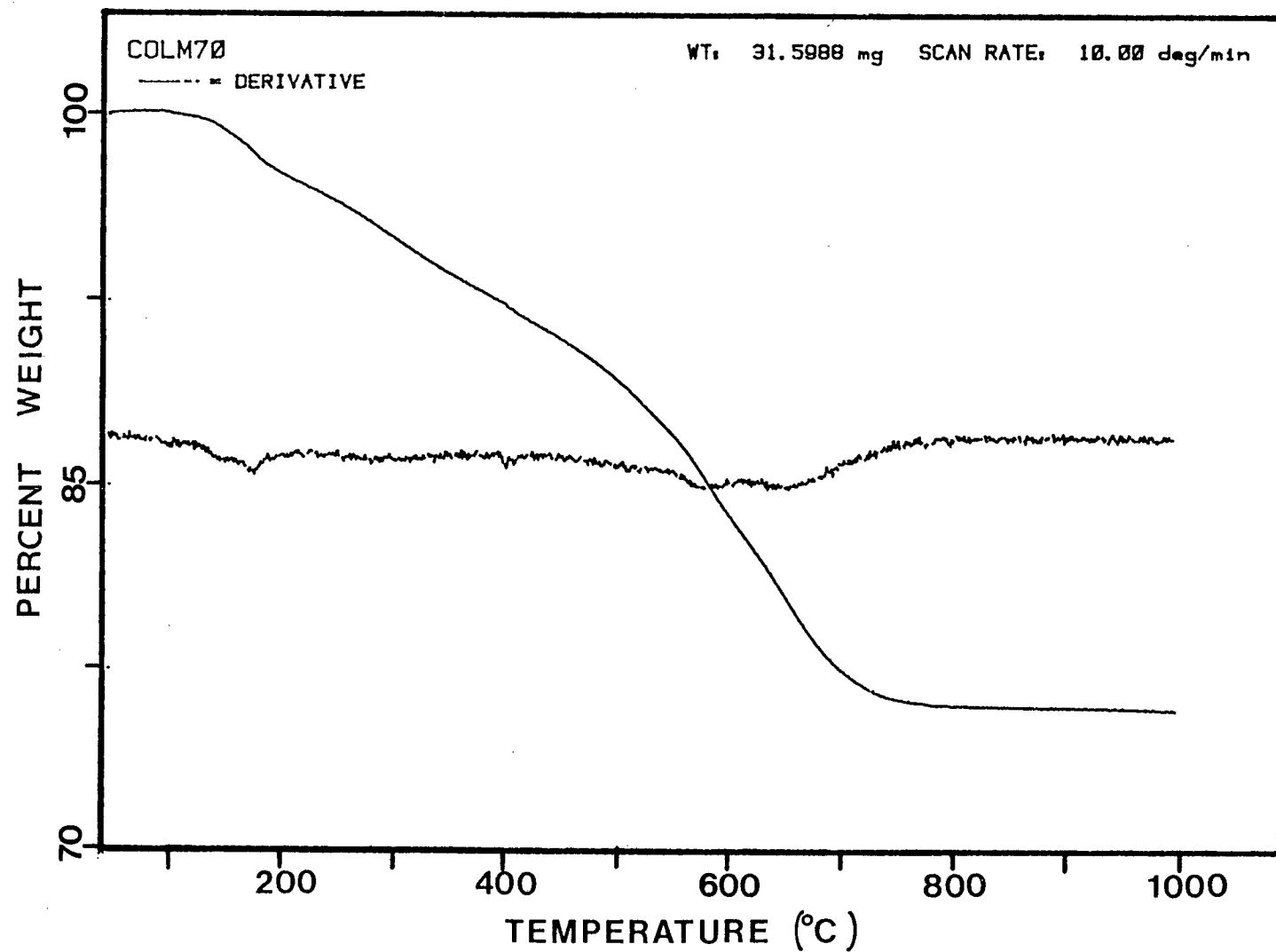
Figure 28: Thermogravimetric data for 70 percent colemanite.
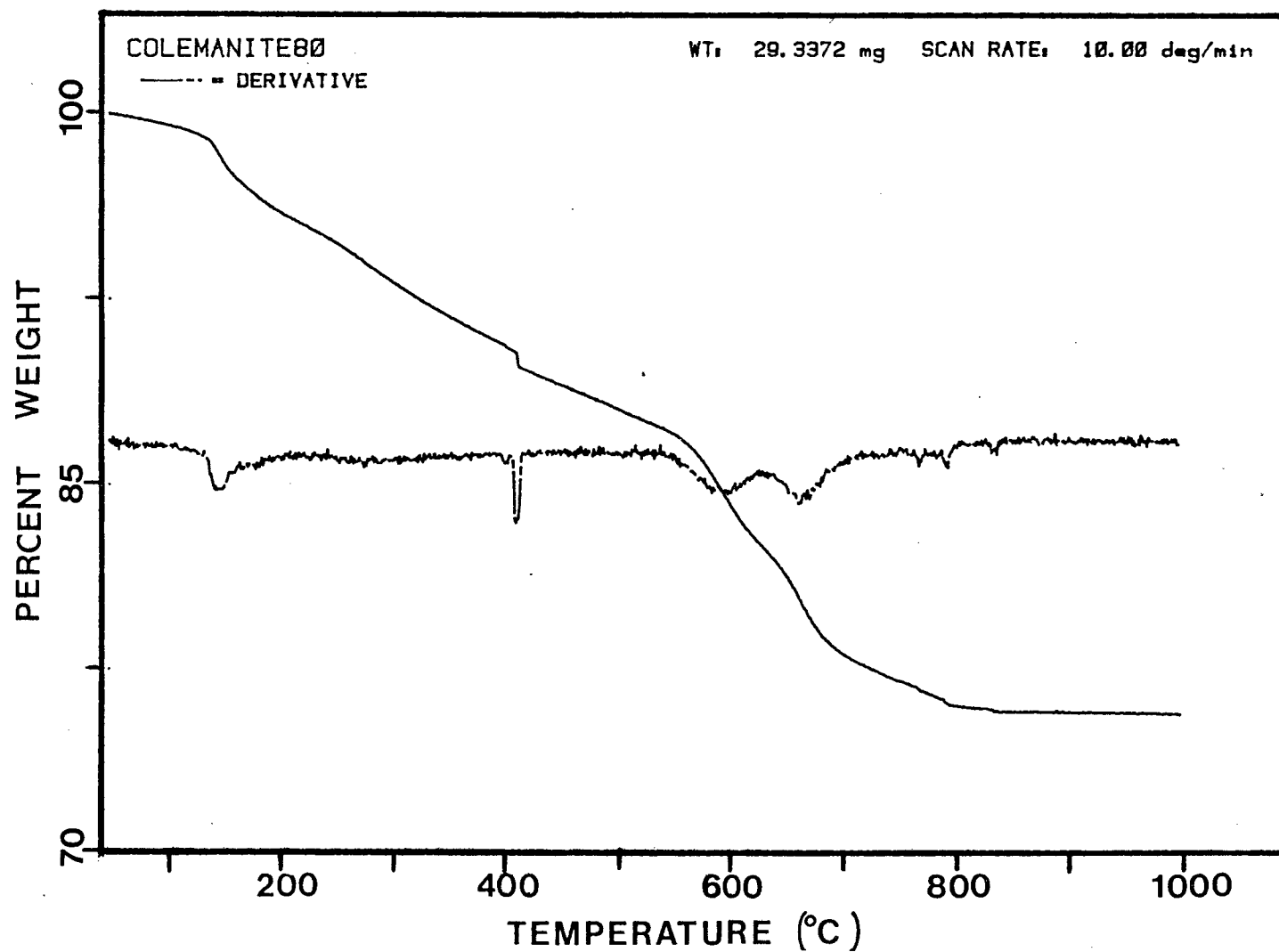
Figure 29: Thermogravimetric data for 80 percent colemanite.

the end of one reaction which is followed by another. These two reactions could be series reactions if the rate of the second reaction is very small below 700°C. When the Figures 27 to 29 are examined it is seen that the curves level off above about 700°C as the percentages of colemanite increases. This indicates that the second phenomena (or reaction) doesn't occur above certain concentrations of colemanite. In order to be able to determine the stoichiometric amount of colemanite necessary for the complete conversion of sodium carbonate it was necessary to know the boron content and the amount of impurity in the colemanite. Boron analyses were performed as described in Appendix I. It was found that the colemanite used in these experiments contains 38 percent B_2O_3 (26). Since pure colemanite contains 50.83 percent B_2O_3, it was not pure, but contained 25.24% impurities. By utilizing the phase diagram shown in Figure 10 it was calculated that the stoichiometric amount of colemanite for the reaction is 63.3% (see Appendix II for calculation).

The results from thermal calorimetric experiments on this reaction done by others (10) also showed the peaks due to the thermal events noted in the thermogravimetric curves at the same temperatures.

The following explanation of the curves can then be made from the results of the boron analyses. For the low colemanite percentages the reaction continues above 700°C because there is not enough B_2O_3 to react with all the Na_2CO_3 available. The unreacted part of the Na_2CO_3 then decomposes by itself at higher temperatures. In the case of colemanite concentrations higher than the stoichiometric amount necessary, the second reaction doesn't occur because there is no

sodium carbonate left unreacted. There is a good match between the colemanite percentage for which the curves level off and the calculated stoichiometric amount, which is 63.3 percent, when the errors which are associated with the boron analyses are considered.

In Figure 30 the output of a run in which 100 percent colemanite was used is shown. The colemanite is not stable over the studied temperature range and loses a considerable amount of weight during heating. The weight loss which is seen around 190°C can be explained as water of dehydration. It was difficult to determine what caused the loss around 410°C. The run with the pure B_2O_3 showed that B_2O_3 loses weight between 150°C and 400°C (Fig. 31). It was thought that this loss around 410°C might be due to the loss coming from free B_2O_3 in the colemanite. There is also a weight loss between 650-750°C. The same phenomena is also seen in the output of 100 percent calcium borate (Fig. 32). This indicates that the loss at this temperature is not coming from the impurities in the colemanite since it is seen in the pure calcium borate case too. Fig. 33 shows the comparison of the curves for these three compounds.

Since colemanite loses weight during heating the thermogravimetric data was recalculated by subtracting a proportion of the colemanite curve from the curves of other runs as described in section 4.2.5. The final form of the data are presented in the Figures 34 through 38 for 20, 30, 40, 50 and 60 percent colemanite concentrations respectively.
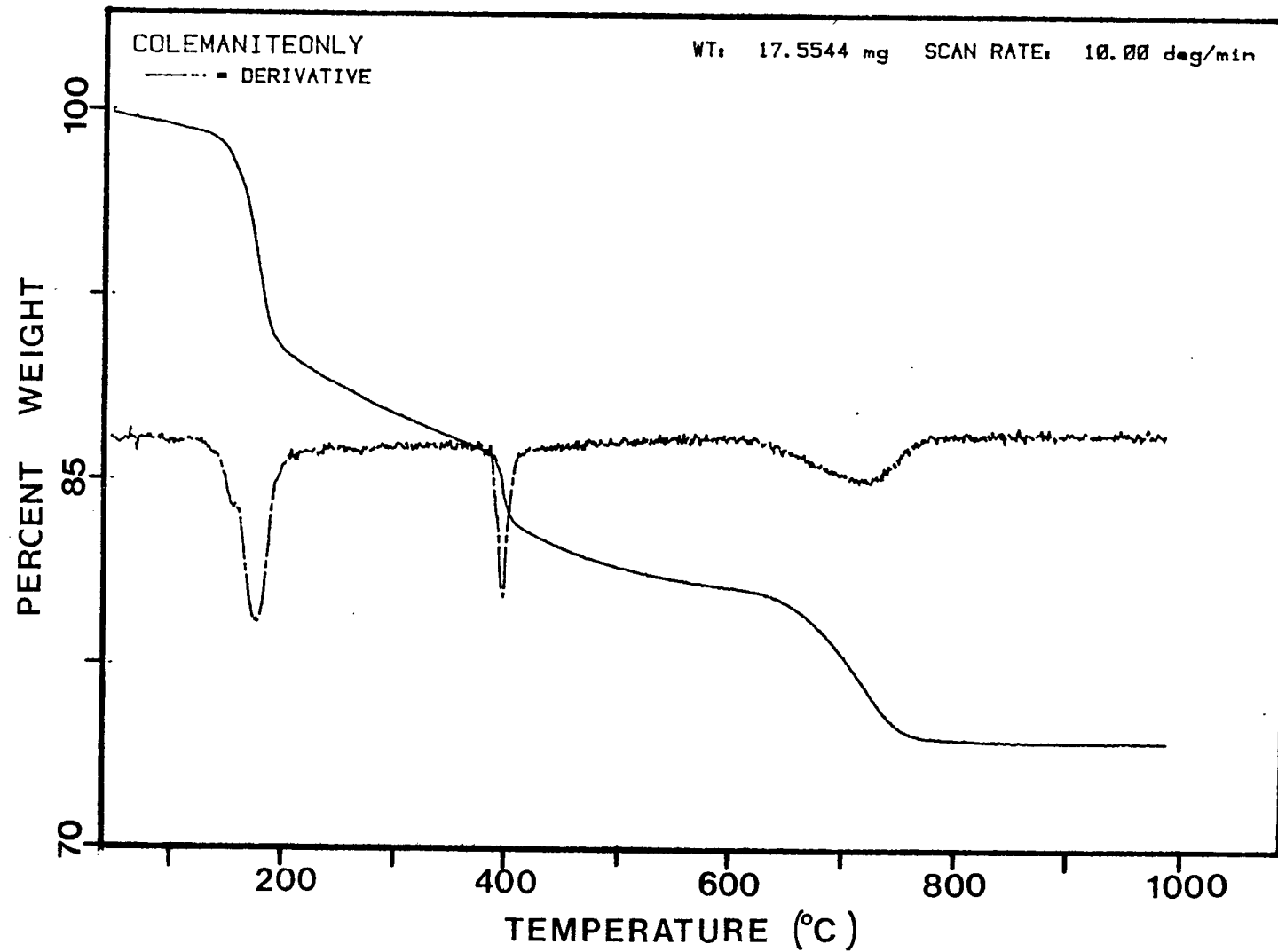
Figure 30: Thermogravimetric data for 100 percent colemanite.
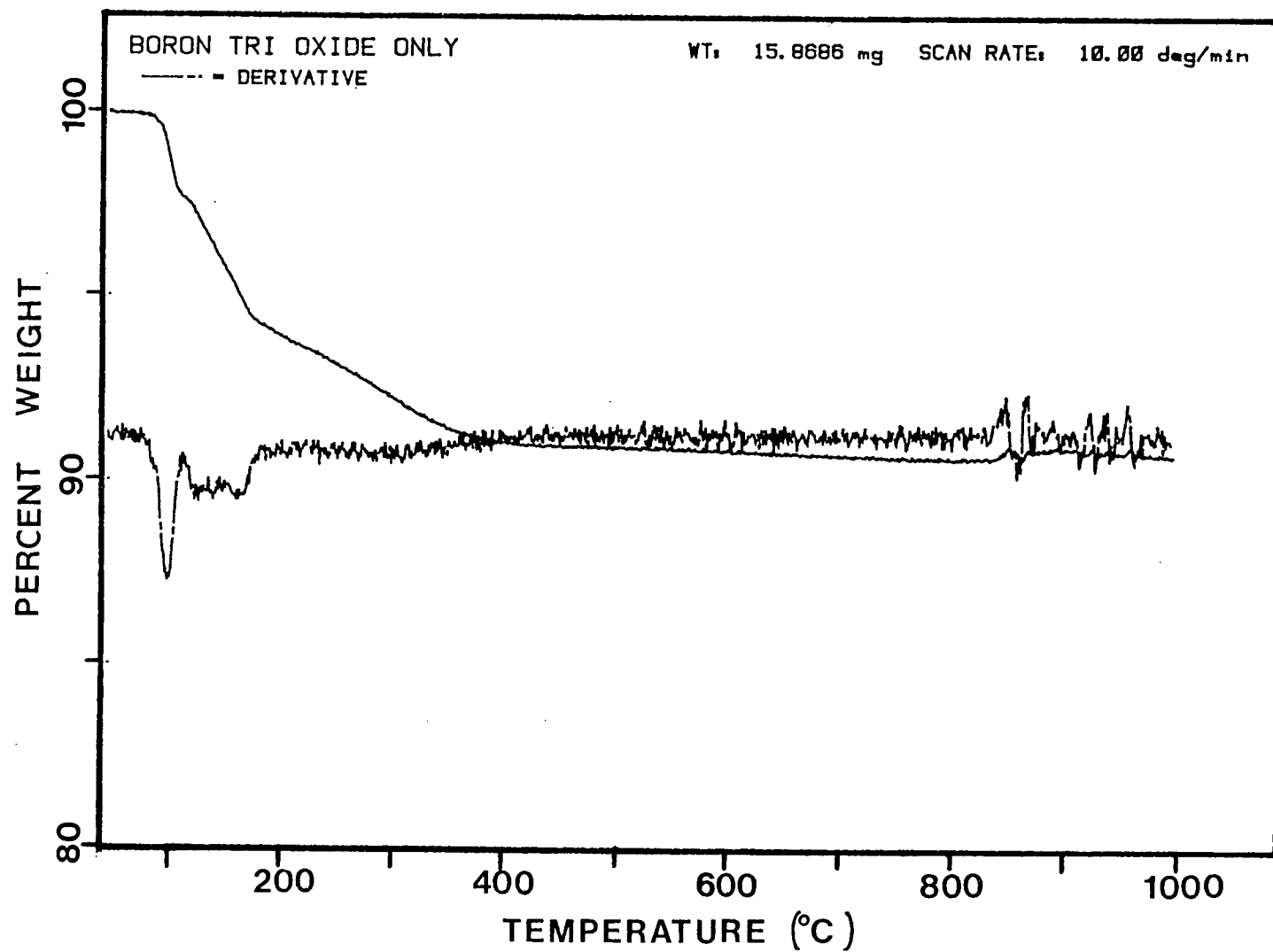
Figure 31: TG results for 100 percent boron trioxide.
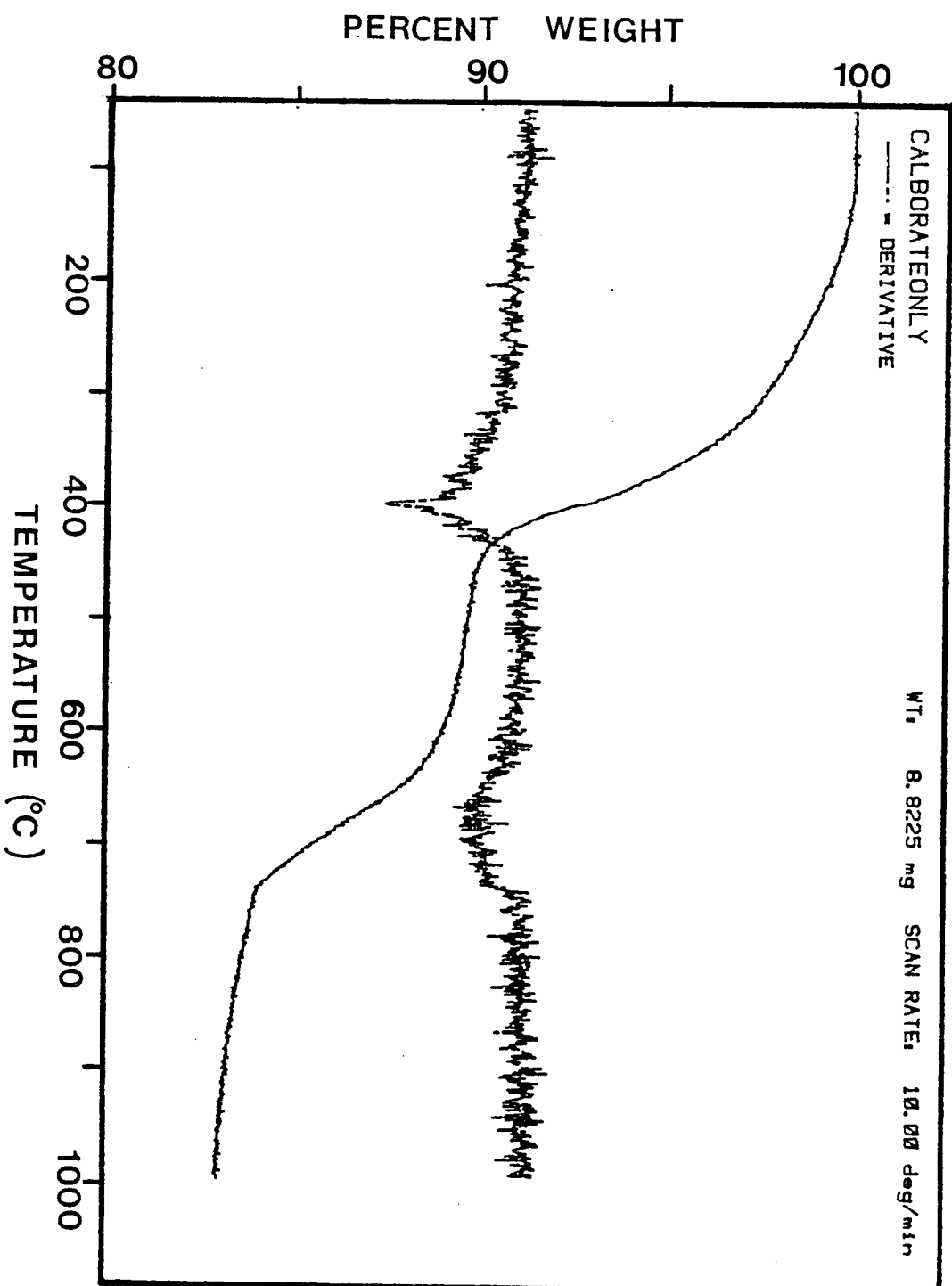
Figure 32: TG results for 100 percent calcium borate.
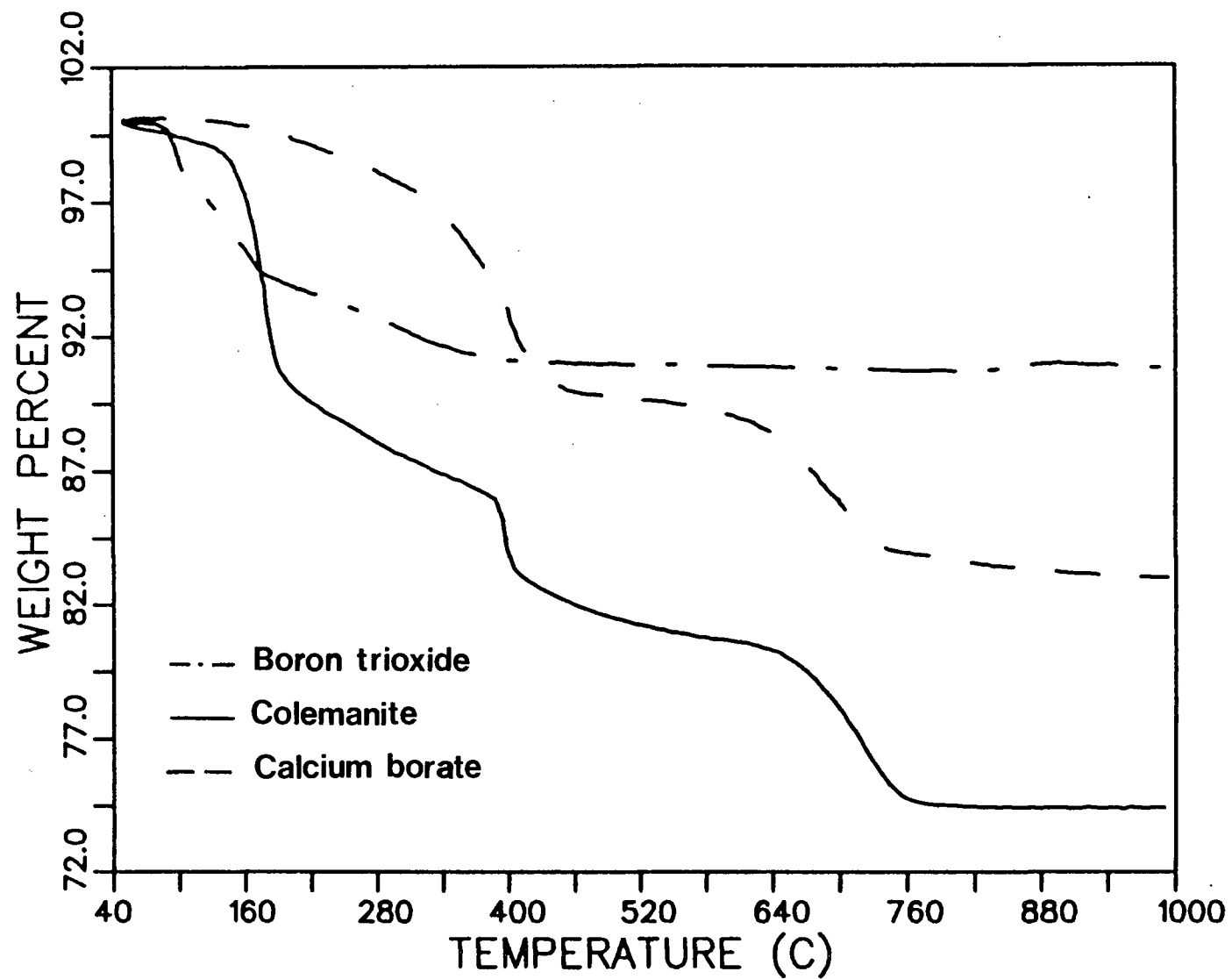
Figure 33: Comparison of TG results for colemanite, boron trioxide and calcium borate.
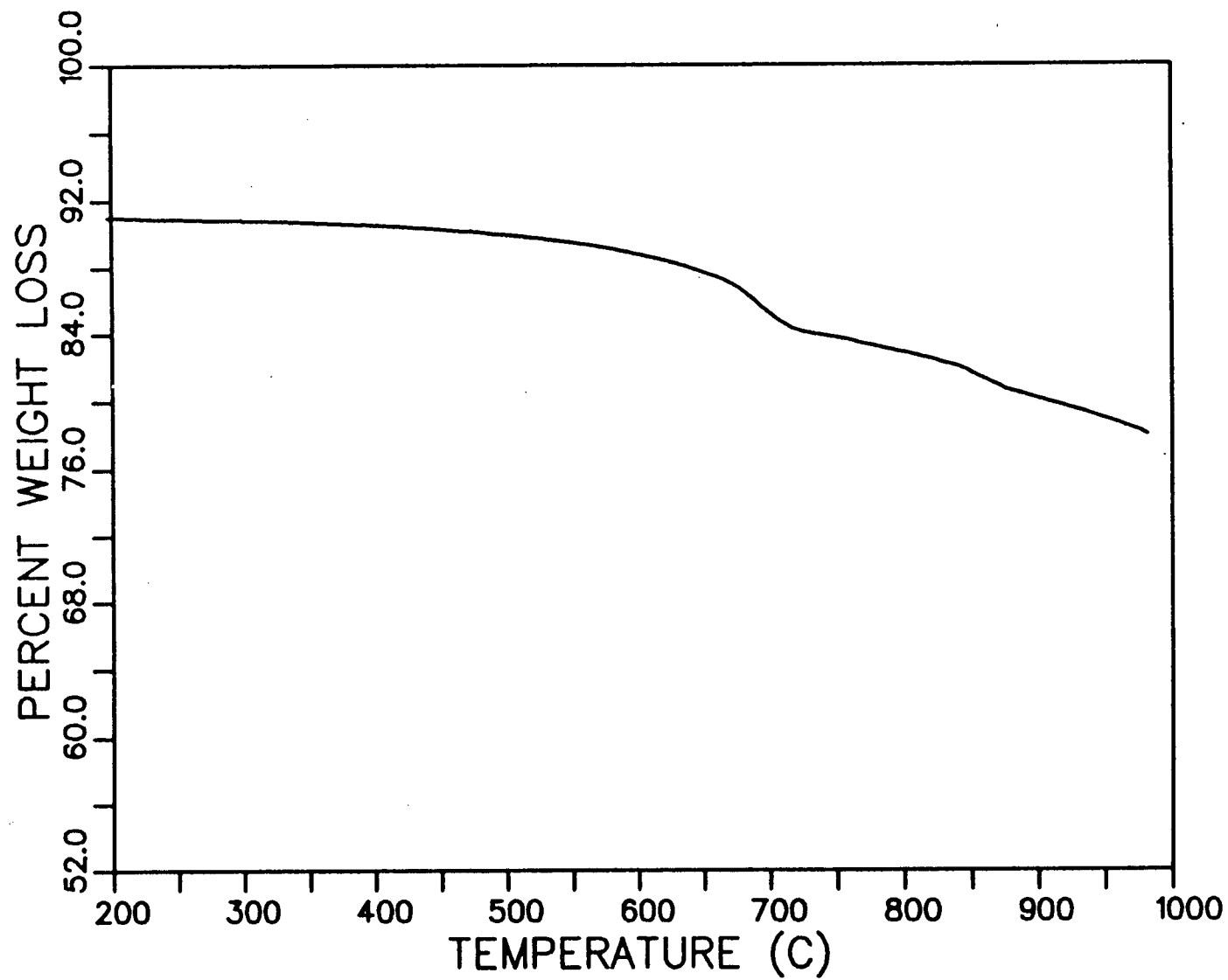
Figure 34: Recalculated Data for 20 Percent Colemanite.
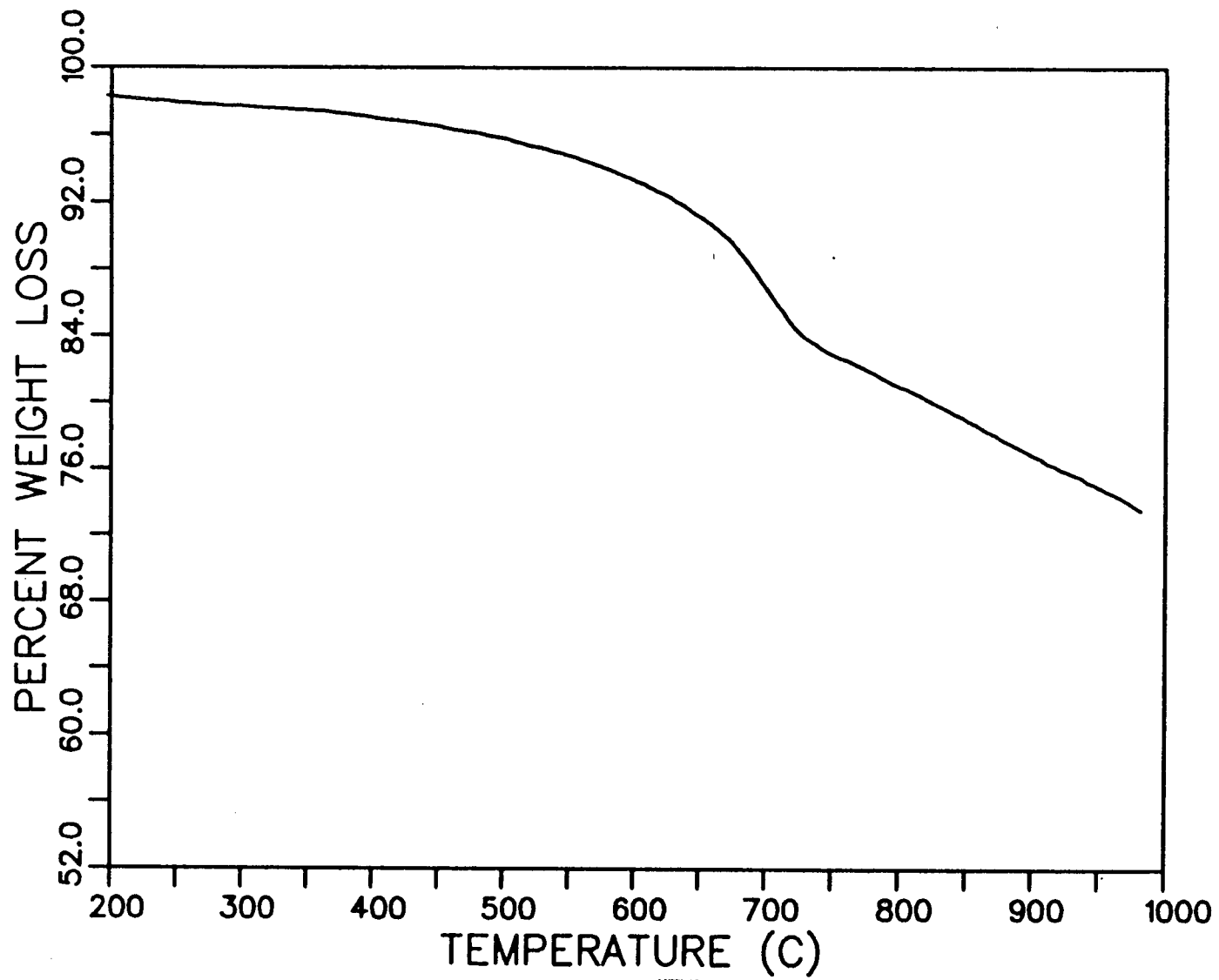
Figure 35:   Recalculated Data for 30 Percent Colemanite.
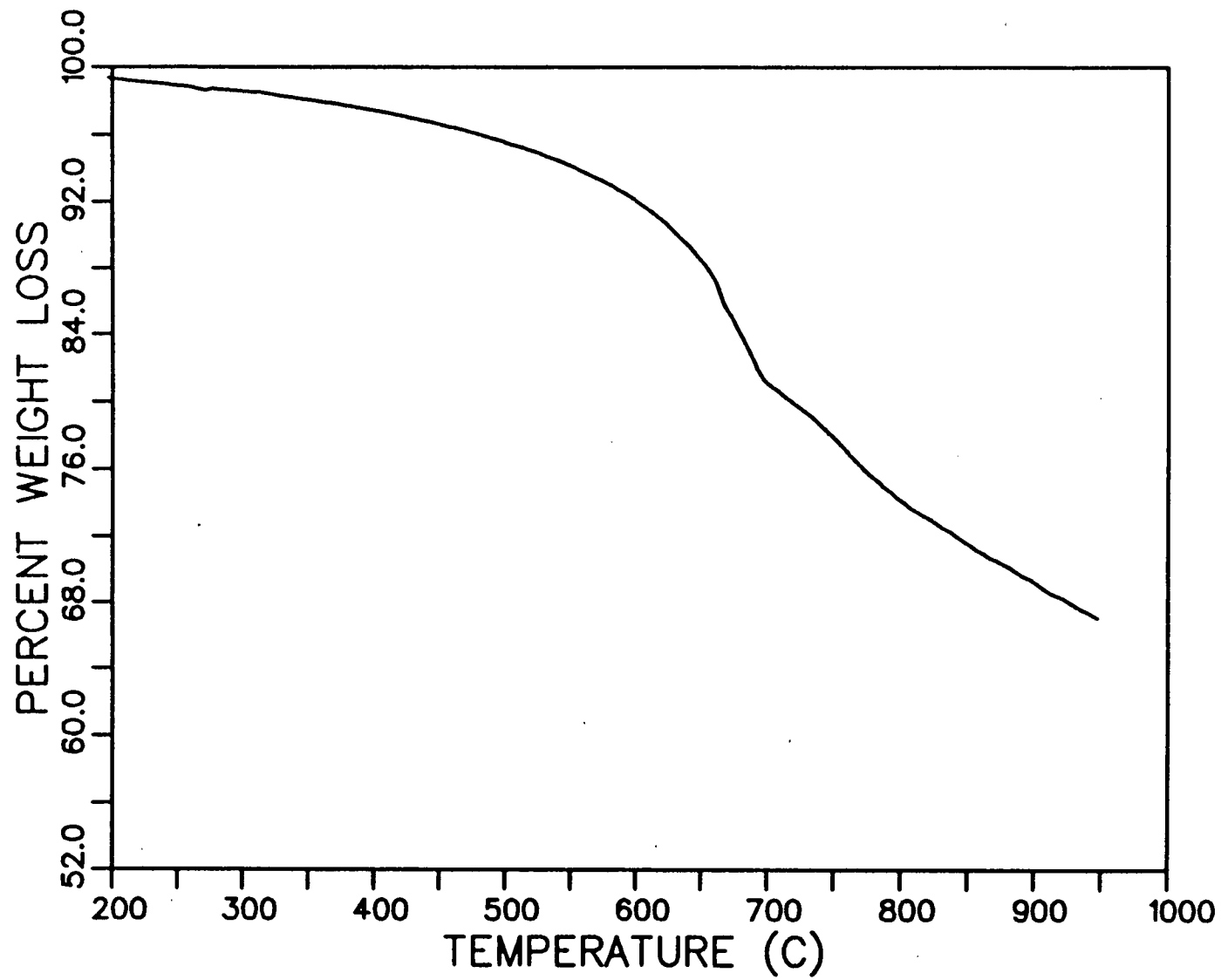
Figure 36: Recalculated Data for 40 Percent Colemanite.
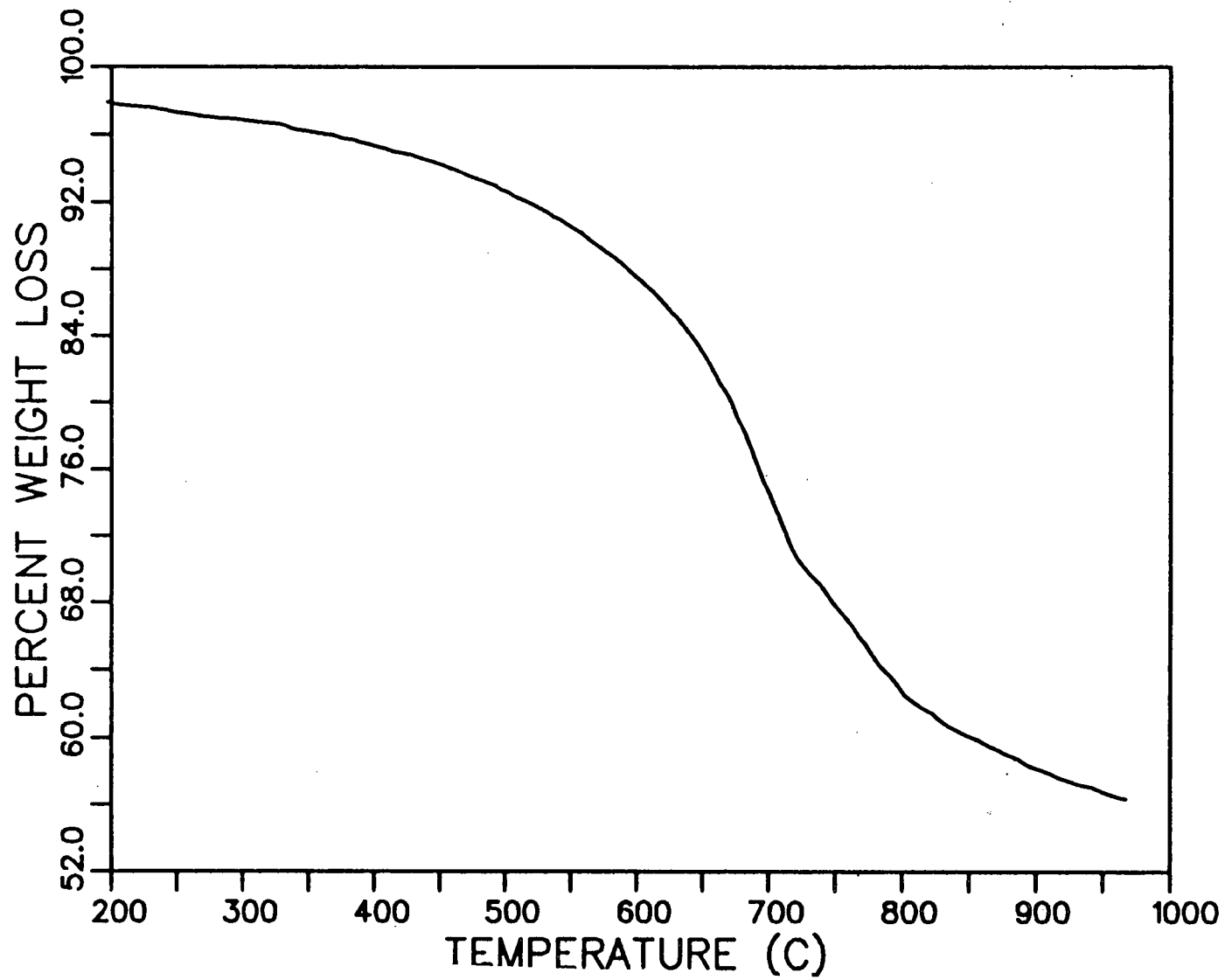
Figure 37: Recalculated Data for 50 Percent Colemanite.
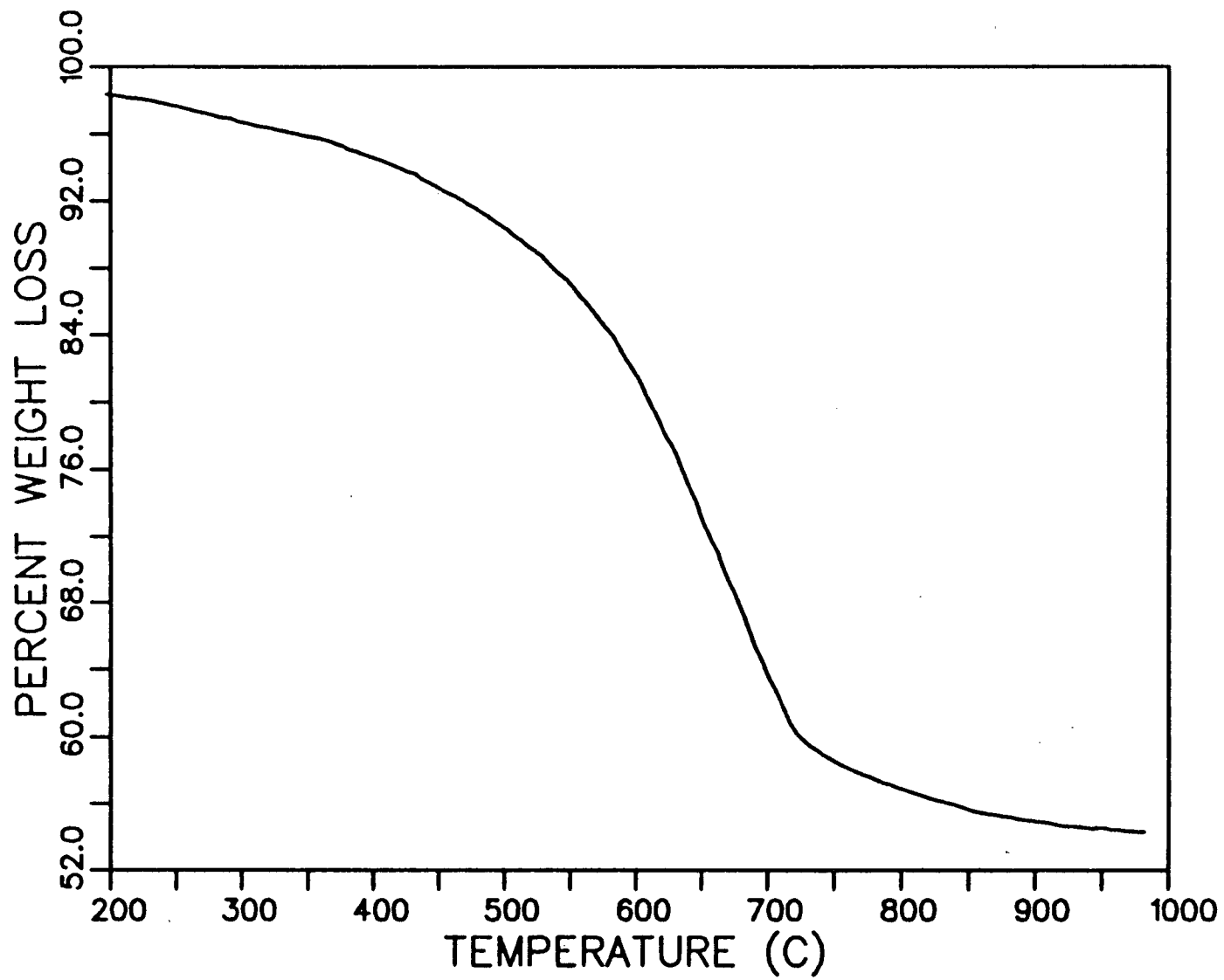
Figure 38: Recalculated Data for 60 Percent Colemanite.

6.2.1 Model of first reaction.

These corrected data were digitized and analyzed to determine a
kinetic model which includes the reaction order, activation energy and
rate constant of the reaction. The expressions for the fractional
conversions of the sodium carbonate and colemanite are also shown in
section 3.2.1 and 3.2.2 respectively. In the derivation of these
equations the following assumptions were made.

- All the weight loss comes from the expulsion of carbon dioxide
so the losses due to sodium or sodium oxide at elevated temperatures
are assumed negligible.

- The effect of the second reaction is very small in the
temperature range of 190-700°C so only one reaction is occurring over
this temperature range.

- The Arrhenius relationship was assumed for the temperature
dependence of the rate constant.

The error which will be produced by the first assumption should
be quite small because sodium will most likely not volatilize below
900°C. It was also reported that the presence of boron decreases the
sodium losses at high temperatures (10). The errors caused by the
second assumption will be discussed after the results of the modelling
have been shown.

The starting point for the first reaction was taken as 192°C.
The temperature at which the first reaction stops and the second
reaction starts was calculated as the point where the boron content of
the colemanite is all consumed so that there is no boron to react
further. The temperatures which were predicted by the computer program

as such were only ∓ 20°C different from the temperatures at which the

break point on the derivative curves occurred for all colemanite

concentrations (see Figure 23 to 29). As is seen from these figures

the temperature at which the derivative curve shows a break doesn't

change with the colemanite concentration.

The iterative procedure for the evaluation of the kinetic

constants was described in section 5.1. Table 16 shows the standard

deviation of B values for different kinds of mechanisms for 60%

colemanite, where m and n are the orders of the reactions and E_1 is the

activation energy.

The standard deviations for the other colemanite percentages are

given in Appendix IV. As can be seen from this table and the standard

deviation results shown in Appendix IV, the minimum of these standard

deviations cannot be chosen easily. Since those values are all very

close to each other and are all reasonably small, choosing the minimum

among them is not necessarily correct. The reason for such results can

be clearly seen from Figure 39. Figure 40 shows that the shape of the

curves for log g(α) (concave up) and $-$log p(x) (concave down) are quite

different from each other as well.

Another approach for choosing the best model is to recheck the

results found from the application of this method by comparing the

fractional conversions found experimentally with the ones predicted by

each proposed model. Figure 41 shows the comparison of the best

fitting models to experimental data for 60 percent colemanite. From

this figure it is seen that the model which best fits the data is zero

Table 16: Standard deviation of B values for 60 percent colemanite.

Proposed Mechanism		Activation Energy (kcal/mol)	Standard deviation δ_{min}
m = 0	m = 0	7.15	0.21028
m = 0	n = 1/3	7.45	0.20946
m = 0	n = 1	8.25	0.21979
m = 1/3	n = 0	7.40	0.20930
m = 1/2	n = 0	7.6	0.20937
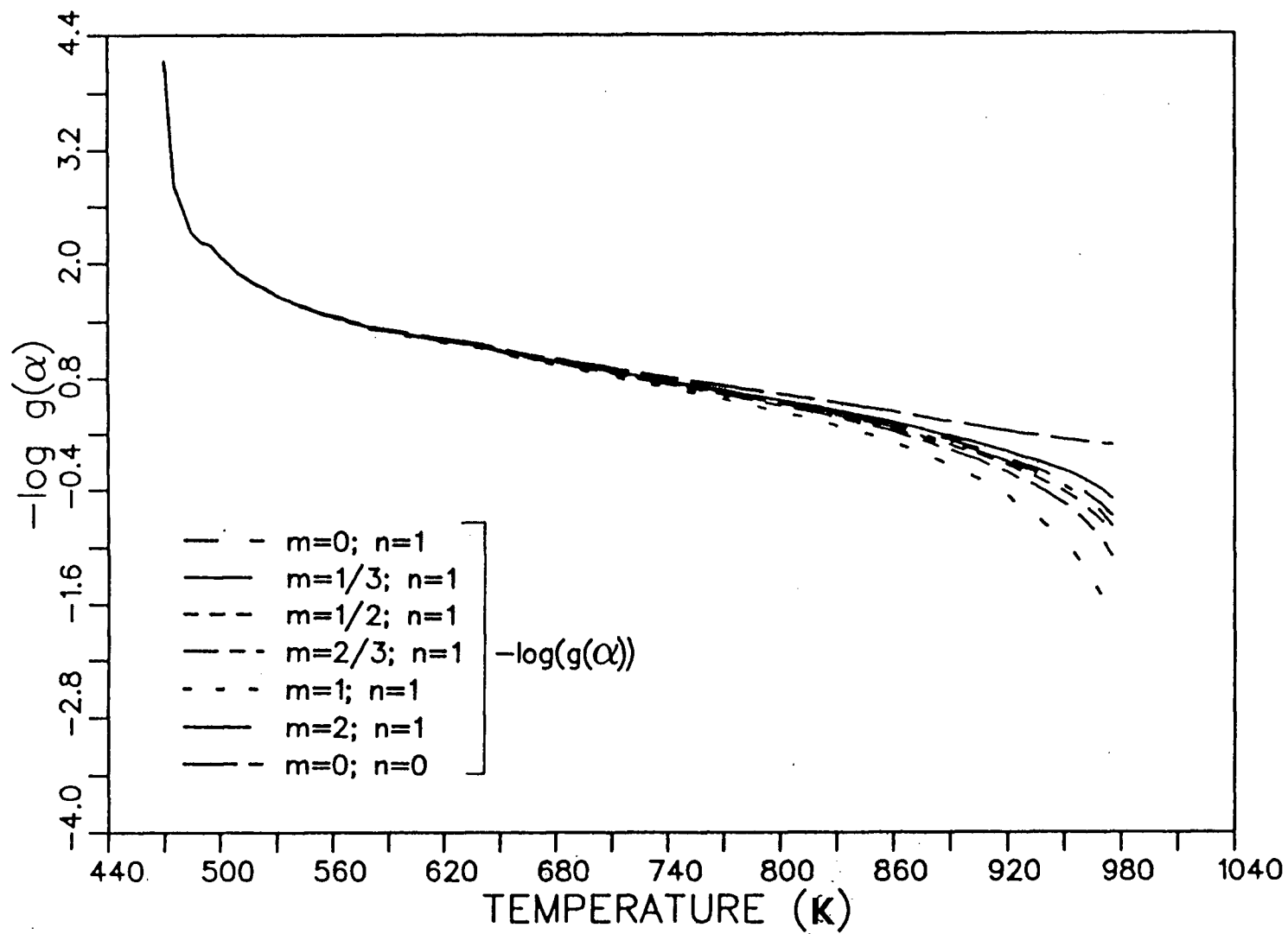
Figure 39: Plot of log g(α) values for 60 percent colemanite.
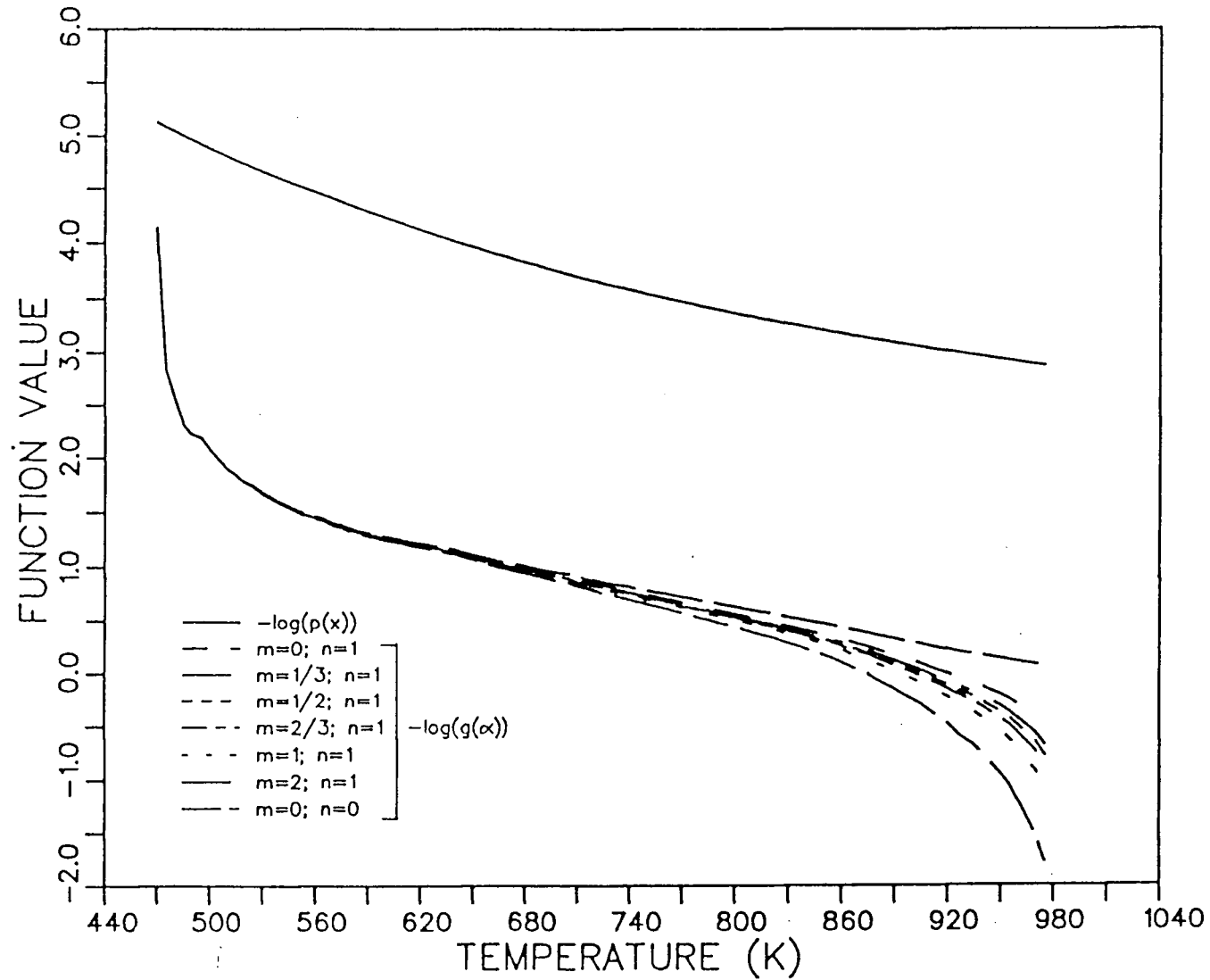
Figure 40:   Comparison of log g(α) values with log p(x) values.
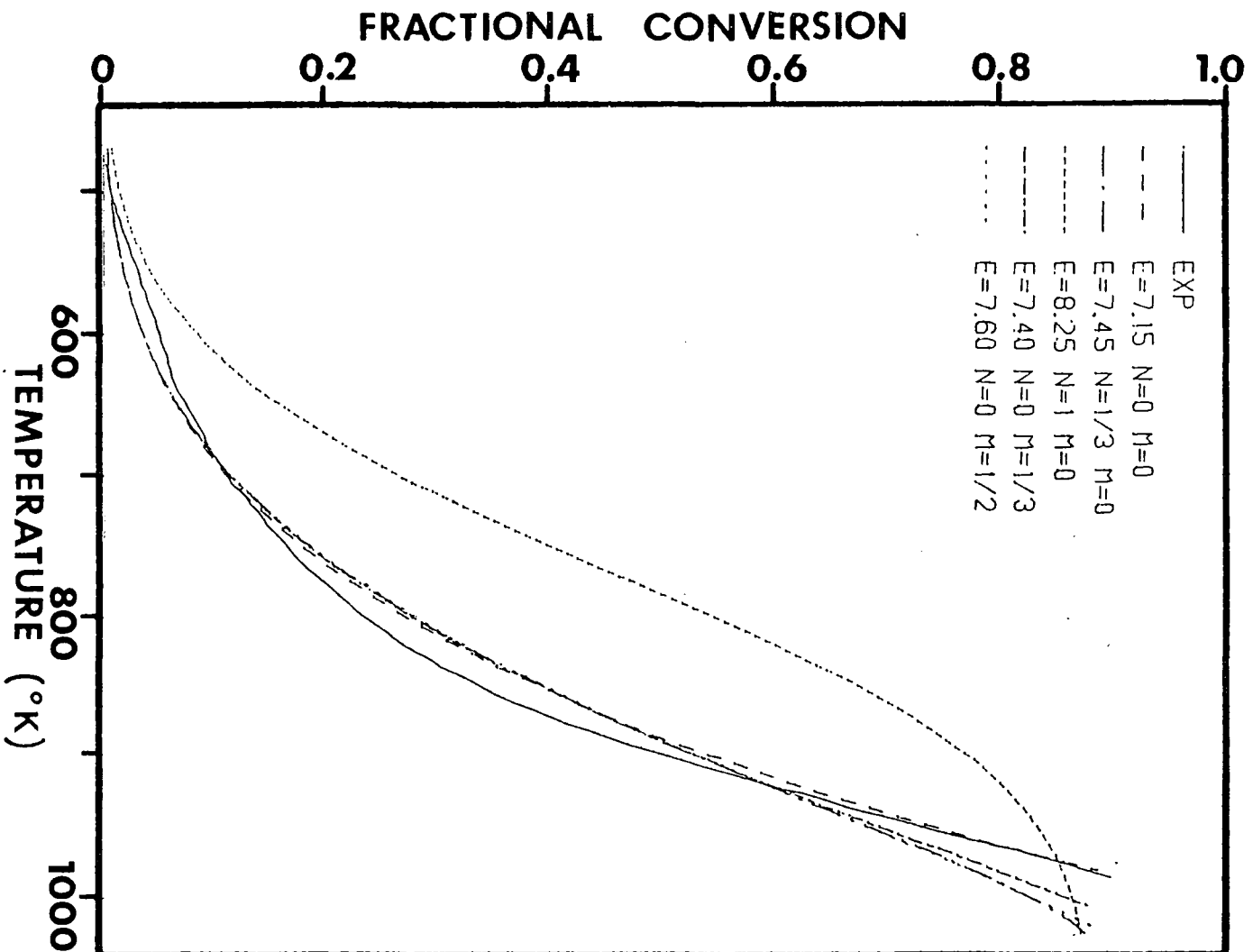
Figure 41: Best fitting models to experimental data for 60 percent colemanite.

order in both sodium carbonate and colemanite concentrations. That is, the rate is solely a function of the reaction temperature. In order to decide on the activation energy of the reaction, standard deviations were found at each colemanite concentration for the E_1 values using the above model. It was noticed that the values of activation energy which gave the minimum standard deviation for the mechanism of $m = 0$ $n = 0$ were different for each case. That is, it was a function of colemanite concentration. The following table shows the activation energies found for each colemanite percentages. The comparison of the model predictions with the experimental results are plotted in Figures 42, 43, 44, and 45 for each case using the activation energies calculated for each. A reasonably good fit was found especially up to 900°K. At higher temperatures the model predicts lower conversions than those found experimentally. This could be due to a contribution from the second reaction when the temperature becomes high enough for the direct decomposition of sodium carbonate and both reactions take place simultaneously. Since the effect of the second reaction was assumed to be negligible in the derivation of the model this high temperature deviation from the model is not unexpected. This explanation is substantiated by the results shown in Figure 45 which shows a perfect fit even at high temperatures for 60 percent colemanite. Since 60 percent is approximately the stoichiometric colemanite concentration necessary for the complete conversion of sodium carbonate, the second reaction doesn't occur. So in this case the second assumption prevails.

Table 17: Activation energies which give best fits to
experimental data.

% Colemanite	Activation Energy (kcal/mol)	Standard deviation ∂_{min}
30	5.5	0.18198
40	6.0	0.19007
50	6.4	0.19007
60	7.15	0.21028
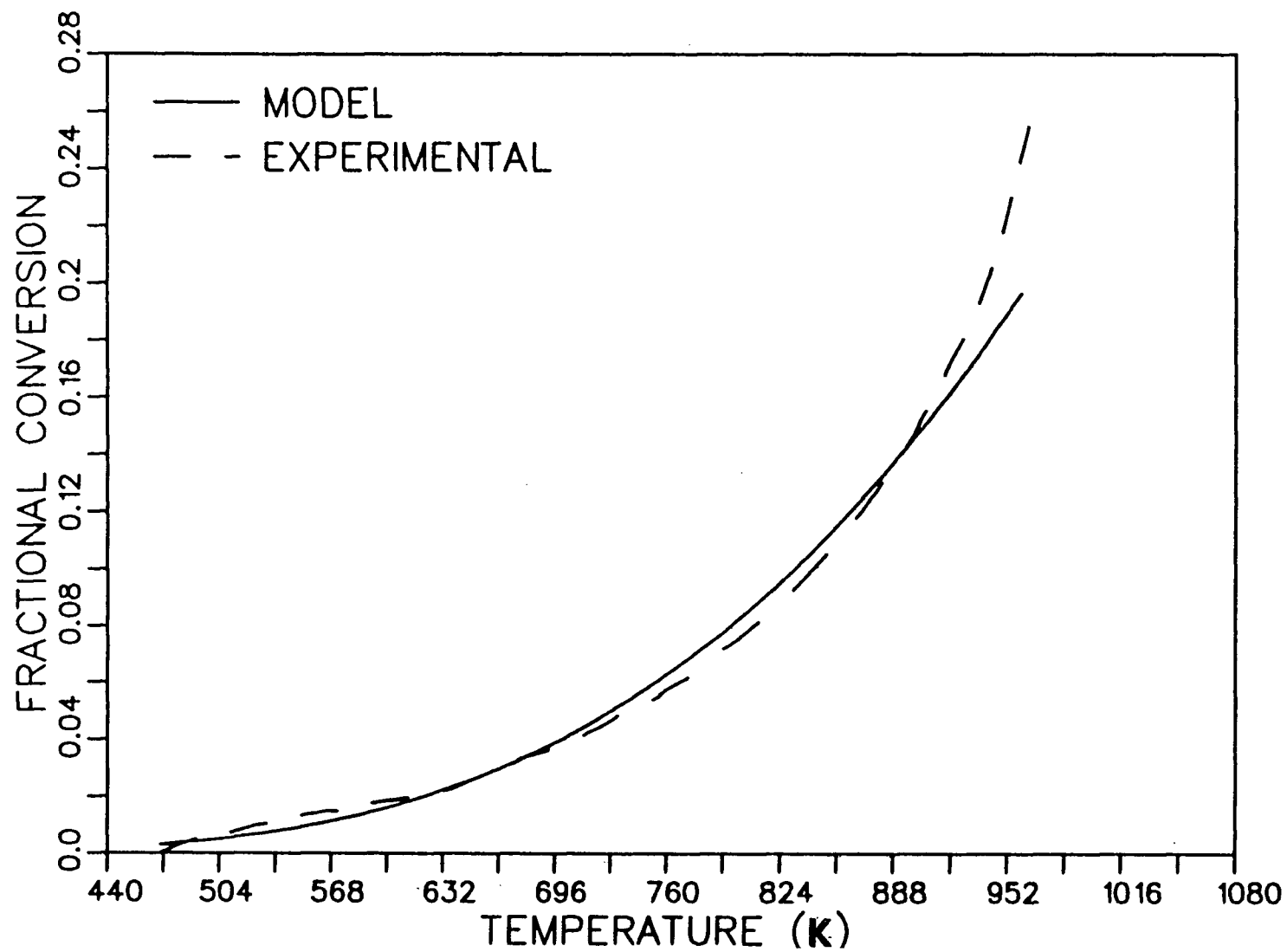
Figure 42: Comparison of the Model Predictions with the
Experimental Results for 30 Percent Colemanite.
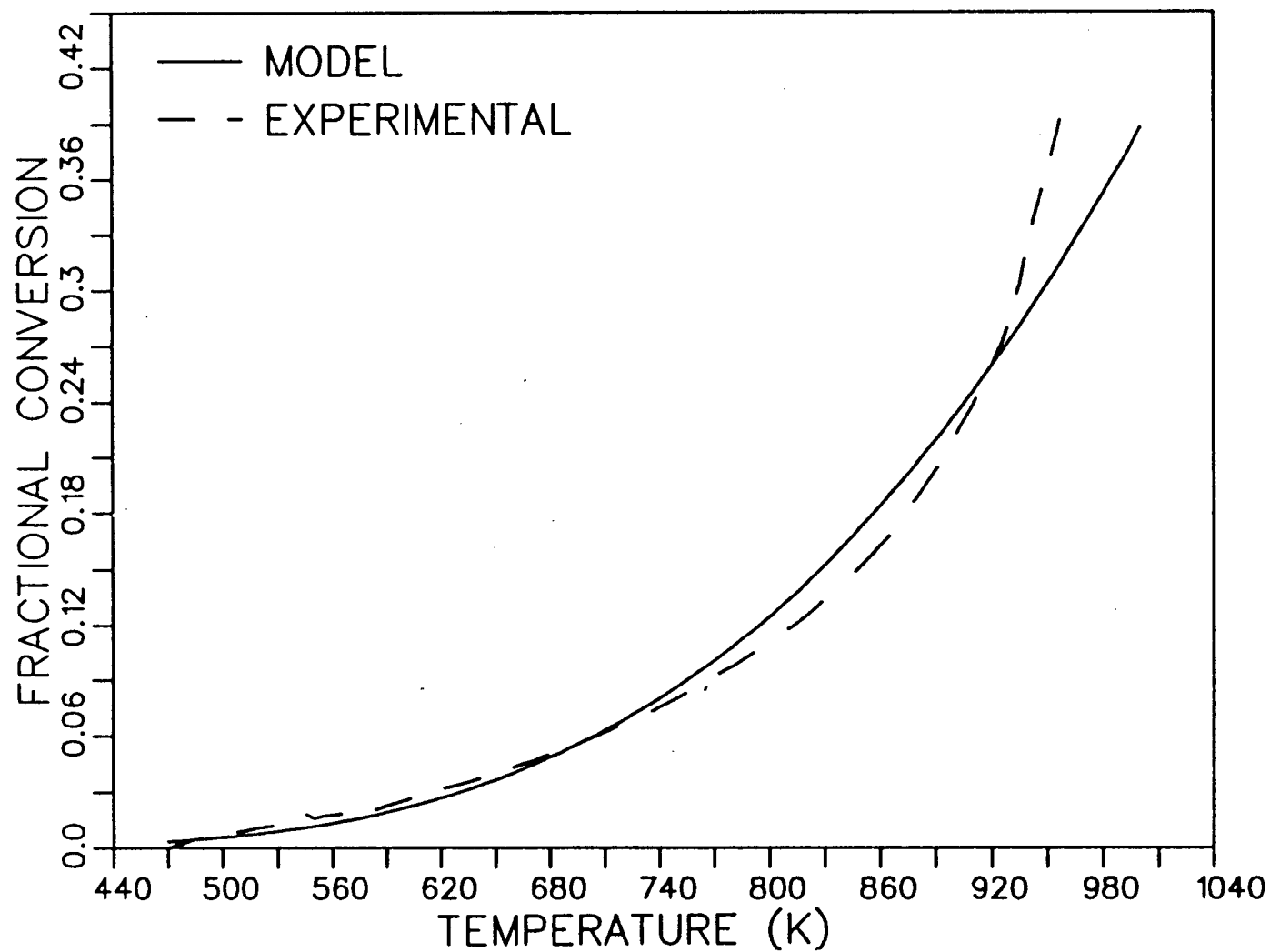
Figure 43:   Comparison of the Model Predictions with the
             Experimental Results for 40 Percent Colemanite.

Figure 44:   Comparison of the Model Predictions with the
            Experimental Results for 50 Percent Colemanite.

Figure 45: Comparison of the Model Predictions with the Experimental Results for 60 Percent Colemanite.

The values of frequency factor, Z_1, were calculated by using the equation 2.24 and using the E_1 values found for each case for the values of m and n equal to zero. Equation 3.13 takes the following form for this specific mechanism

$$g(\alpha) = \frac{ZE}{Rq} \, W_{s_o}^{-1} \, p(x) \qquad (6.1)$$

This can also be written in the logarithm form as

$$\log g(\alpha) - \log p(x) = \log \left(\frac{ZE}{Rq} W_{s_o}^{-1}\right) = B \qquad (6.2)$$

Sample calculations of Z_1 and k_1 values are shown in Appendix II. Table 18 shows the parameters calculated for the model at 900°C. As can be seen from this table the rate constant of the reaction is a function of colemanite concentration as a result of both activation energy and frequency factor being functions of the colemanite concentration. These results were in conflict with the model which determines the rate as zero order on both reactant concentrations. Colemanite concentration indirectly affects the rate constant k_1 which is expected to be constant at constant temperature. This could indicate a very complex rate equation for this reaction. The effect of the colemanite concentration on the activation energy, E_1, and frequency factor, Z_1, is shown in Figures 46 and 47 respectively. In both of these figures it is seen that there is a systematic change in these kinetic constants with the change in colemanite percentage. This shows that this change doesn't come from the experimental errors and it

Table 18: Kinetic constants for the first reaction.*

Percent Colemanite	Activation energy (E_1) cal/mol	Frequency factor (Z_1) g/min	Rate constant (k_1) g/min
30	5500	16.802	1.587
40	6000	37.180	2.833
50	6400	69.003	4.430
60	7150	180.172	8.383

* Rate constants are calculated at 900°C.
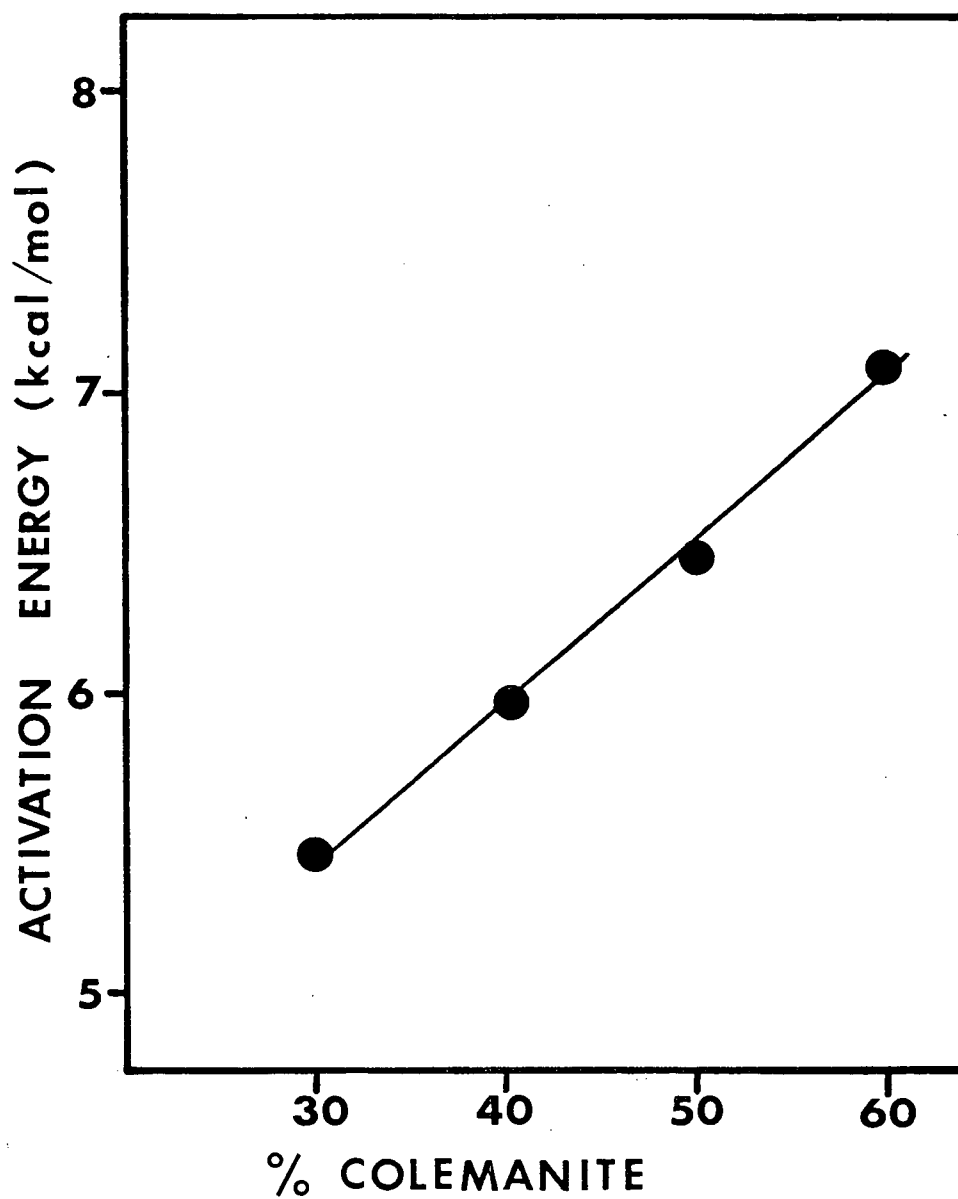
Figure 46: Effect of colemanite concentration on the activation energy, E_1.
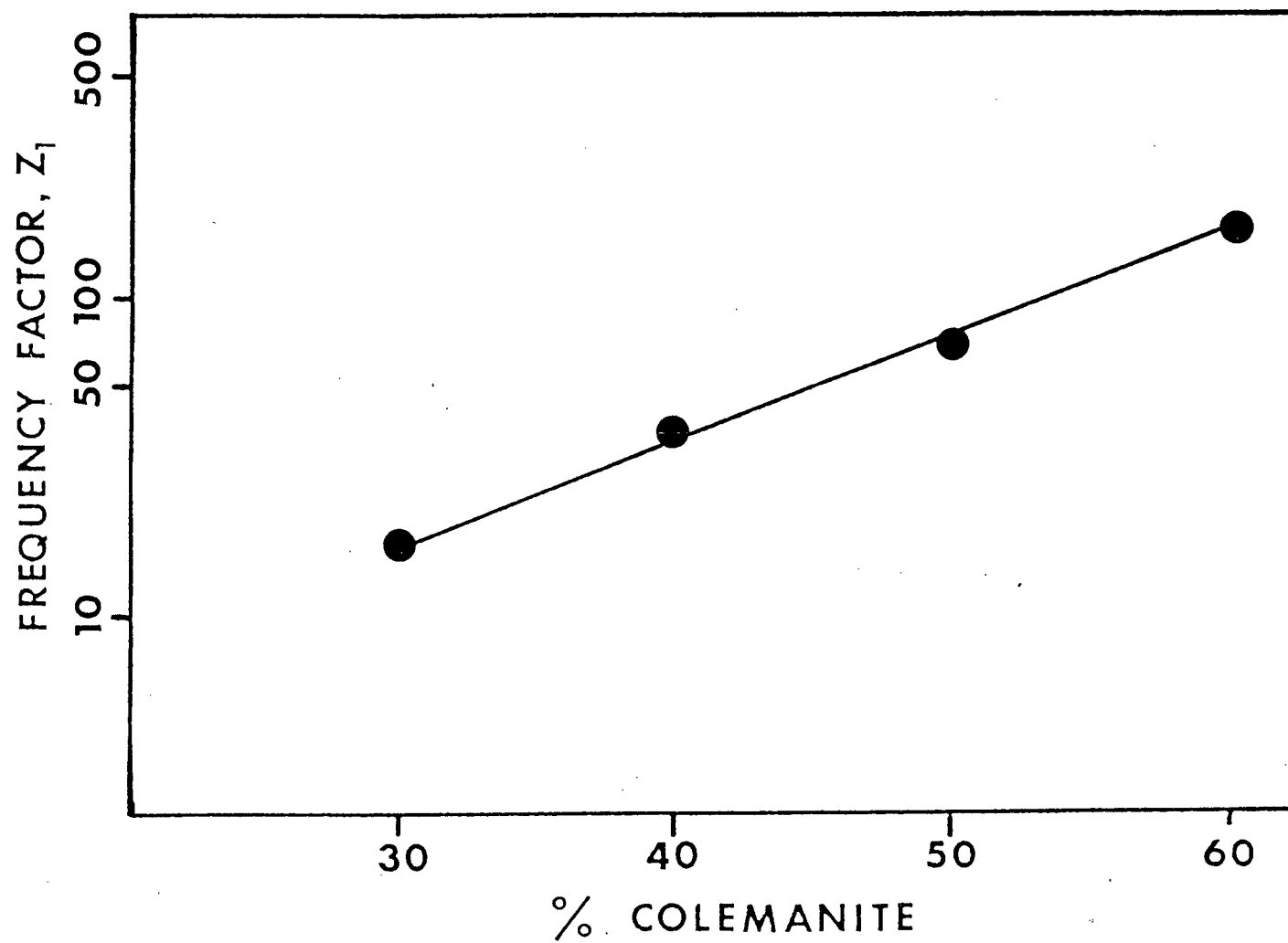
Figure 47: Effect of colemanite concentration on the
frequency factor, Z_1.

is specific for this reaction system. At this point it is evident that further studies must be made of this reaction by modifying the model to take into consideration the effect of the colemanite concentration on the kinetic constants.

In order to be able to express the activation energy and frequency factor in terms of the colemanite concentration, the points on Figures 46 and 47 were fitted to an equation by using the OLSF subroutine from the U.B.C. computing centre library. As a result it was found that the activation energy changes with colemanite percentage linearly according to the following equation

$$E_1 = 3.75 + 0.055 \, Y_c \qquad\qquad (6.3)$$

The change in the frequency factor, Z_1, was found to be exponential and expressed as

$$Z_1 = 1.384 \, e^{0.08 Y_c} \qquad\qquad (6.4)$$

So the equation of the rate constant for the first reaction can be written as in the following form.

$$k_1 = 1.384 \, e^{0.08 Y_c} \exp \left(- \frac{3.75 + 0.05 \, Y_c}{RT} \right) \qquad\qquad (6.5)$$

The kinetic constants which are recalculated by using these equations are tabulated in Table 19.

Table 19: Kinetic constant for the first reaction calculated
by using equation 6.3, 6.4 and 6.5.

Percent Colemanite	Activation energy (E_1) cal/mol	Frequency factor (Z_1) g/min	Rate constant (k_1) g/min
30	5400	15.400	1.520
40	5950	35.620	2.773
50	6500	75.010	4.613
60	7050	174.024	8.452

Figures 48 to 51 show the results after the modification of the
model according to the new values of activation energy and frequency
factor, calculated from equation 6.3 and 6.4. These figures show
similar fit to the ones found by using the activation energy values
which are found for each case specifically.

6.2.2 Model of Second Reaction.

The thermogravimetric data was also analyzed in the temperature
range of ~ 700-1000°C where the second reaction takes place. As was
mentioned before this reaction could be the decomposition of sodium
carbonate either by itself or in the presence of the impurities in
colemanite. The impurities in colemanite consist of alumina, iron
oxide and silica which are also believed to have an autocausticizing
effect on the reaction. So these substances might further react with
the unreacted part of the sodium carbonate. The method of analysis of
this reaction was similar to that used for the analysis of the first
reaction and described in section 5.2. The losses due to the
volatilization of sodium at high temperatures were assumed negligible.

The minimum, δ_{min}, of the standard deviations was searched for
at 0.1 Kcal increments of E_a for each mechanism as was done for the
analysis of the first reaction. The starting temperature of this
reaction is taken as the temperature where the first reaction stops.
It was found that the reaction is first order with respect to the
sodium carbonate concentration even though some of the other mechanisms
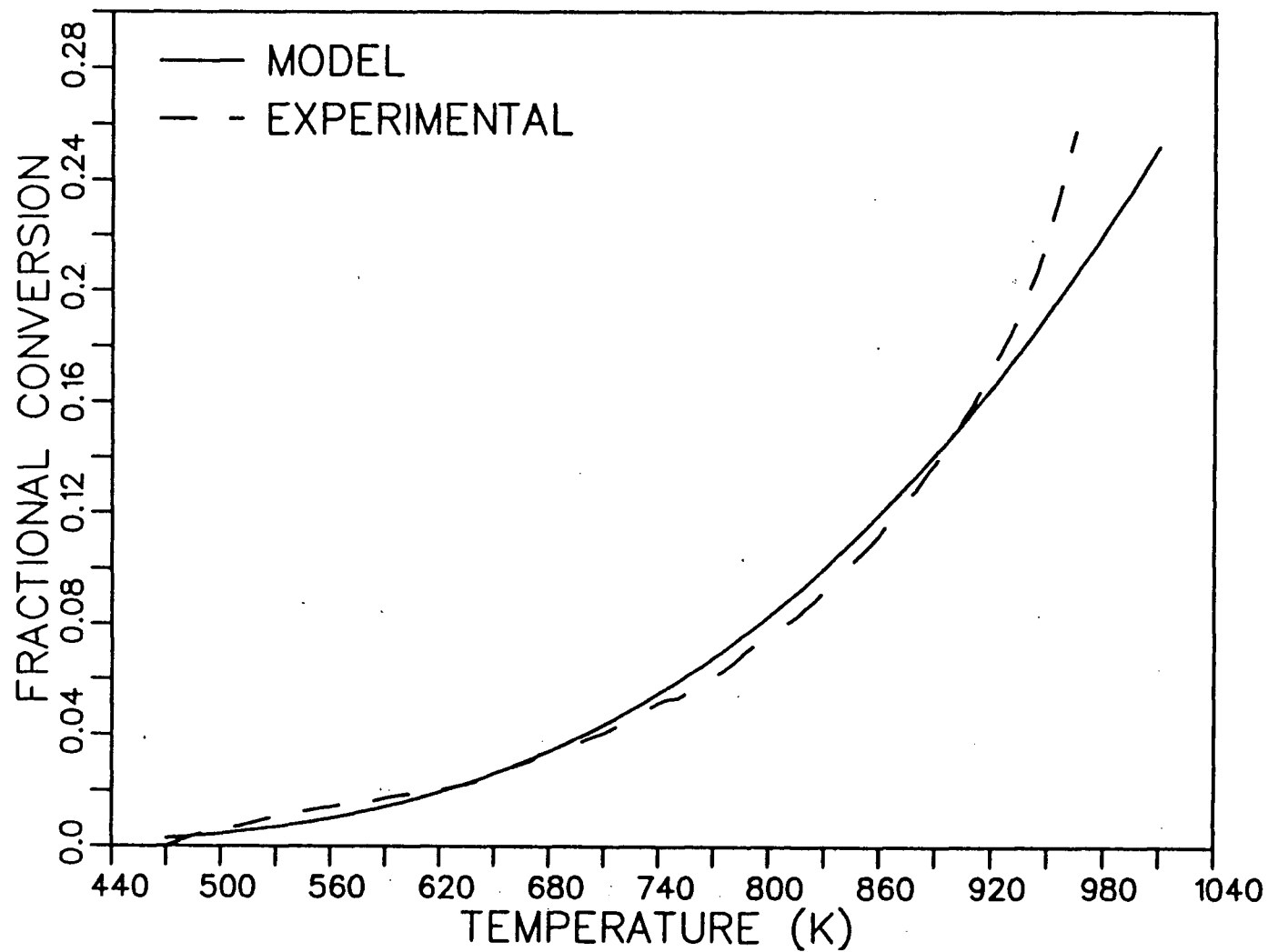
Figure 48: Comparison of the Results after the Modification of the Model for 30 Percent Colemanite.
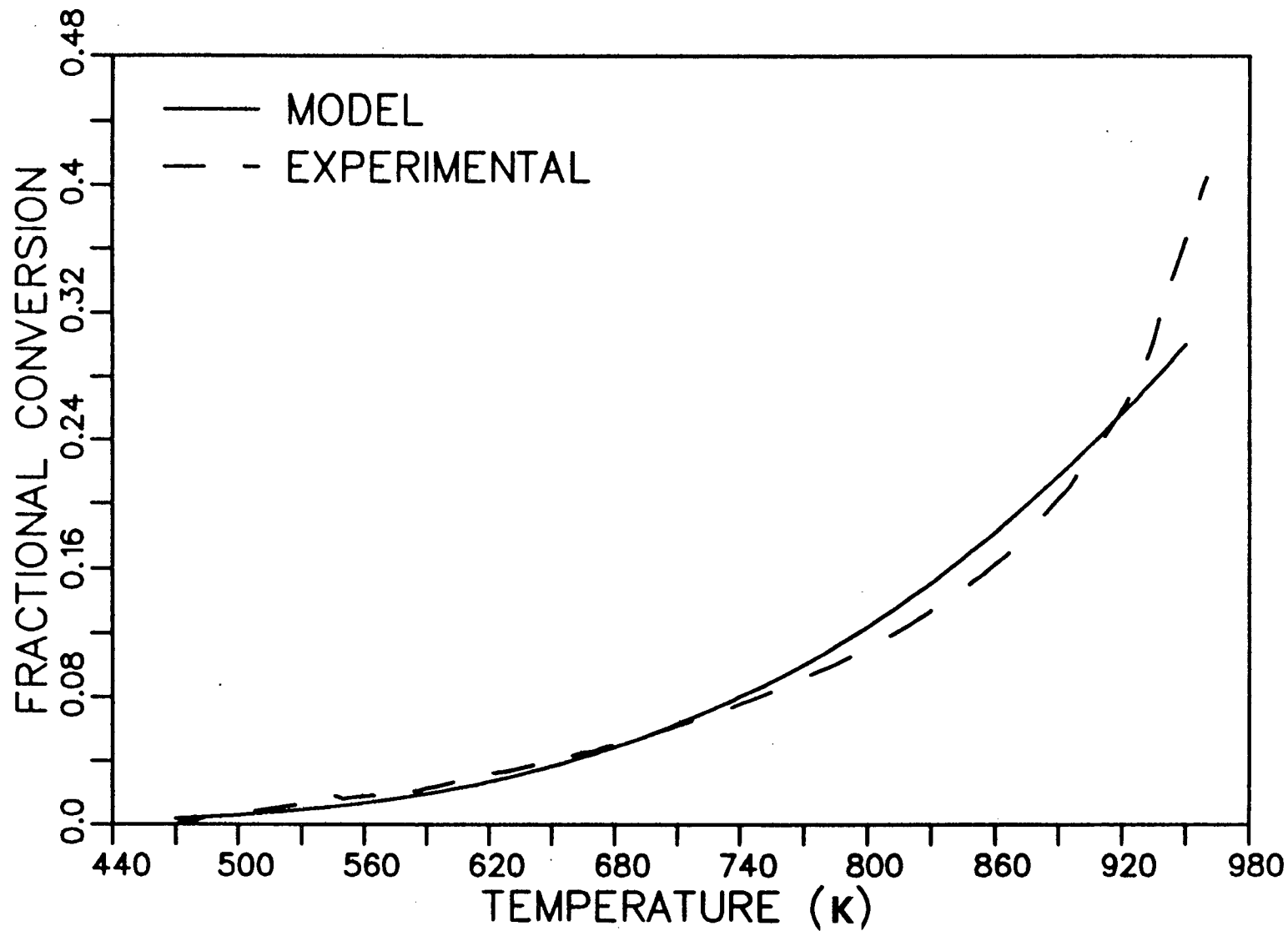
Figure 49:   Comparison of the Results after the Modification
of the Model for 40 Percent Colemanite.
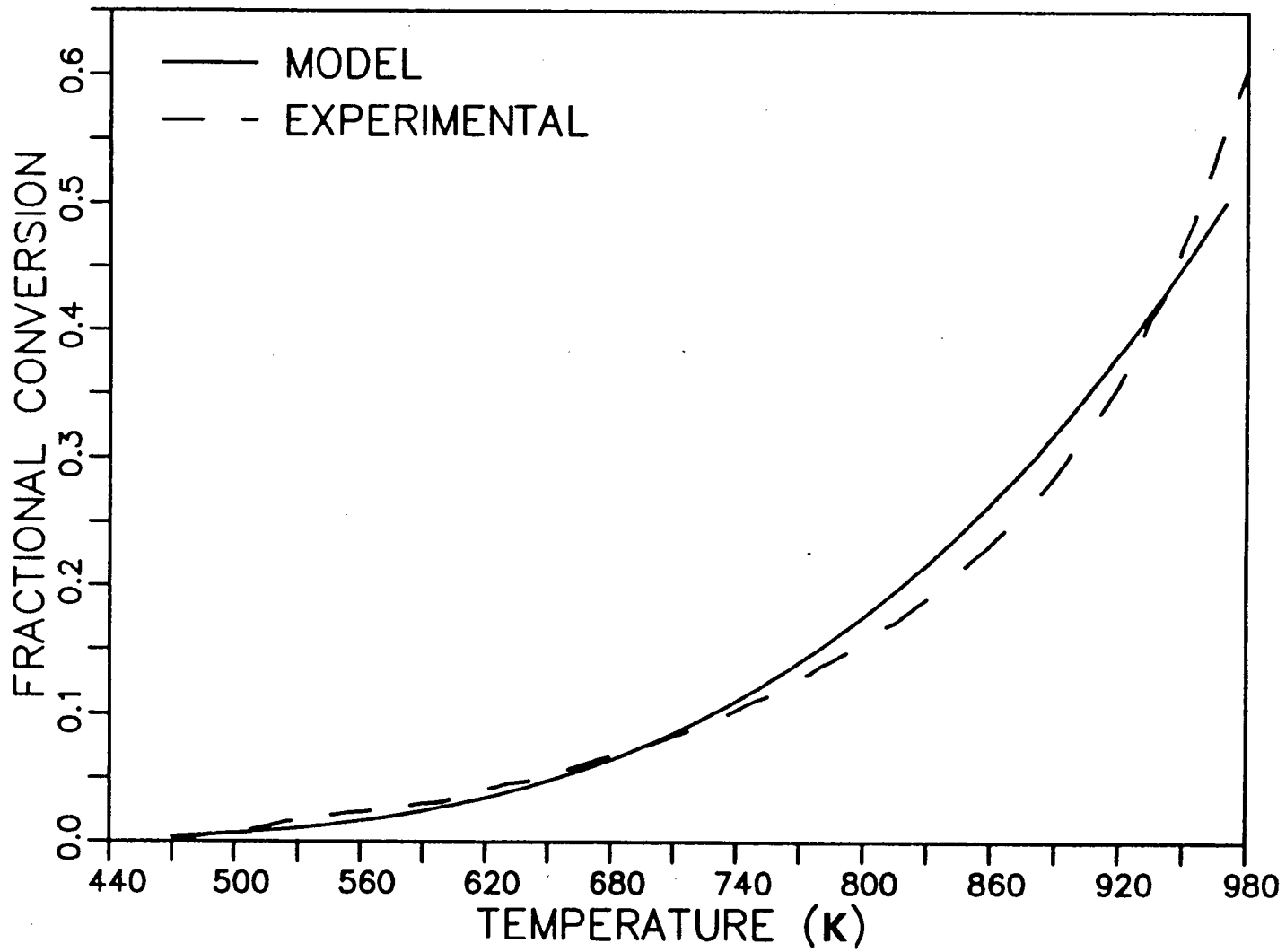
Figure 50: Comparison of the Results after the Modification
of the Model for 50 Percent Colemanite.
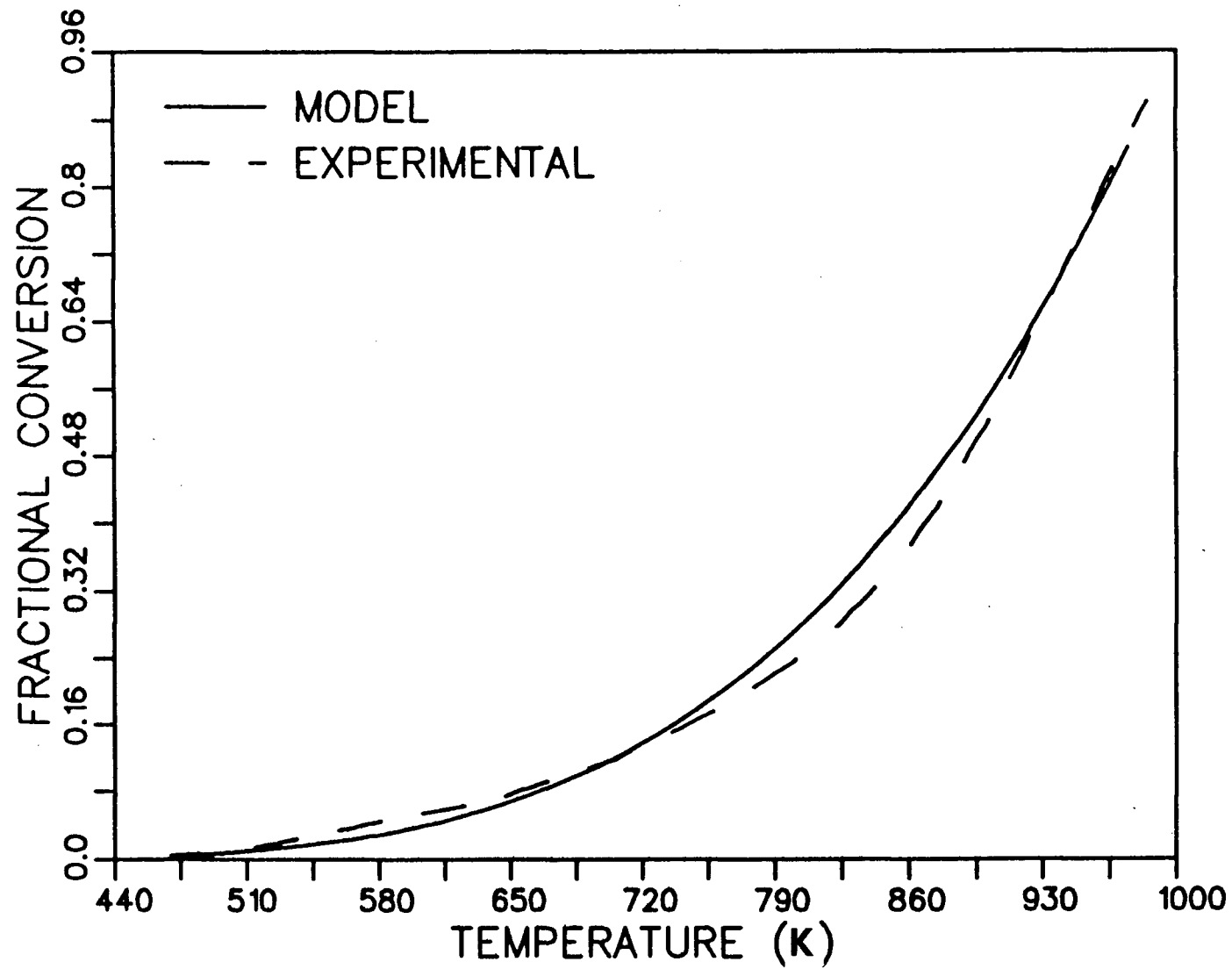
Figure 51:   Comparison of the Results after the Modification
of the Model for 60 Percent Colemanite.

show minimum standard deviations lower than the minimum value obtained

for the first order case. When the fractional conversions were

plotted, first order is the one which gives the best fit to the

experimental data. These results are shown in Figures 52, 53, 54 and

55 for 20, 30, 40 and 50 percent colemanite percentages respectively.

These all show extremely good fits even at high temperatures. When the

final values for conversions are examined for all colemanite

percentages it can be concluded that the substances or impurities in

the colemanite act as agents or possibly catalysts for the conversion

of sodium carbonate to sodium oxide because there is a considerable

amount of conversion due to the second reaction which cannot be

achieved by the self-decomposition of sodium carbonate (see Fig. 22).

These results also show that it is possible to obtain conversions as

high as 60 percent even by using the colemanite in concentrations as

small as 30 percent. This is an important factor in the choice of

colemanite as the best autocausticizing agent when the possibility of

having problems due to the use of colemanite in large quantities in the

mill application is considered. Even though the use of colemanite

in stoichiometric amounts (63.35 percent) gives much better results at

lower temperatures, the decision on how much colemanite should be used

must be found by an economic evaluation.

Rate constants for the second reaction were also calculated by

using the same technique used in the first part. A sample calculation

of frequency factor and rate constants is shown in Appendix II. The

results are tabulated in Table 20. As is seen from this table
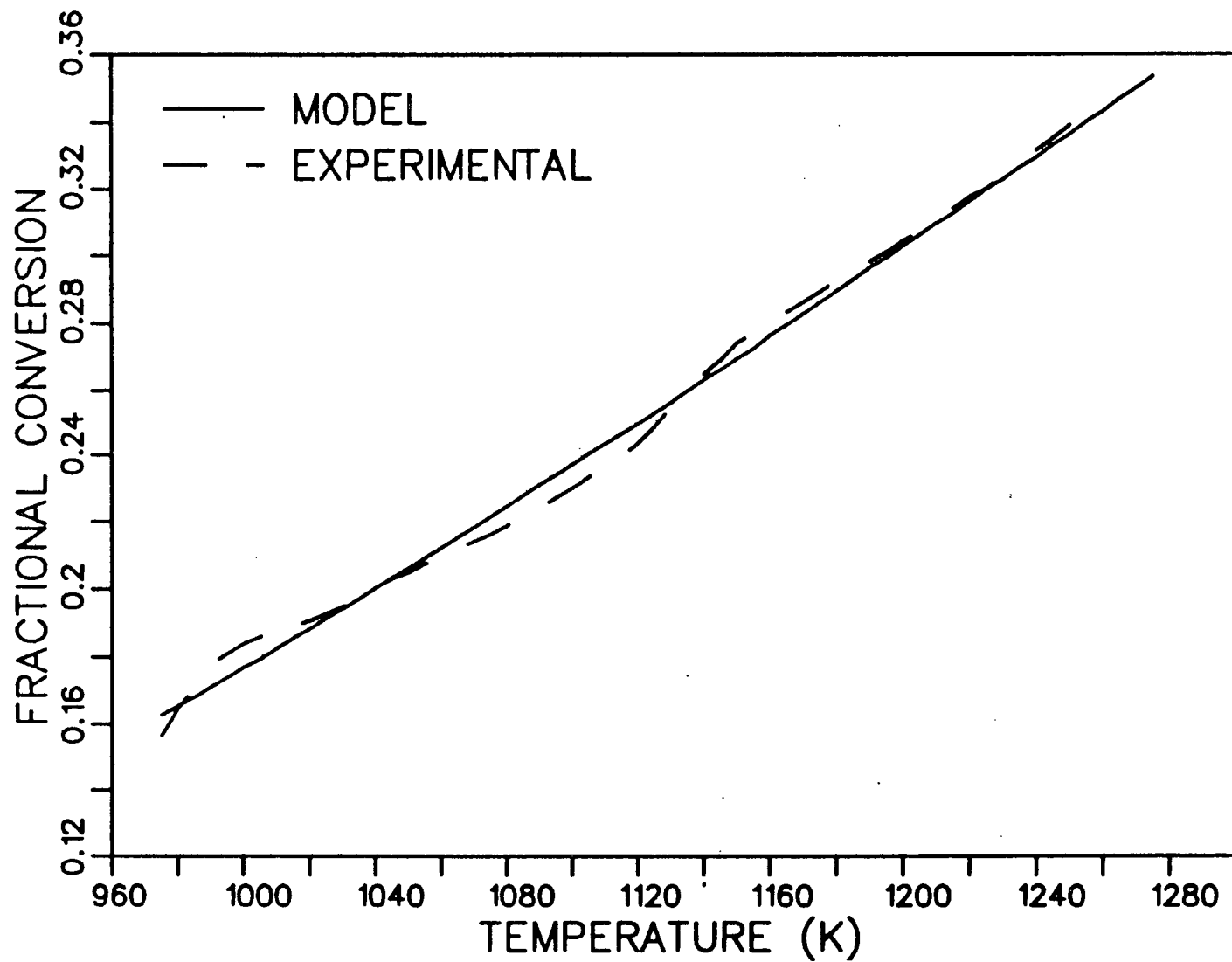
Figure 52: Comparison of the Model with the Experimental Results for Second Reaction for 20 Percent Colemanite.
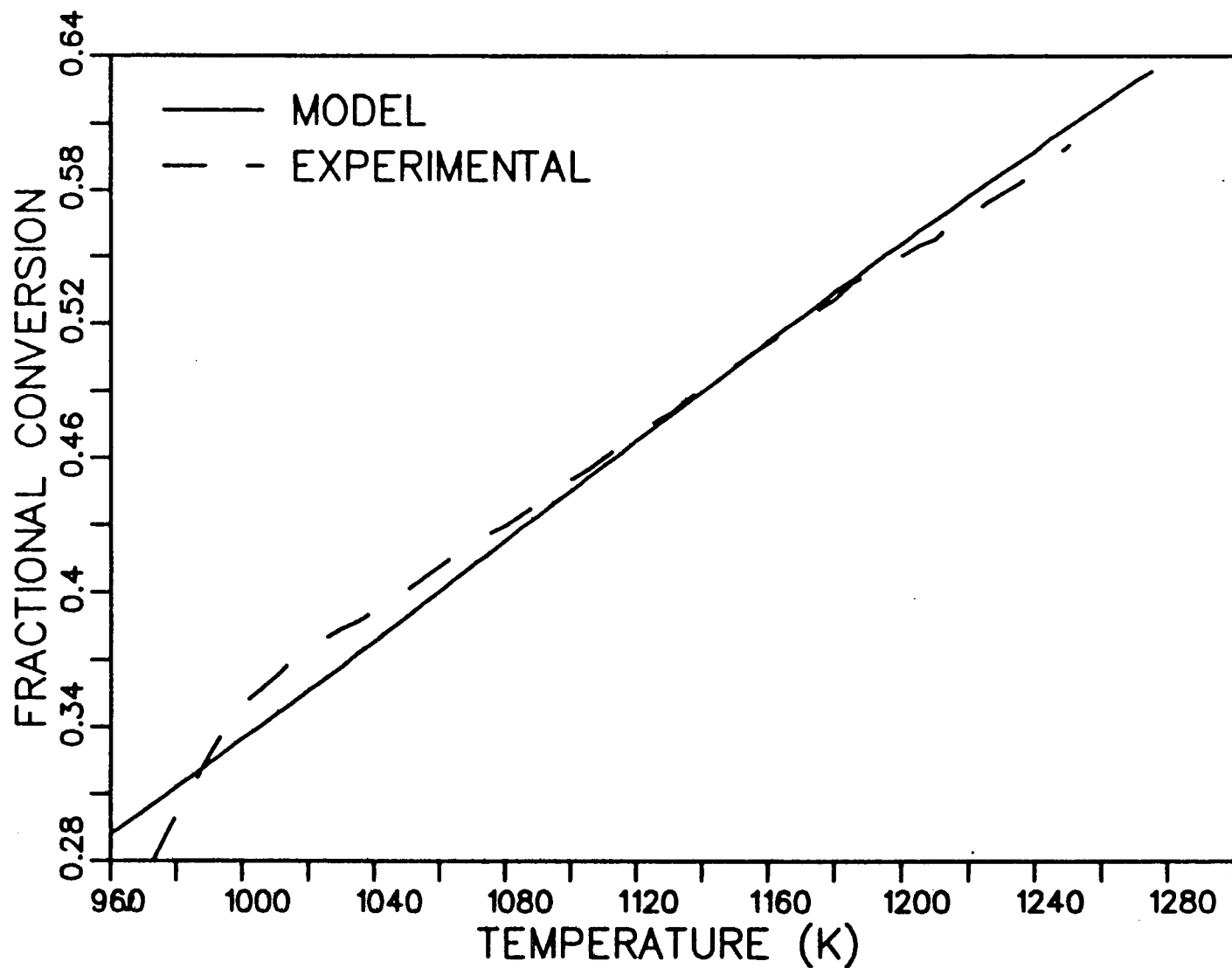
Figure 53: Comparison of the Model for the Second Reaction with the Experimental Results for 30 Percent Colemanite.
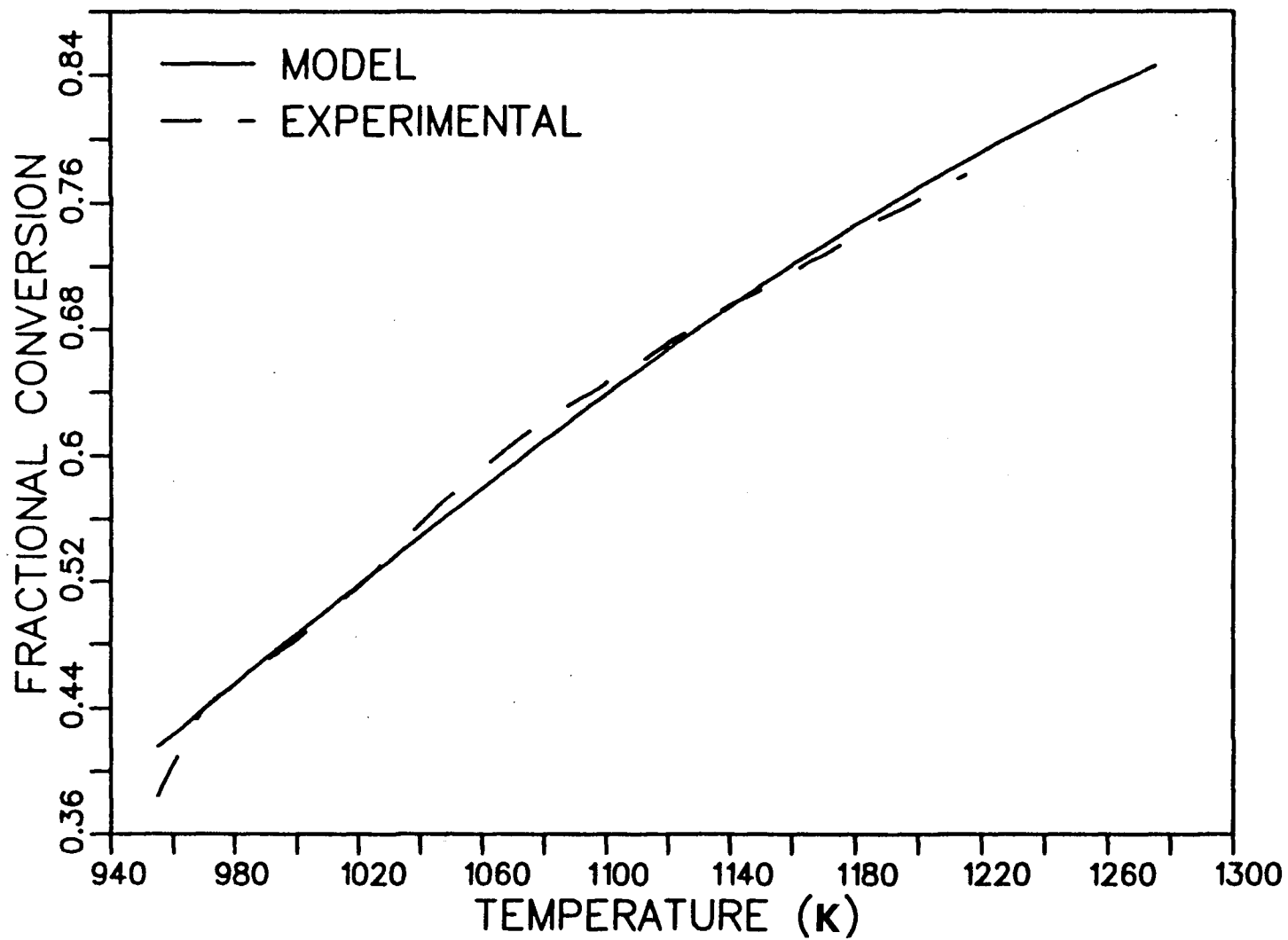
Figure 54:   Comparison of the Model for the Second Reaction
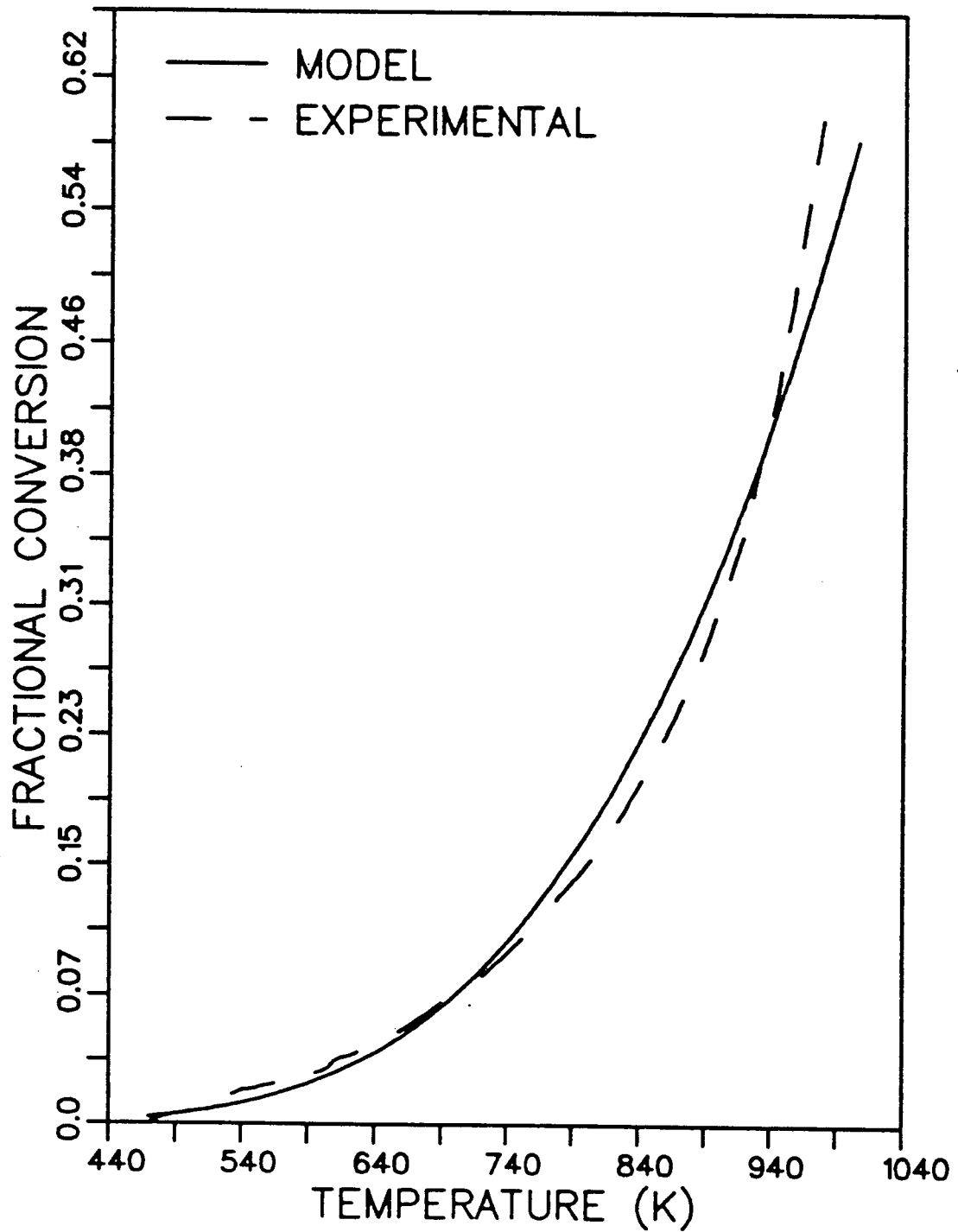with the Experimental Results for 40 Percent
Colemanite.
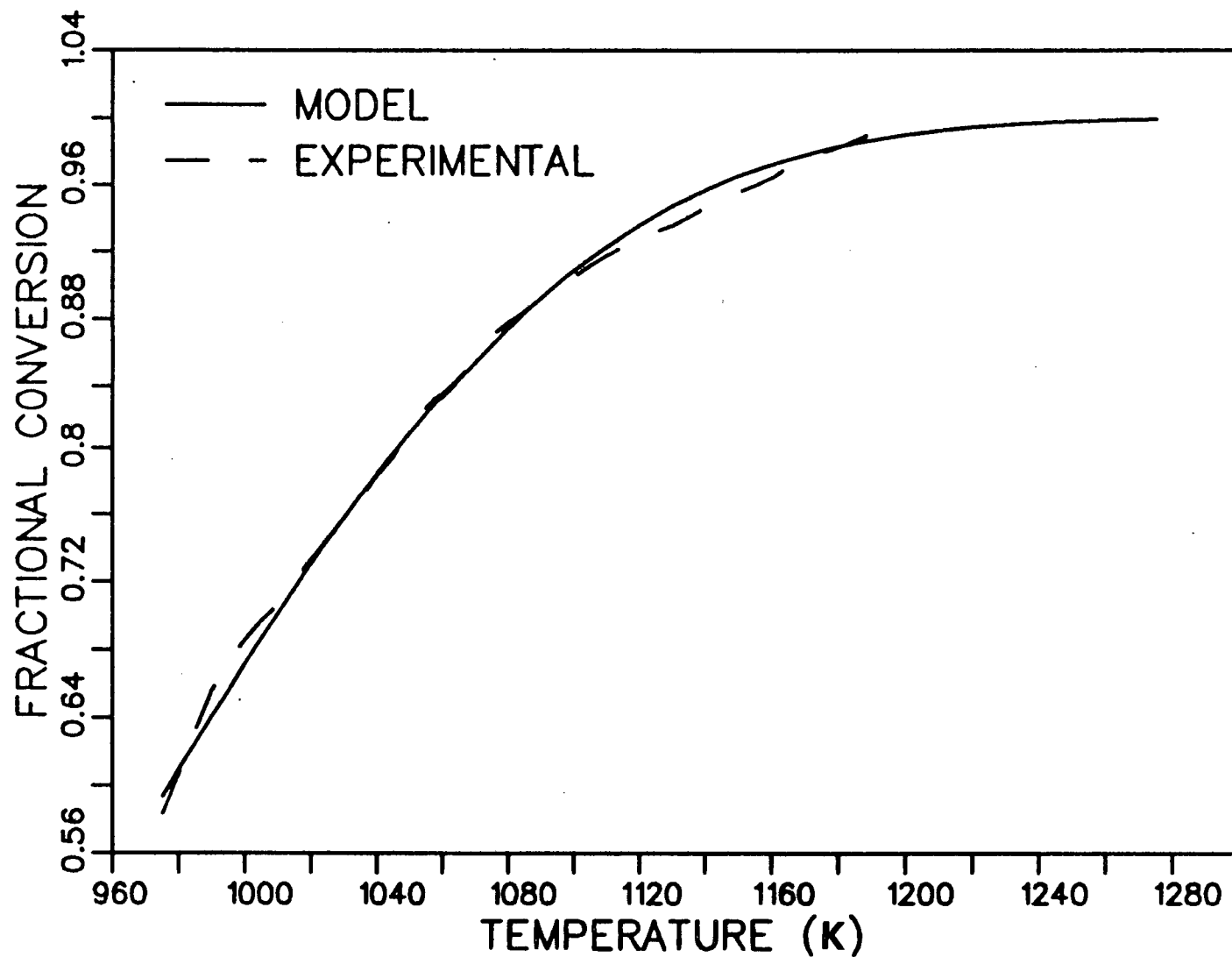
Figure 55:   Comparison of the Model for the Second Reaction
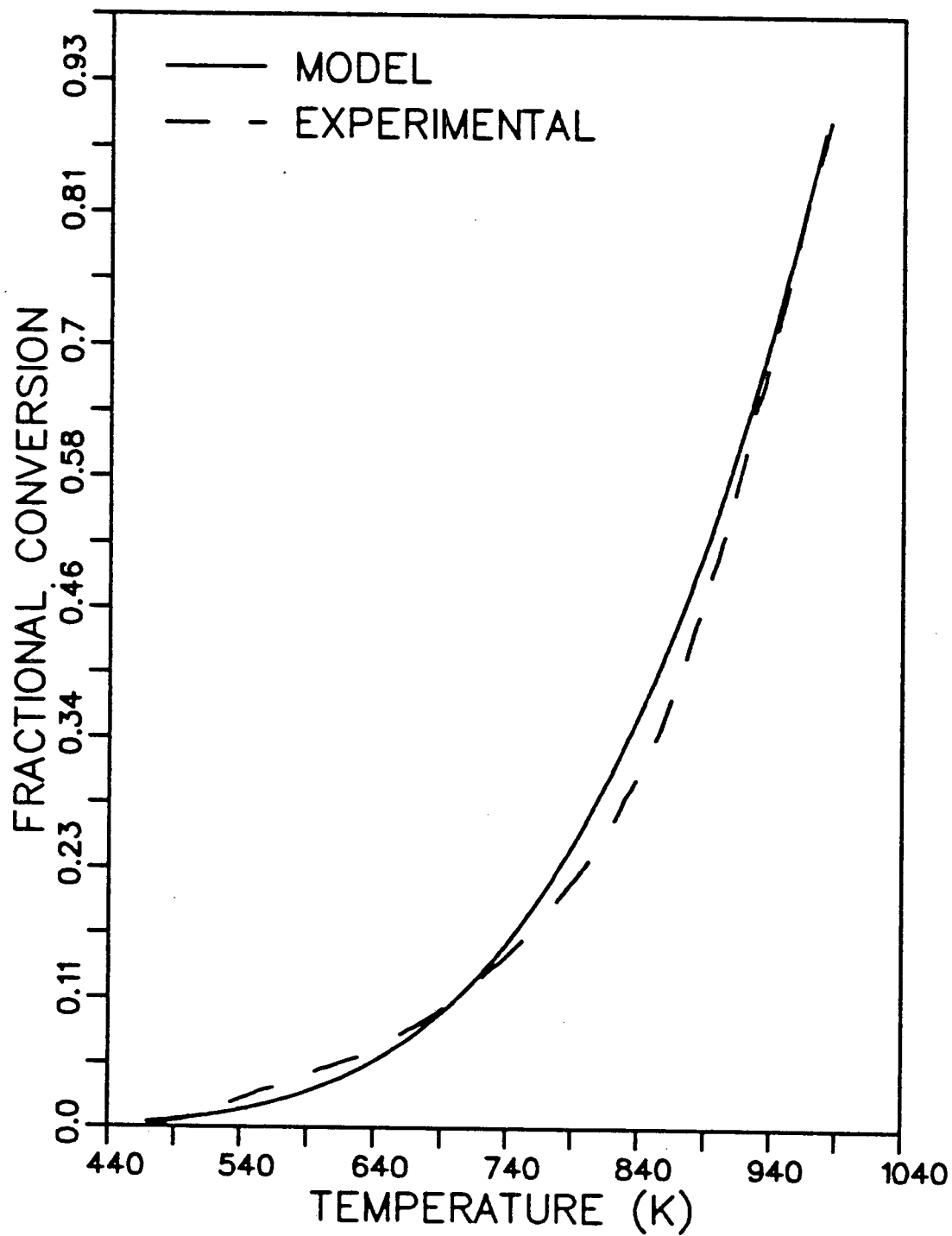with the Experimental Results for 50 Percent
Colemanite.

Table 20: Kinetic constants for the second reaction.*

Percent Colemanite	Activation energy (E_2) cal/mol	Frequency factor (Z_2) (min^{-1})	Rate constant (k_2) (min^{-1})
20	3900	0.049	9.27×10^{-3}
30	4700	0.174	0.024
40	5800	0.567	0.048
50	13000	64.47	0.244

* Rate constants are calculated at 900°C.

the kinetic constants change with the concentration of colemanite. The
model assumes that the colemanite, or more correctly, the substances in
it other than boron act as a true catalyst so that their concentration
doesn't change throughout the reaction. So the changes in E_2 and Z_2
with the change in colemanite percentage are unpredictable. An attempt
was made to least square fit the points on Figures 56 and 57 in order
to be able to express the changes in both activation energy, E_2, and
frequency factor, Z_2, with the change in colemanite concentration. It
was found that the change in both kinetic constants with the colemanite
percentage (in the range of 10-60 percent colemanite) can be described
by a third order polynomial. The goodness of fit for these equations
was very high. The output of the computer program which shows the
coefficients of this polynomial is in Appendix V. As a result, the
following equations for the activation energy and frequency factor can
be written

$$E_2 = -19999.0013 + 2518.23627 \ Y_c - 85.4970639 \ Y_c^2$$
$$+ 0.966638716 \ Y_c^3 \tag{6.6}$$

$$Z_2 = -252.342474 + 27.3482681 \ Y_c - 0.947228943 \ Y_c^2$$
$$+ 0.0105397707 \ Y_c^3 \tag{6.7}$$
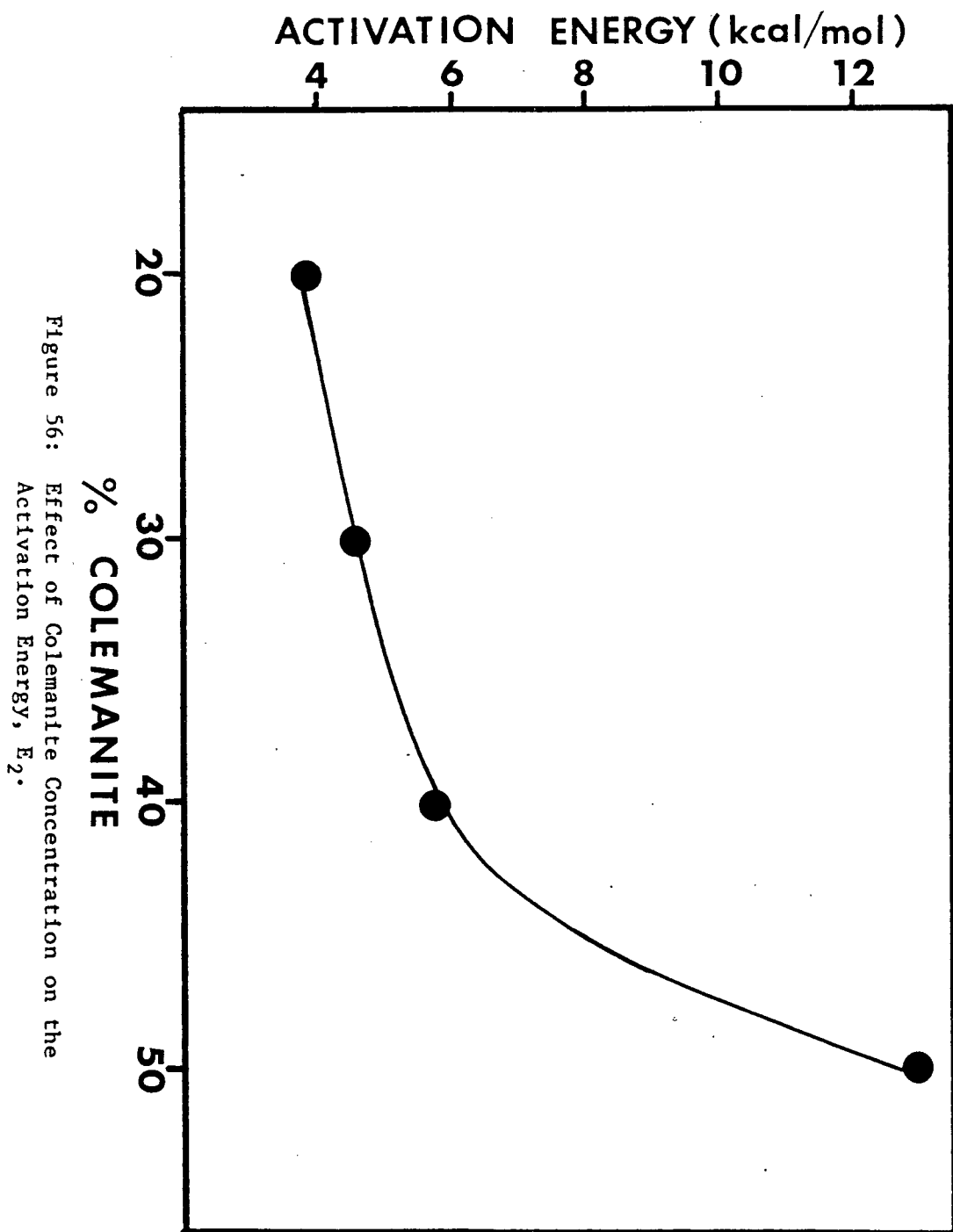
Figure 56: Effect of Colemanite Concentration on the Activation Energy, E_2.
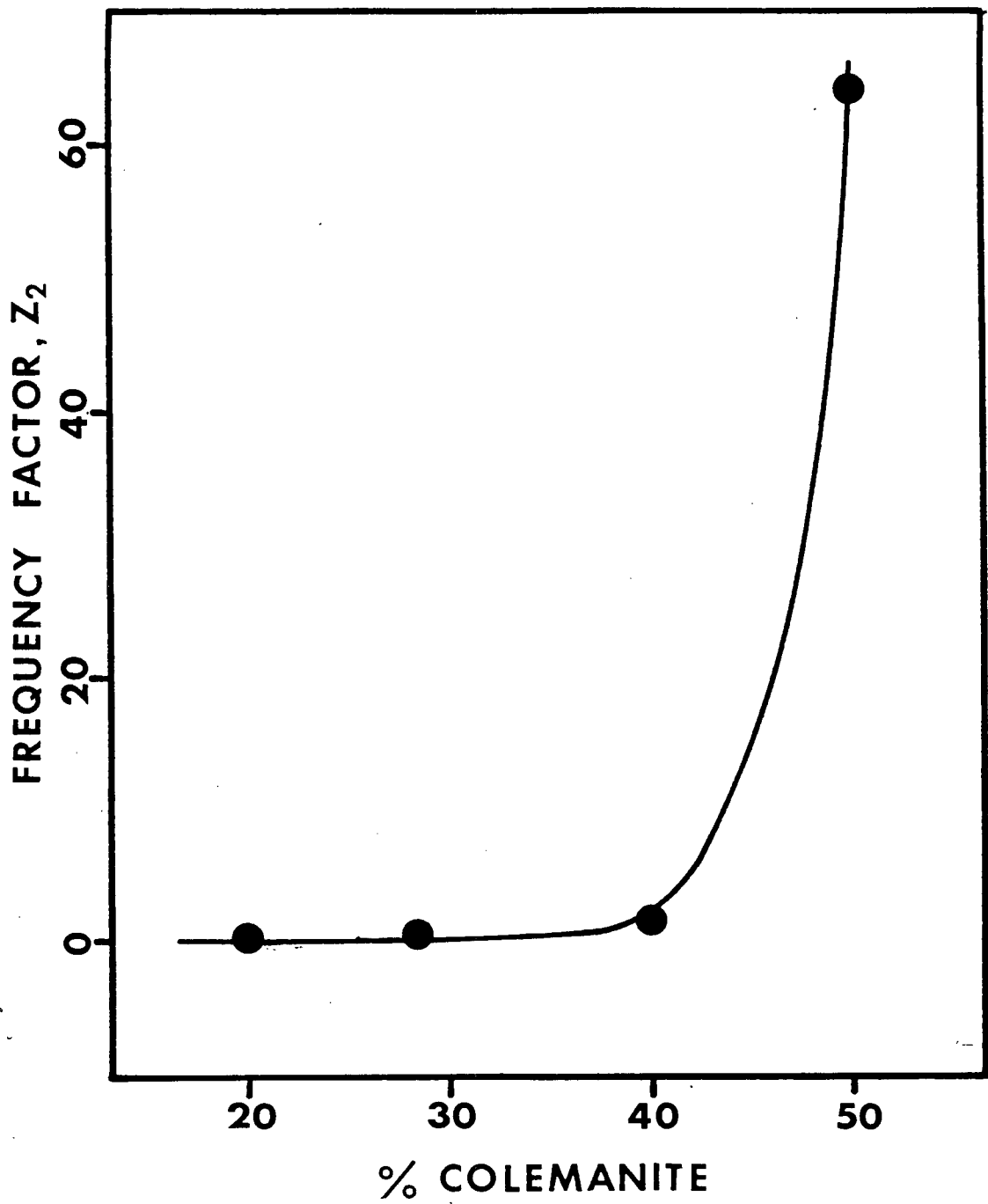
Figure 57: Effect of Colemanite Concentration on the Frequency Factor, Z_2.

The values of the kinetic constants which were calculated using equations 6.6 and 6.7 are tabulated in Table 21 and were used for further calculations. The rate constant for the second reaction can be written as

$$k_2 = (- 252.34 + 27.348 \ Y_c - 0.947 \ Y_c^2 + 0.010 \ Y_c^3) \ *$$

$$\exp \left[- \frac{(- 19999 + 2518.23 \ Y_c - 85.49 \ Y_c^2 + 0.966 \ Y_c^3)}{RT} \right] (6.8)$$

Recalling that the rate of first reaction is independent of the reactant concentrations and the rate of the second raction is first order of the sodium carbonate concentration, the final forms of the rate expressions can be written as

$$\frac{d\alpha_1}{dt_1} = k_1' \tag{6.9}$$

where $k_1' = k_1 \ W_{s_o}^{-1}$

$$\frac{d\alpha_2}{dt} = k_2 \ (1 - \alpha_2) \tag{6.10}$$

where k_1 and k_2 are the rate constants given as functions of the colemanite concentration by eq. (6.5) and eq. (6.8) for the 1st and 2nd reaction respectively.

Table 21: Kinetic constants for the second reaction
calculated by using equation 6.6 and 6.7.*

Percent Colemanite	Activation energy (E_2) cal/mol	Frequency factor (Z_2) (min^{-1})	Rate constant (k_2) (min^{-1})
20	3900	0.052	9.75×10^{-3}
30	4699	0.182	0.024
40	5800	0.588	0.048
50	13000	64.51	0.244

* Rate constants are calculated at 900°C.

6.3 Comparison of the Model with the Results of Isothermal Experiments.

The reaction model in its final form was used to calculate the final conversions at 900°C for different reaction times and the results were compared with the results of the isothermal experiments for each colemanite concentration. As was stated before the first and second reactions are different in nature. The previous results showed that the first reaction stops when the active part of the colemanite is finished, because colemanite acts as a reactant rather than a catalyst. So until this point is reached both reactions take place at the same time and then the second reaction continues until the amount of sodium carbonate available is all consumed. A possible reason why the first and the second reactions take place at the same time even though the second reaction doesn't seem to start before the first reaction finishes or a certain temperature is reached during the thermogravimetric experiments is that the second reaction might not start before the temperature at which the mixture is all melted. In fact the DTA work on the same reaction showed a physical change which could be melting around the temperature where the second reaction started (26). When the samples were placed into the furnace at 900°C both reactions could take place simultaneously because the temperature is high enough for melting to occur and for the second reaction to take place at an appreciable rate. Thus at the beginning of the reaction the overall rate of the reaction is expressed as

$$\frac{d\alpha}{dt} = k_1' + k_2 (1-\alpha) \tag{6.11}$$

or

$$\int_0^{\alpha'} \frac{d\alpha}{k_1' + k_2 - k_2\alpha} = \int_0^{t_1} dt$$

The time at which the first reaction ceased can be calculated from the integrated form of eq. (6.9) by knowing the conversion value at the end of the first reaction from the Figures 24 to 26 for each colemanite percentage. These times are found to be

$t_1 = 17.05$ min for 30% colemanite

$t_1 = 15.083$ min for 40% colemanite

$t_1 = 12.693$ min for 50% colemanite

For times longer than these the following equation which is the integrated form of the equation (6.10) is used to find the conversions.

$$\alpha_2 = 1 - [(1-\alpha') \exp (-k_2(t_2-t_1))] \tag{6.12}$$

The following table shows the rate constants as well as the fractional conversions.

These results are compared with the results of the isothermal experiments in Figures 58, 59 and 60 for the 30, 40 and 50 percent colemanite cases respectively. These figures show that this model predicts the conversion values very well specially in the first 10

Table 22: Rate constants and fractional conversions for the 1st and 2nd reaction.

Percent Colemanite	k_1 g/min	k_2 (min^{-1})	t (min)	α'	α_2
30	1.520	0.024	10	0.351	0.351
			20	0.552	0.582
			30	0.552	0.672
			40	0.552	0.743
			50	0.552	0.798
40	2.773	0.048	10	0.596	0.596
			20	0.804	0.846
			30	0.804	0.905
			40	0.804	0.942
			50	0.804	0.964
50	4.613	0.244	5	0.841	0.841
			10	1.0	1.0
			20	1.0	1.0
			30	1.0	1.0
			40	1.0	1.0
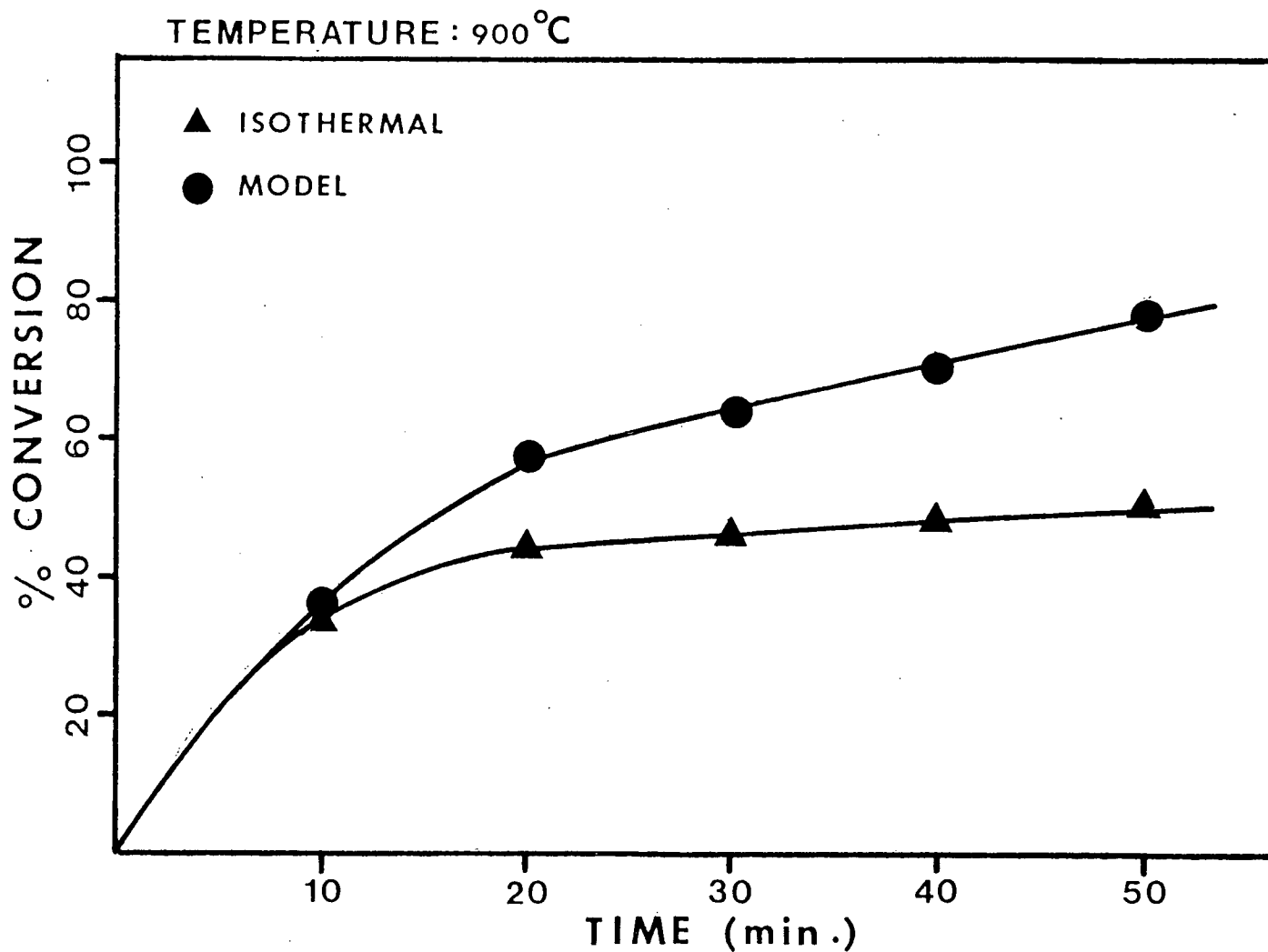
Figure 58:   Comparison of the Model with the Results of
Isothermal Experiments for 30 Percent Colemanite.
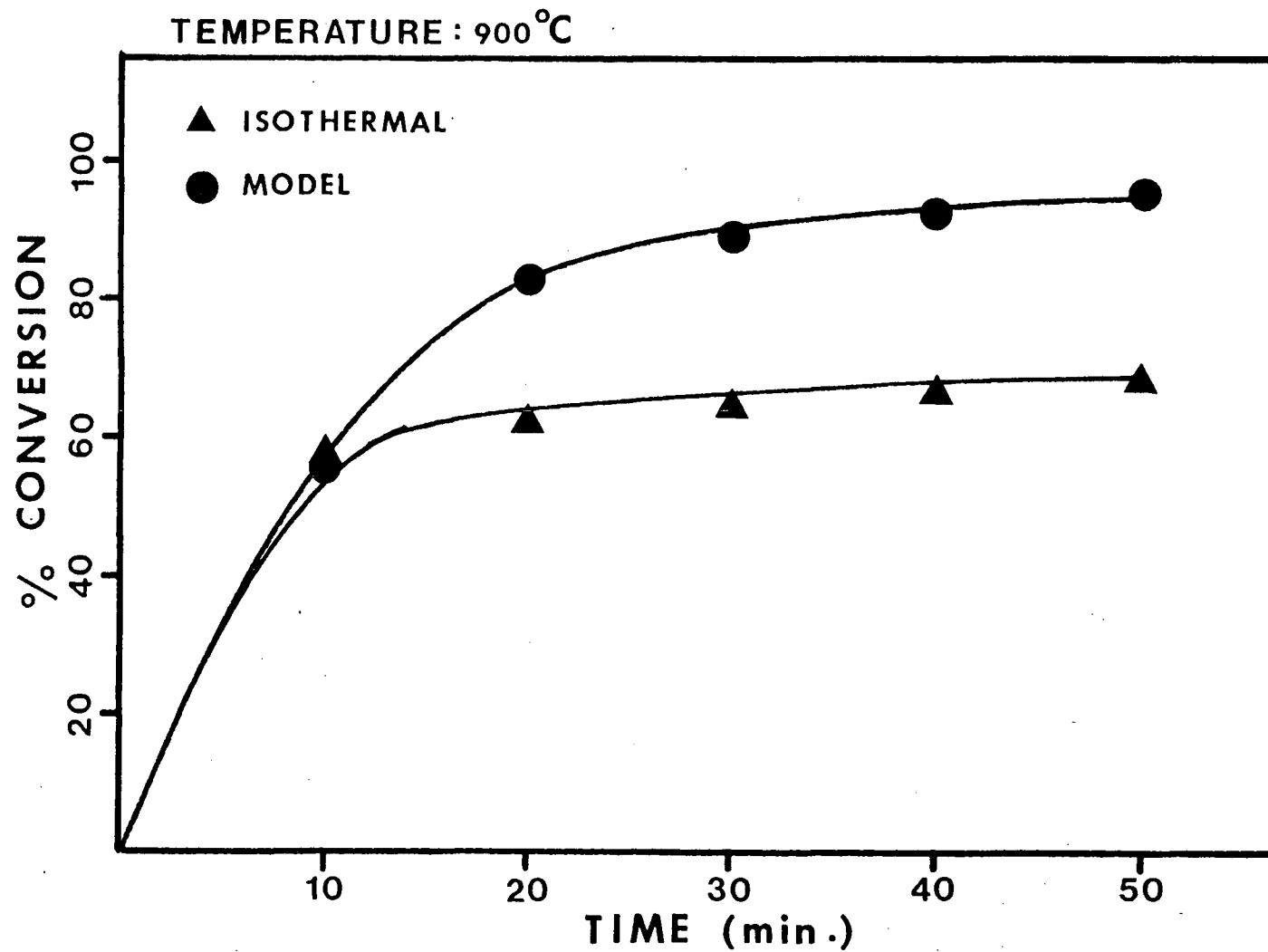
Figure 59:   Comparison of the Model with the Results of
             Isothermal Experiments for 40 Percent Colemanite.
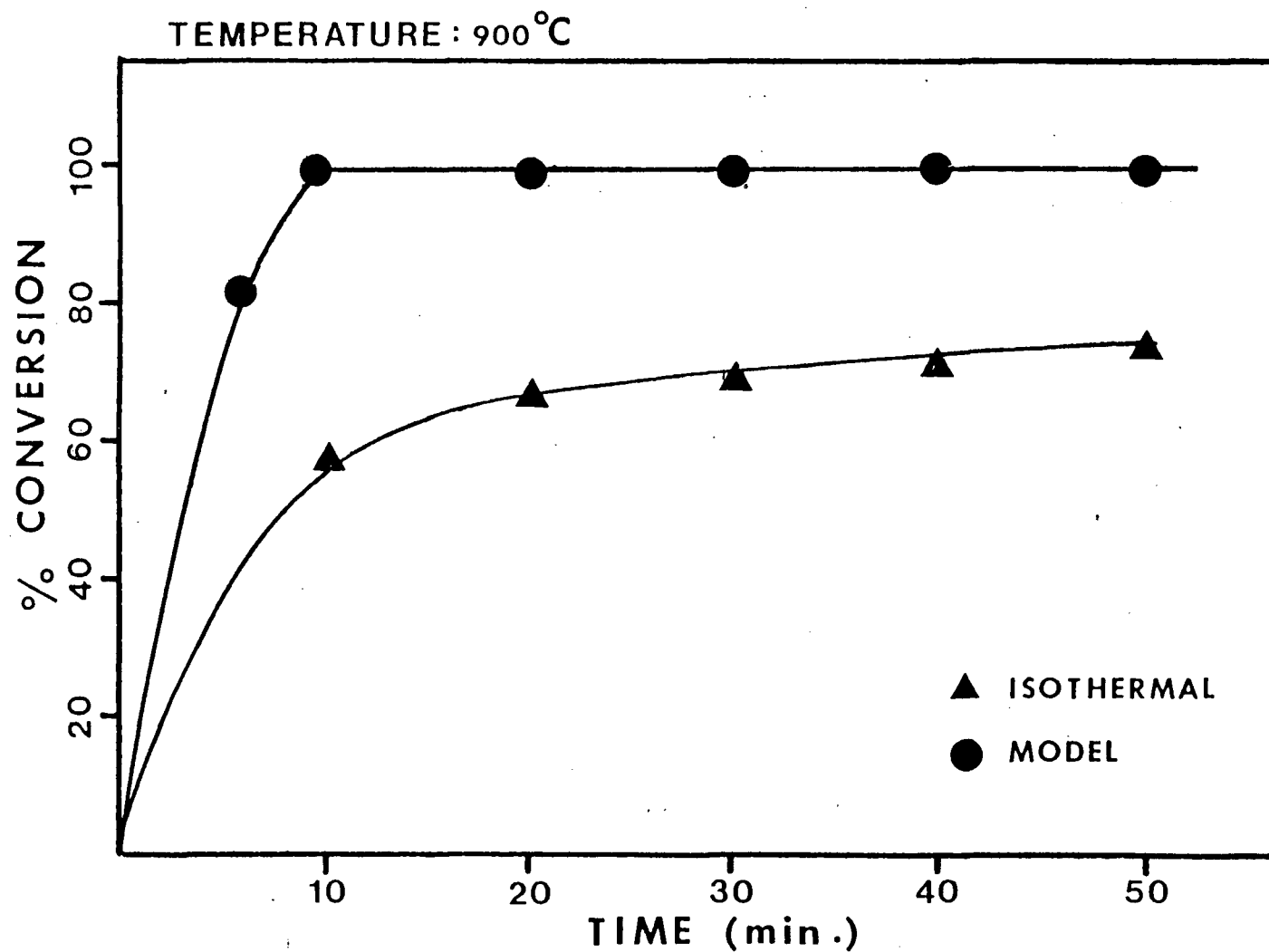
Figure 60: Comparison of the Model with the Results of
Isothermal Experiments for 50 Percent Colemanite.

minutes of the reaction. For longer times the model predicts higher

conversions than the ones obtained experimentally. This could result

from the errors due to the poor experimental technique used in the

isothermal experiments. As was mentioned previously, at high

temperatures, samples are fused into a solid mass which made the

recovery of the reaction product from the crucibles very difficult.

This was even more difficult for the samples which were kept in the

oven for a long time. During the dissolution of the samples some

spitting occured and also a part of the product was left in the

crucibles. These losses might cause lower conversion values than the

model prediction. The isothermal results may also include some

titration errors. For the 50 percent colemanite case the prediction of

the model doesn't seem as good as the ones for 30 and 40 percent

colemanite cases even in the first ten minutes of the reaction. This

can be explained as before, especially since as the colemanite

concentration increases the solid mass becomes more difficult to

dissolve from the crucibles. In fact the two sets of results were

obtained in two totally different ways. Therefore, some difference

between them would be expected. The kinetic constants were obtained by

using a very small amount of sample. For larger amounts of sample the

kinetics of the liberation of carbon dioxide might be different; the

diffusion of the carbon dioxide through the sample thickness might

become more important as well. The conditions inside the furnaces were

not the same in both cases either. If there was any carbon dioxide

pressure built up in the big oven this would retard the liberation of

carbon dioxide considerably. From these results it seems that it is

possible to obtain complete conversion of sodium carbonate in ten minutes at 900°C. This makes colemanite superior to the titanium dioxide and also brings some advantages from the heat economy and operation point of view.

The kinetic constants reported in this chapter are specific for this study. Since they are dependent on factors such as sample size and conditions inside the furnace these values can not be applied directly to plant scale operations. In a sprayed sample the particles would have a large area, and should have kinetics closer to that of the small TG samples. However in a molten mass at the bottom of the furnace the isothermal results may hold. The true answer will be most likely between the two obtained here.

6.4 Recycle of Colemanite

The recyclability of the colemanite was also studied in this project. The results obtained from the thermogravimetric analysis of recycled colemanite and sodium carbonate mixtures are shown in Figures 61, 62 and 63 for the first, second and third recycle of the colemanite respectively. When these figures are compared with the Figure 25 which shows the weight loss for 40 percent colemanite it is seen that the shape of the curves are the same. This means that the mechanism of the reaction stays the same when the colemanite is reused. It is also seen that the weight changes are about the same in both cases. The weight changes are also the same for the first, second and third recycle tests. This is a promising result for the use of colemanite in the pulping process. Quantitative values for the conversions of sodium

COLEMANITE CARBONATED RECYCLE   WT: 27.6788 mg   SCAN RATE: 10.00 deg/min
——·· = DERIVATIVE

98.6%

FROM: 192.12
TO: 987.72
WT. % CHANGE: 21.7

76.89%
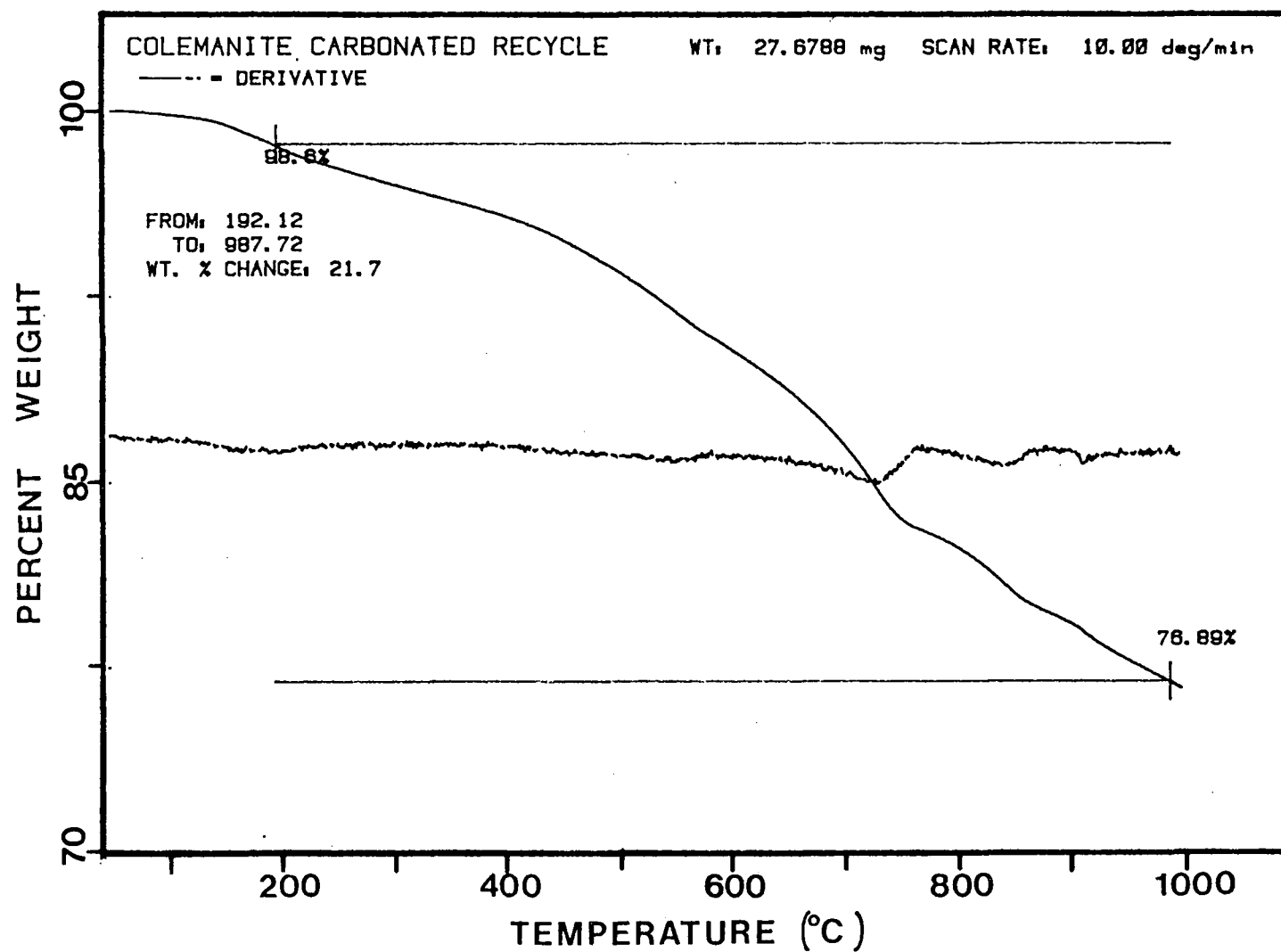
Figure 61: TG Results for the First Recycle.
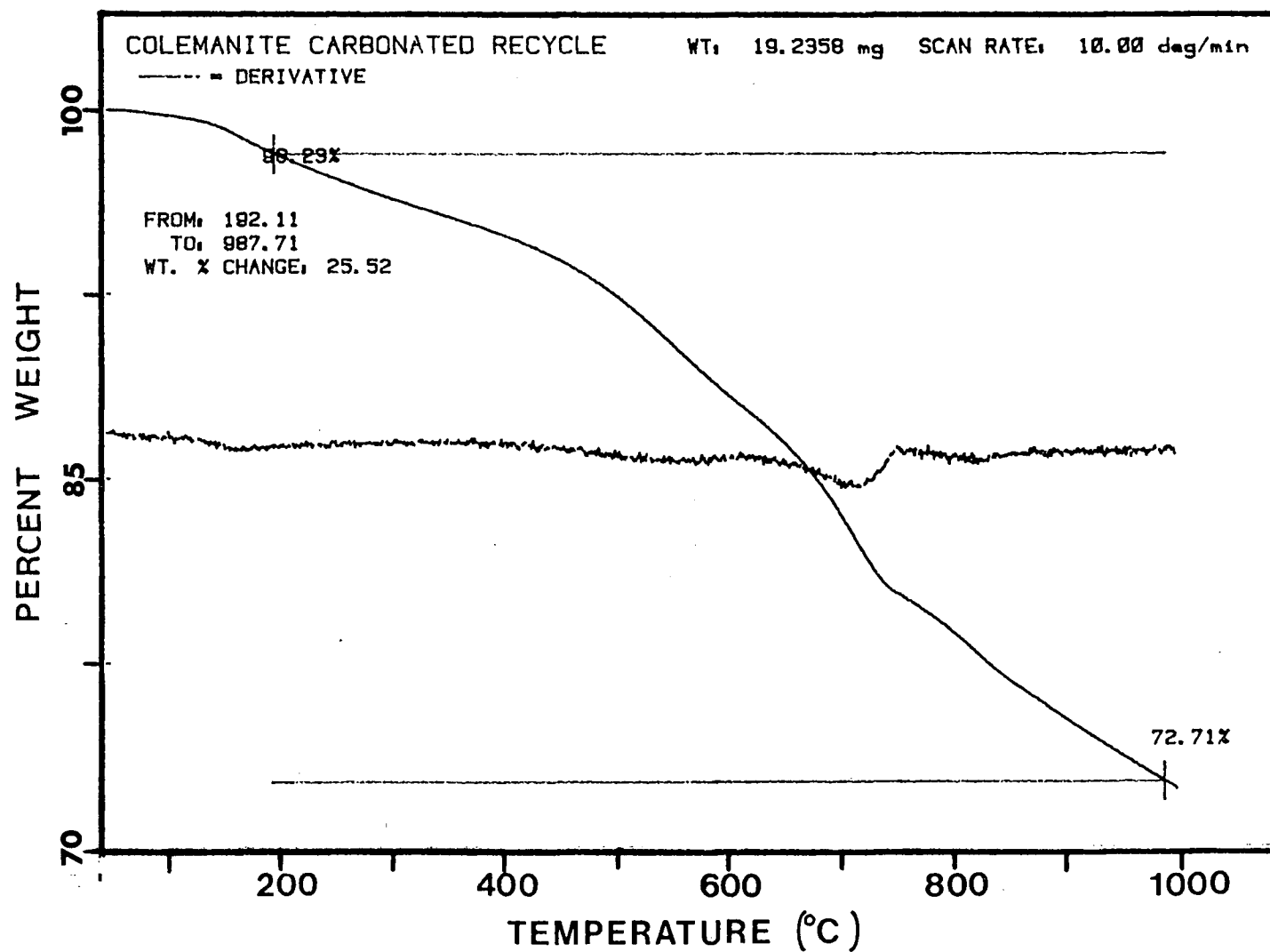
Figure 62: TG Results for the Second Recycle.
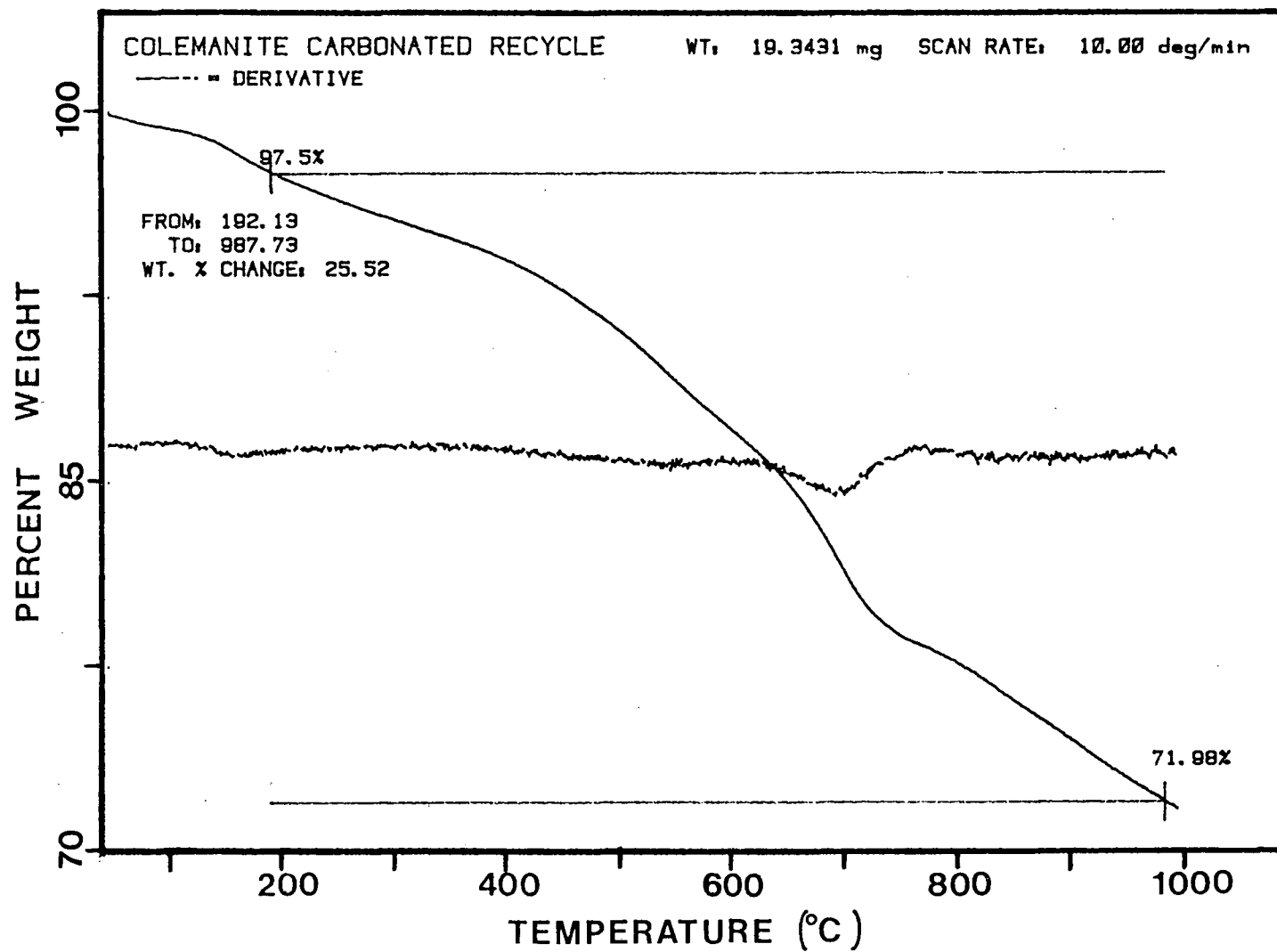
Figure 63: TG Results for the Third Recycle.

carbonate when the recycled colemanite is used can not be found from this data because the analysis of these curves can not be made without knowing the losses of colemanite when it is reused. Besides this, three recycle tests are not enough to make a definitive statement on the recyclibility of colemanite.

From the process point of view, if colemanite can be reused, it would be partially separated from the sodium hydroxide and recycled back to the furnace without going through the whole cycle because of the partial solubility of colemanite. The work done by K.L. Pinder (26) on the solubility of colemanite showed that only 40 percent of the colemanite is soluble at 20°C. Therefore the soluble borate would go throughout the pulping cycle and would assist pulping as it does in the case of sodium borates (11). The make-up should be only that colemanite which is lost during pulp washing etc. Colemanite seems to be the best autocausticizing agent from this point of view as well.

7. CONCLUSIONS AND RECOMMENDATIONS

The results of this study show that colemanite is a good agent for the autocausticization of black liquor. It seems superior to the other amphoteric oxides studied before from the following points of view.

1. It gives quite high conversions at temperatures found in Kraft furnaces. It was found that for Na:B molar ratio of 1.15 the reaction goes to completion at 700°C. Thus is won't be necessary to go to temperatures as high as 1000°C as is the case with titanium dioxide. This could result in a considerable saving of energy.

2. Colemanite is partially soluble and about 60 percent of it is settled out (26) and returned directly to the furnace. Thus there is less total hold-up and not as large a dead load on the evaporators. This is the main difference between colemanite and sodium borate which is completely soluble and carried through the whole process.

In Figure 64 is shown the process proposed from this research for the autocausticizing of Kraft liquor with colemanite. When this figure is compared with Figure 1 it can be seen that there is a considerable saving in capital equipment in the new process. Elimination of the lime kiln brings savings in both energy and capital investments.

In addition to these advantages colemanite is very cheap compared to other agents. However its actual performance can only be determined by pilot plant scale tests.
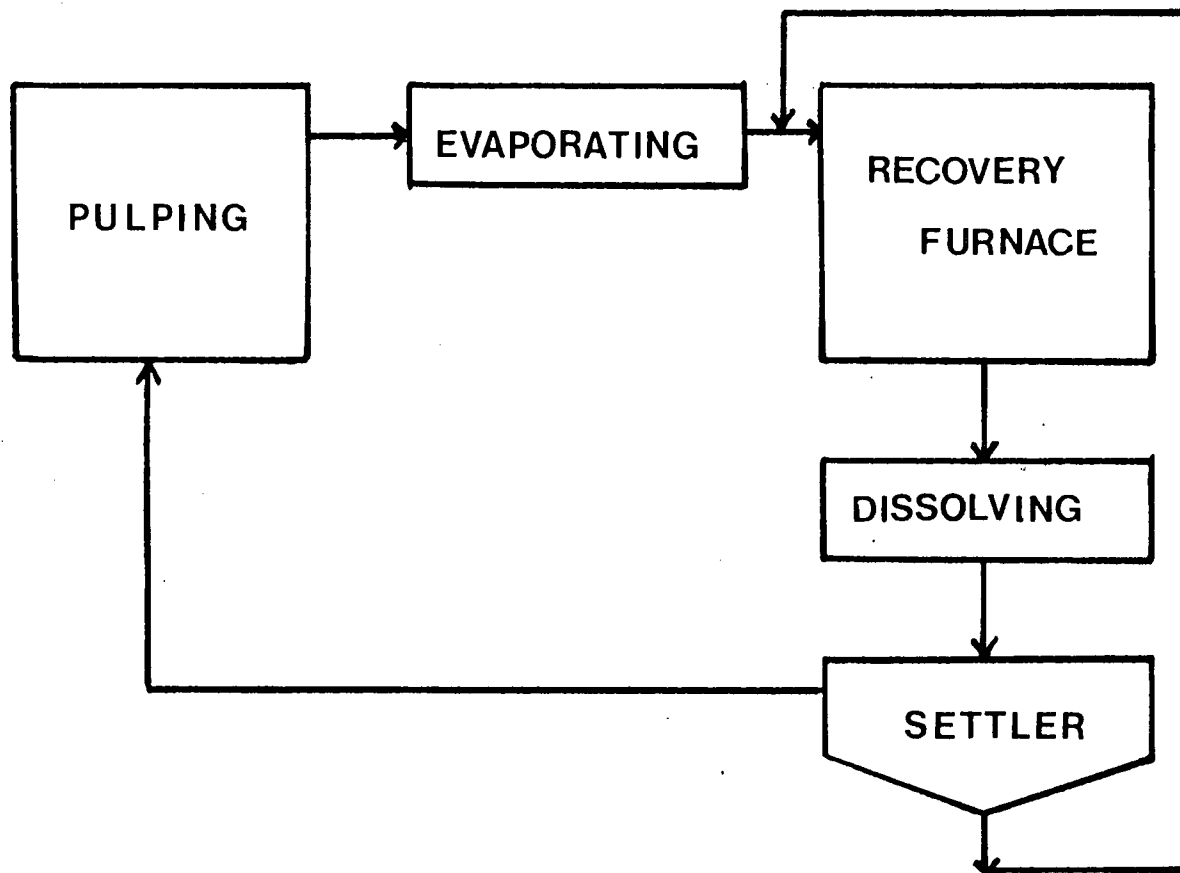
Figure 64:   Schematic of Proposed Process

Experimental results showed that there are two different main reactions in the temperature range from 190-1000°C. The first reaction is between colemanite and sodium carbonate in the temperature range of 192 and 700°C. This reaction goes practically to completion at 700°C. Then the unreacted part of the sodium carbonate is catalyzed by the substances other than boron which are present in the colemanite at temperatures between 700 and 1000°C. The first reaction was found to be zero order in sodium carbonate and a complex function of the colemanite concentration. Thus the reaction depends only on the temperature and the colemanite concentration. The second reaction was found to be first order on the sodium carbonate concentration and a complex function of the impurities in colemanite. The derived model gave very good fits to the experimental data taken in this study. Further studies will be needed to determine whether modifications must be made to the models.

The comparison of the results of isothermal experiments and the results of TG analysis agreed reasonably well except for the difference in conversions at high temperatures for the longer runs. This may be the result of increased importance of diffusion in the bulk isothermal tests.

Colemanite can be reused several times without losing its activity as an autocausticizing agent. So it is most likely recyclable.

Although the results of this study are very promising it is difficult to say from such small scale tests whether this process could satisfactorily replace the conventional Kraft Recovery Process.

Further research is recommended in order to answer the following questions.

1. Since this method will be utilized in Kraft mills, what would be the effect of sodium sulfide (Na_2S) on this reaction?

2. Does the use of this process have any effect on the pulp yield and paper quality?

3. Does colemanite cause any scaling problem as it is carried throughout the process?

Although the TGA is a very effective technique for measuring the kinetics of such reactions and for distinguishing between mechanisms a pilot plant study or a small mill trial is necessary to answer all these questions prior to industrial scale operations. Such tests would not be subject to such large errors caused by the carbonate losses during the dissolution of the product. The efficiency of the recycle step will also be better tested.

NOMENCLATURE

A_2 Avrami and Erofev equation for random nucleation

A_3 Avrami and Erofev equation for random nucleation

B_i difference of the logarithms of $g(\alpha)$ and $p(x)$ for a specific temperature

$\bar{B}$ arithmetical mean of B_i values

C percent conversion of sodium carbonate to sodium oxide

D_1 function $g(\alpha)$ for one-dimensional diffusion controlled reaction

D_2 function $g(\alpha)$ for two-dimensional diffusion controlled reaction

D_3 function $g(\alpha)$ for a diffusion controlled reaction in sphere

E_a activation energy of the reaction (cal/mol)

E_1 activation energy of the first reaction (cal/mol)

E_2 activation energy of the second reaction (cal/mol)

$f(\alpha)$ function which shows the dependence of the rate of reaction on the reaction mechanism

$f_1(\alpha)$ function $f(\alpha)$ for one-dimensional diffusion controlled reaction

$f_2(\alpha)$ function $f(\alpha)$ for two-dimensional diffusion controlled reaction

$f_3(\alpha)$ function $f(\alpha)$ for a diffusion controlled reaction in sphere

$g(\alpha)$ a function which is obtained after the integration of $f(\alpha)$

H_c percentage of humidity in colemanite

I_c percentage of impurity in colemanite

k reaction rate constant [unit depends on mechanism]

k_1 rate constant of the first reaction (g/min)

k_1' constant defined in equation 6.9 (min^{-1})

k_2	rate constant of the second reaction (min^{-1})
k_r	combined rate constant (min^{-1})
$k*$	modified rate constant defined in equation (3.14) [unit depends on mechanism]
m	order of the first reaction on sodium carbonate
M	molarity of the sulfuric acid
MW_c	molecular weight of colemanite (g/g-mole)
MW_{CO2}	molecular weight of carbon dioxide (g/g-mole)
MW_s	molecular weight of sodium carbonate (g/g-mole)
n	order of the first reaction on colemanite
N	constant defined in equation (3.24)
$p(x)$	function which shows the dependence of the rate of the reaction on temperature and the activation energy
q	heating rate (°K/min)
r	number of experimental data points
R	the gas constant (cal/mol-°K)
R_1	rate of the first reaction (min^{-1})
R_2	rate of the second reaction (min^{-1})
t	time (min)
t_1	time at which the first reaction ceased (min)
t_2	integration time limit for the second reaction (min)
T	temperature (°K)
V_1	volume of the acid to titrate total carbonate (ml)
V_2	volume of the acid to titrate sodium hydroxide (ml)
W	weight of the sample at any moment of the reaction (g)
W_A	weight of the compound A (g)
W_B	weight of the compound B (g)

W_{A_o} initial weight of the compound A (g)

W_{B_o} initial weight of the compound B (g)

W_{C_o} initial weight of colemanite (g)

W_{S_o} initial weight of sodium carbonate (g)

X_c weight fraction of colemanite

Y_c percentage of colemanite

Z frequency factor [unit depends on reaction mechanism]

Z_1 frequency factor for the first reaction (g/min)

Z_2 frequency factor for the second reaction (min^{-1})

α weight fraction converted

α_A weight fraction of compound A converted

α_B weight fraction of compound B converted

α_c weight fraction of colemanite converted

α_s weight fraction of sodium carbonate converted

α_1 fractional conversion at the end of time t_1

α_2 fractional conversion at the end of time t_2

α' weight fraction converted from the combination of first and second reaction

δ standard deviation of B_1 values

δ_{min} minimum of the standard deviation, δ

ν order of the second reaction on sodium carbonate

REFERENCES

1. Achar, B.N.N., Brindley, G.W., Sharp, J.H., Proceedings of the International Clay Conference, Jerusalem, Israel (1966) 1, 67-73.

2. Achar, B.N.N., Brindley, G.W., Sharp, J.H., Numerical Data for Some Commonly Used Solid State Reaction Equations, Journal of American Ceramic Society, 49, 379-382 (1966).

3. Berg, L.G., "Thermografiya" [Thermal Analysis], p. 473-5, Moscow, (1944).

4. Covey, G.H., "Development of the Direct Alkali Recovery System and Potential Applications", Journal of Pulp and Paper, 83, 92-6, (1982).

5. Doyle, C.D., "Kinetic Analysis of Thermogravimetric Data", Journal of Applied Polymer Science, 5, 285-292, (1961).

6. Grace, M.T., "Improved Energy Efficiency, Safety Likely in Future Recovery Systems", Pulp and Paper, 2, 90, (1981).

7. Hall, F.P., Insley, H., "Phase Diagrams for Ceramists", The Journal of American Ceramic Society, 33, 21, (1947).

8. Janson, J., U.S. Patent 4,116,759 (1978). "Preparation of Liquor for Delignification or Alkali Treatment by Autocausticization".

9. Janson, J., "The Use of Unconventional Alkali in Cooking and Bleaching", Paperi ja Puu, 59, 425-30, (1977).

10. Janson, J., "Alkali Cooking of Wood with the Use of Borates", Paperi ja Puu, 59, 546-57, (1977).

11. Janson, J., "Oxygen-alkali Cooking and Bleaching with the Use of Borate", Paperi ja Puu, 60, 89-93, (1978).

12. Janson, J., "Kraft Cooking with the Use of Borate", Paperi ja Puu, 60, 348-57, (1978).

13. Janson, J., "Autocausticizing Reactions", Paperi ja Puu, 61, 20-30, (1979).

14. Janson, J., "Autocausticizing of Sulphur Containing Model Mixtures and Spent Liquors", Paperi ja Puu, 61, 98-103, (1979).

15. Janson, J., "Pulping Processes Based on Autocausticizable Borate", Svensk Papperstidn, 83, 392-5, (1980).

16. Janson, J., "Mill Scale Development of the Borate-based Kraft Process", International Conference on Chemical Recovery, Vancouver, B.C. (1981).

17. Kato, K., Canadian Patent 54,70 (1975). "Method for Directly Converting Sodium Carbonate into Caustic Soda and Application of Said Method to Pulp and Paper".

18. Kiiskila, E., Virkola, N.E., "Recovery of Sodium Hydroxide from Alkaline Pulping Liquors by Autocasticizing", Paperi ja Puu, 60, 129-32, (1978).

19. Kiiskila, E., "Reaction Between Sodium Carbonate and Titanium Dioxide", Paperi ja Puu, 61, 394-401, (1979).

20. Kiiskila, E., "Alkali Distribution in Titanium Dioxide Causticizing", Paperi ja Puu, 61, 453-63, (1979).

21. Kiiskila, E., Valkonen, N., "Causticizing of Sodium Carbonate by Ferric Oxide", Paperi ja Puu, 61, 505-10, (1979).

22. Kiiskila, E., "Comparison of Various Causticizing Chemicals", Paperi ja Puu, 61, 639-50, (1979).

23. Kiiskila, E., "Recovery of Sodium Hydroxide from Alkaline Pulping Liquors by Causticizing Molten Sodium Carbonate with Amphoteric Oxides", Paperi ja Puu, 62, 339-50, (1980).

24. Kojo, M., "Profitability of Recausticizing", Paperi ja Puu, 61, 581-3, (1979).

25. Othmer, Kirk, "Encyclopedia of Chemical Technology", 2nd edition, John Wiley & Sons, Inc., New York, (1964) 3, 602-680.

26. Pinder, K.L., Personal communication on the DTA analysis of colemanite and sodium carbonate mixtures and boron analysis.

27. Satava, V., Skvara, F., "Mechanism and Kinetics of the Decomposition of Solids by a Thermogravimetric Method", Journal of American Ceramic Society, 52 [11], 591-5, (1969).

28. Sestak, J., Satava, V, Rihak, V., "Algorithm for Evaluating Kinetic Data from Non-Isothermal Thermogravimetric Curve", Silikaty, 11 [4], 315-24, (1967).

29. Sestak, J., "Errors of Kinetic Data Obtained from Thermogravimetric Curves at Increasing Temperatures", Talanta, 13, 567-79, (1966).

30. Wendlandt, W.W., "Thermal Methods of Analysis", 2nd edition, England, (1966) p. 29-40.

31. Zsako, J., "Kinetic Analysis of Thermogravimetric Data", The Journal of Physical Chemistry, 72 [7], 2406-11, (1968).

32. The manuals of Perkin-Elmer Thermogravimetric Analysis System.

APPENDIX I: GENERAL PROCEDURE FOR DETERMINATION OF
ACID SOLUBLE BORON

A.   SCOPE OF PROCEDURE

This procedure can be used to determine boron at levels of 0.05 to 5% in boron-containing substances such as boron minerals (except tourmaline and elemental boron), soils and organic substances impregnated with borates.

B.   REAGENTS

1. Standard 0.1 $\underline{N}$ sodium hydroxide.

2. Concentrated hydrochloric acid.

3. 1 $\underline{N}$ sodium hydroxide.

C.   SOLUTION OF SAMPLE FOR ANALYSIS

1. Weigh 5 grams and record weight to nearest 1 mg. Transfer to a 250-ml wide-mouthed erlenmeyer flask and heat the contents under reflux for two hours with 3 ml of conc. hydrochloric acid and 150 ml of water.

2. Cool the solution, filter and wash the residue.

3. The filtrate is used for the barium carbonate procedure, which follows.

D.   BARIUM CARBONATE PROCEDURE FOR DETERMINING B_2O_3

1. OUTLINE OF METHOD

The "Barium Carbonate Method" is a procedure used to remove heavy metals from solutions of crude borates, such as Rasorite, colemanite or ulexite, which would normally interfer with the determination of B_2O_3 by titration.

The heavy metals, iron, alumina, soluble silica and manganese are removed by the addition of barium carbonate to boric

acid. The resulting solution acts like a buffer with the proper hydrogen-ion concentration to precipitate the metals as hydroxides. Insoluble barium compounds are also formed of the acidic compounds present, such as silica. Barium borate itself is quite soluble.

This method is useful in precepitating almost all heavy metals except ferrous iron which must first be oxidized to the ferric state by the addition of bromine water. It is necessary to remove the excess bromine by boiling, as it would otherwise decolorize the methyl-red indicator.

2. PROCEDURE

a. Neutralize the filtrate with 1$\underline{N}$ NaOH to the methyl red end point. Make slightly acid to methyl red with HCl.

b. Add a few drops of bromine water and boil to remove the excess.

c. Add to this solution about two g of barium carbonate powder and boil for 2-3 minutes. Add more barium carbonate until there is a slight excess in the bottom of the beaker.

d. Allow the solution to stand at room temperature for two hours.

e. Filter the solution and wash with hot water. If a strong colour persists which would interfer with the perception of the endpoint, add a small amount of activated charcoal, bring to a boil and filter again.

f. Acidify the filtrate with HCl and boil to remove carbon dioxide.

g. Neutralize the filtrate with 0.1 $\underline{N}$ NaOH using methyl red as an indicator.

h. Add three heaping teaspoonsful of mannitol and seven drops of 1% phenolphthalein indicator solution.

i. Titrate with standard 0.1 $\underline{N}$ sodium hydroxide solution. The color of the solution in the presence of borate will change from red to yellow and then to pink at the phenolphthalein end point as sodium hydroxide is added.

j. Calculation:

$$\% \text{ B} = \frac{(\text{Volume of NaOH}) \times (\text{Normality of NaOH}) \times 1.082}{(\text{Sample Weight})}$$

APPENDIX II: SAMPLE CALCULATIONS AND DERIVATIONS

i. - Calculation of conversion from the titration data taken in the isothermal runs.

Define percent conversion as:

$$C = \frac{\text{moles of reacted } Na_2CO_3}{\text{moles of reacted } Na_2CO_3 + \text{moles of unreacted } Na_2CO_3} \times 100$$

The reactions are

$$Na_2CO_3 \rightarrow Na_2O + CO_2$$

$$Na_2O + H_2O \rightarrow 2NaOH$$
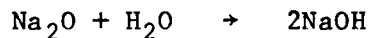
Let V_1: volume of acid to titrate NaOH and unreacted sodium carbonate

Let V_2: volume of acid to titrate sodium hydroxide

Let molarity of acid: M

Therefore moles of NaOH = $M \cdot V_2 \cdot 2$

moles of unreacted $Na_2CO_3 = (V_1 - V_2) \cdot M$

Then percent conversion = $\dfrac{1/2 \ (M \cdot V_2 \cdot 2)}{1/2 \ (MV_2 \cdot 2) + (V_1 - V_2)M} \times 100$

$$C = \frac{MV_2}{MV_2 + MV_1 - MV_2} \times 100$$

$$C = \frac{V_2}{V_1} \times 100$$

ii - Calculation of the stoichiometric amount of colemanite for the direct reduction of sodium carbonate.

Data for this calculation:

Formula of colemanite: $2CaO3B_2O_3 \cdot 5H_2O$

MW of B_2O_3: 69.6 g/g mole

MW of Na_2O: 62 g/g mole

MW of Na_2CO_3: 106 g/g mole

MW of colemanite: 410.8 g/g mole

MW of $Na_2O B_2O_3$: 131.6 g/g mole

From the phase diagram shown in Figure 10 it is seen that the compound which will form as a reaction product would be $Na_2O B_2O_3$ for Na:B ratio of greater than 0.999. The percentage of Na_2O and B_2O_3 in this compound can be calculated as follows:

$\% \ Na_2O$: $\dfrac{69.6}{131.6} \times 100 = 47.1$

$\% \ B_2O_3$: $\dfrac{62}{131.6} \times 100 = 52.9.$

Then what would be the percentage of colemanite in the mixture of colemanite and sodium carbonate in order to have $Na_2O B_2O_3$ as the product?

Basis: 100 gr $Na_2O \cdot B_2O_3$ which will form as a reaction product.

weight of sodium carbonate needed: $\frac{47.1}{62}$ x 106 = 80.53 g

weight of pure colemanite needed: $\frac{1}{3}$ x $\frac{52.9}{69.6}$ x 410.8 = 104.08 g

Since the colemanite which is used in this study was not pure and contained 38% B_2O_3 rather than 50.83% B_2O_3 actual needed amount of colemanite:

$$104.08 \text{ x } \frac{50.83}{38} = 139.22 \text{ g.}$$

So the total weight of the mixture should be:

$$80.53 + 139.22 = 219.75 \text{ g.}$$

Then weight % of Na_2CO_3: 36.65

weight % of colemanite: 63.35

iii — Calculation of frequency factor, Z_1, and rate constant, k_1, for the first reaction.

Starting with the equation (3.13)

$$g(\alpha) = \frac{Z_1 E_1}{Rq} W_{S_o}^{m-1} W_{C_o}^{n} p(x)$$

Since the reaction is zero order on both sodium carbonate and colemanite concentration the values of m and n are zero. Then the equation becomes

$$g(\alpha) = \frac{Z_1 E_1}{Rq} W_{S_o}^{-1} p(x)$$

Taking the logarithms of both sides

$$\log g(\alpha) = \log \frac{Z_1 E_1}{Rq} - \log W_{S_o} + \log p(x)$$

rearranging

$$\log g(\alpha) - \log p(x) = \log \frac{Z_1 E_1}{Rq W_{S_o}} = \bar{B}$$

therefore

$$\log Z_1 + \log E_1 - \log Rq W_{S_o} = \bar{B}$$

So $$\log Z_1 = \bar{B} - \log \frac{E_1}{Rq W_{S_o}}$$

$$Z_1 = \log^{-1} [\bar{B} - \log \frac{E_1}{Rq W_{S_o}}]$$

Rate constant can be calculated from the Arrhenius equation (6.3)

$$k_1 = Z_1 \exp \left(- \frac{E_1}{RT}\right)$$

where T is the temperature.

Sample calculation for 60 percent colemanite:

Data for this calculation:

$R = 1.987 \times 10^{-3}$ kcal/mol-°K

$W_{s_o} = 98.56$ g

$q = 10$ °K/min

$Y_c = 60$

$E_1 = 7.15$ kcal/mol

$\bar{B} = 2.8392$ (from figure 45)

$$\log Z_1 = 2.8392 - \log \frac{7.15}{(1.987 \times 10^{-3})(10)(98.56)}$$

$Z_1 = 180.172$ g/min

$$k_1 = 180.172 \exp \left[- \frac{7.15}{(1.987 \times 10^{-3})(T)}\right]$$

at $T = 1173$°K (900°C)

$k_1 = 8.383$ g/min

iv - Calculation of frequency factor, Z_2, and rate constant, k_2, for the 2nd reaction.

Starting with the following equation

$$g(\alpha) = \frac{Z_2 E_2}{Rq} W_{S_0}^{\nu-1} p(x)$$

Since the reaction is first order on the sodium carbonate concentration $\nu = 1$ therefore;

$$g(\alpha) = \frac{Z_2 E_2}{Rq} p(x)$$

Taking the logrithms of both sides

$$\log g(\alpha) = \log \frac{Z_2 E_2}{Rq} + \log p(x)$$

rearranging

$$\log g(\alpha) - \log p(x) = \log \frac{Z_2 E_2}{Rq} = \bar{B}$$

therefore

$$\log Z_2 = \bar{B} - \log \frac{E_2}{Rq}$$

$$Z_2 = \log^{-1} [\bar{B} - \log \frac{E_2}{Rq}]$$

and $\quad k_2 = Z_2 \exp(-\frac{E_2}{RT})$

Sample calculation for 30 percent colemanite:

Data for this calculation:

$R = 1.987$ cal/mol °K

$q = 10$ °K/min

$E_2 = 4700$ cal/mol

$\bar{B} = 1.6134$ (From figure 53)

$Z_2 = \log^{-1} [\bar{B} - \log \frac{E}{Rq}]$

$Z_2 = \log^{-1} (1.6134 - \log \frac{4700}{(1.987)(10)})$

$Z_2 = 0.1736$ min^{-1}

$k_2 = 0.1736 \exp (- \frac{4700}{(1.987)(T)})$

at $T = 900°C$ (1173 °K)

$k_2 = 0.1736 \exp (- \frac{4700}{(1.987)(1173)})$

$k_2 = 0.02311$ min^{-1}

v - Derivation of a combined rate expression.

The rate expression for the 1st reaction is

$$\frac{d\alpha}{dt} = R_1 = k_1' \qquad (1)$$

where

$$k_1' = k_1 \dot{W}_{S_o}^{-1}$$

The rate expression for the 2nd reaction is

$$\frac{d\alpha}{dt} = R_2 = k_2(1-\alpha) \qquad (2)$$

When these two reactions take place at the same time the overall rate of the reaction would be

$$\frac{d\alpha}{dt} = k_1' + k_2(1-\alpha) \qquad (3)$$

rearranging it

$$\frac{d\alpha}{k_1' + k_2 - k_2\alpha} = dt \qquad (4)$$

let $k_1' + k_2 = k_r$

then $\displaystyle\int_0^{\alpha'} \frac{d\alpha}{k_r - k_2\alpha} = \int_0^{t_1} dt$ \qquad (5)

Integration of this equation gives the following solution

$$-\frac{1}{k_2} \ln (k_r - k_2 \alpha) \Big|_0^{\alpha'} = t \Big|_0^{t_1}$$

$$\ln (k_r - k_2 \alpha') - \ln k_r = -k_2 t_1$$

$$\ln \frac{k_r - k_2 \alpha'}{k_r} = -k_2 t_1$$

$$\frac{k_r - k_2 \alpha'}{k_r} = \exp (-k_2 t_1)$$

$$k_r - k_2 \alpha' = k_r \exp (-k_2 t_1)$$

$$\alpha' = \frac{k_r - k_r \exp (-k_2 t_1)}{k_2} \tag{6}$$

Since the 1st reaction stops when the boron oxide content of the colemanite finishes there would be a specific time for each colemanite percentage at which the first reaction stops. This time can be calculated from the integration of equation 1 which will result in $\alpha_1' = k_1 t_1$ by knowing the final conversions at the end of the 1st reaction from the fractional conversions vs temperature plots. After the time t_1 is reached only the 2nd reaction takes place so the rate of the reaction is expressed as eq. 2. When eq. 2 is integrated

$$\int_{\alpha'}^{\alpha_2} \frac{d\alpha}{(1-\alpha)} = k_2 \int_{t_1}^{t_2} dt \tag{7}$$

$$- \ln (1-\alpha) \Big|_{\alpha'}^{\alpha_2} = k_2 \, t \Big|_{t_1}^{t_2}$$

$$- \ln \frac{1-\alpha_2}{1-\alpha'} = k_2 \ (t_2-t_1)$$

$$\frac{(1-\alpha_2)}{(1-\alpha')} = \exp \ (- \ k_2(t_2-t_1))$$

$$(1-\alpha_2) = (1-\alpha') \exp \ (- \ k_2(t_2-t_1))$$

$$\alpha_2 = 1 - [(1-\alpha') \exp \ (- \ k_2(t_2-t_1))] \tag{8}$$

where α_2 will be the final conversion at the end of the time t_2.

Sample calculation for 30 percent colemanite:

$$W_{S_o} = 99.6 \text{ g}$$

From Figure 42 $\alpha_1 = 0.26$

From Table 22 $k_1 = 1.520 \text{ g/min}$

$$k_2 = 0.024 \text{ min}^{-1}$$

$$k'_1 = (k_1)(W_{S_o})^{-1}$$

therefore $k'_1 = (1.520)(99.6)$

$$k'_1 = 0.01525 \text{ min}^{-1}$$

$$t_1 = \frac{0.26}{0.01525} = 17.05$$

$$k_r = k'_1 + k_2 = 0.03949$$

$$\alpha' = \frac{0.03949 - 0.03949 \exp[(-0.024)(17.05)]}{0.024}$$

$$\alpha' = 0.552$$

For $t_2 = 30 \text{ min.}$

$$\alpha_2 = 1 - [(1-0.552) \exp[-(0.024)(30-17.05)]]$$

$$\alpha_2 = 0.672$$

Table A1: Na:B ratios for different colemanite concentrations.

% colemanite	Na:B for Na_2CO_3 + colemanite	Na:B for Na_2CO_3 + calcium borate
30	4.04	5.16
40	2.59	3.35
50	1.73	2.24
60	1.15	1.5

APPENDIX III: TURKISH COLEMANITE PRODUCT SPECIFICATIONS AND
TYPICAL ANALYSIS

Chemical Analysis	Contract Specifications Max.	Min.	Typical Analysis
B_2O_3	40.0	38.0	39.50
Na_2O	0.5		0.15
CaO	27.5	24.5	27.00
Fe_2O_3	0.3		0.09
SiO_2	7.0		5.14
Al_2O_3	1.0		0.38
SrO	1.5		0.95
MgO	3.0		1.95
SO_3	0.8		0.74
LOI (1600°F for 30 min)	26.5		24.30
H_2O (60°C for 2 hrs.)	2.0		0.80

* Analysis done by the American Borate Company

Physical Analysis

U.S. Screen Size	Cumulative Weight Percent Retained	
Mesh	Max.	Min.
+ 60	.05	
+ 70	.25	
+100	3.25	
+140	9.25	
+200	20.00	
-200		80.

Other Physical Data

Specific Gravity	2.4	
Reactivity with Steel	None	
Angle of Repose-Settled	25°	
Bulk Density (lbs./cu. ft.)		
Tap	90	
Pour	70	
Hardness (Mohs Scale)		
Colemanite	4.5	
Calcite	3.0	

* Analysis done by the American Borate Company

APPENDIX IV: STANDARD DEVIATION TABLES FOR THE
FIRST AND SECOND REACTIONS

Table A2. Standard deviation of the B (as defined by Equation 2.24)
values (STD) for various reaction mechanisms and activation
energies (E) for the first reaction at 30% by weight colemanite

$E\left(\dfrac{CAL}{MOL}\right)$		N=1/3 M=O	N=1/2 M=O	N=2/3 M=O	N=1 M=O	N=O M=1/3	N=O M=1/2	N=O M=O
5000	B	1.4658	1.4779	1.4903	1.5162	1.4474	1.4498	1.4427
	STD	0.19176	0.19641	0.20226	0.21781	0.18651	0.18696	0.18570
5200	B	1.5590	1.5710	1.5835	1.6094	1.5406	1.5430	1.5358
	STD	0.18812	0.19208	0.19728	0.21167	0.18399	0.18430	0.18346
5400	B	1.6511	1.6632	1.6756	1.7015	1.6327	1.6351	1.6279
	STD	0.18540	0.18863	0.19312	0.20623	0.18246	0.18263	0.18222
5600	B	1.7423	1.7544	1.7668	1.7927	1.7239	1.7263	1.7192
	STD	0.18374	0.18621	0.18995	0.20164	0.18203	0.18205	0.18209
5800	B	1.8326	1.8447	1.8571	1.8830	1.8142	1.8166	1.8094
	STD	0.18304	0.18471	0.18766	0.19786	0.18256	0.18243	0.18290
5500	B	1.6968	1.7089	1.7214	1.7472	1.6785	1.6809	1.6737
	STD	0.18440	0.18726	0.19138	0.20379	0.18208	0.18217	0.18198
5700	B	1.7876	1.7996	1.8121	1.8380	1.7692	1.7716	1.7644
	STD	0.18322	0.18530	0.18865	0.19961	0.18212	0.18207	0.18232

Table A3. Standard deviation of the B (as defined by Equation 2.24) values (STD) for various reaction mechanisms and activation energies (E) for the first reaction at 40% by weight colemanite

$E\left(\dfrac{CAL}{MOL}\right)$		N=1/3 M=0	N=1/2 M=0	N=2/3 M=0	N=1 M=0	N=0 M=1/3	N=0 M=1/2	N=0 M=0
5000	B	1.6162	1.6276	1.6393	1.6638	1.6015	1.6051	1.5944
	STD	0.20997	0.21540	0.22198	0.23889	0.20407	0.20514	0.20214
6000	B	2.0735	2.0849	2.0966	2.1211	2.0588	2.0624	2.0516
	STD	0.19154	0.19387	0.19746	0.20896	0.18999	0.19005	0.19007
7000	B	2.5115	2.5229	2.5346	2.5591	2.4968	2.5004	2.4896
	STD	0.19706	0.19577	0.19562	0.19961	0.20019	0.19923	0.20228
6200	B	2.1624	2.1738	2.1855	2.2100	2.1477	2.1513	2.1406
	STD	0.19067	0.19227	0.19513	0.20526	0.19008	0.18992	0.19059
5800	B	1.9838	1.9952	2.0069	2.0314	1.9691	1.9727	1.9620
	STD	0.19335	0.19637	0.20065	0.21344	0.19084	0.19112	0.19050
5900	B	2.0288	2.0402	2.0519	2.0764	2.0141	2.0177	2.0069
	STD	0.19239	0.19507	0.19901	0.21118	0.19035	0.19053	0.19022
6100	B	2.1181	2.1295	2.1412	2.1657	2.1034	2.1070	2.0962
	STD	0.19094	0.19290	0.19614	0.20696	0.18986	0.18982	0.19016

Table A-4. Standard deviation of the B (as defined by Equation 2.24) values (STD) for various reaction mechanisms and activation energies (E) for the first reaction at 50% by weight colemanite

$E\left(\frac{CAL}{MOL}\right)$		N=1/3 M=0	N=1/2 M=0	N=2/3 M=0	N=1 M=0	N=0 M=1/3	N=0 M=1/2	N=0 M=0
5000	B	1.7478	1.7597	1.7719	1.7975	1.7369	1.7428	1.7252
	STD	0.22433	0.23121	0.23931	0.25951	0.21840	0.22098	0.21383
6000	B	2.2012	2.2130	2.2252	2.2509	2.1902	2.1961	2.1786
	STD	0.19648	0.20049	0.20591	0.22147	0.19353	0.19459	0.19208
7000	B	2.6353	2.6472	2.6594	2.6850	2.6244	2.6303	2.6127
	STD	0.19185	0.19201	0.19357	0.20179	0.19268	0.19188	0.19488
8000	B	3.0550	3.0668	3.0791	3.1047	3.0440	3.0499	3.0324
	STD	0.21159	0.20811	0.20573	0.20542	0.21574	0.21336	0.22089
6200	B	2.2894	2.3012	2.3134	2.3390	2.2784	2.2843	2.2668
	STD	0.19351	0.19680	0.20152	0.21581	0.19129	0.19198	0.19057
6400	B	2.3768	2.3887	2.4009	2.4265	2.3659	2.3718	2.3543
	STD	0.19153	0.19407	0.19805	0.21098	0.19006	0.19038	0.19007
6600	B	2.4636	2.4755	2.4877	2.5133	2.4526	2.4585	2.4410
	STD	0.19063	0.19239	0.19558	0.20703	0.18993	0.18987	0.19069

Table A4. Continue

$E\left(\dfrac{CAL}{MOL}\right)$		N=1/3 M=O	N=1/2 M=O	N=2/3 M=O	N=1 M=O	N=O M=1/3	N=O M=1/2	N=O M=O
6800	B	2.5498	2.5616	2.5738	2.5995	2.5388	2.5447	2.5272
	STD	0.19078	0.19173	0.19412	0.20398	0.19084	0.19041	0.19233
6300	B	2.3332	2.3451	2.3573	2.3829	2.3223	2.3282	2.3107
	STD	0.19240	0.19532	0.19968	0.21332	0.19054	0.19105	0.19019
6500	B	2.4203	2.4322	2.4444	2.4700	2.4094	2.4153	2.3978
	STD	0.19104	0.19319	0.19678	0.20898	0.18994	0.19008	0.19033

Table A5. Standard deviation of the B (as defined by Equation 2.24) values (STD) for various reaction mechanisms and activation energies (E) for the second reaction at 30% by weight colemanite

$E\left(\dfrac{CAL}{MOL}\right)$		M=0	M=1/3	M=1/2	M=2/3.	M=1	M=2	D1	D2	D3	A2	A3
2000	B	0.3787	0.4191	0.4399	0.4611	0.5047	0.6454	0.0228	-.1988	-.7666	0.6196	0.6579
	STD	0.02528	0.03254	0.03694	0.04176	0.05243	0.09113	0.11713	0.13607	0.15812	0.01995	0.03868
3000	B	0.8416	0.8820	0.9028	0.9240	0.9676	1.1083	0.4857	0.2640	-.3037	1.0825	1.1208
	STD	0.02087	0.02202	0.02438	0.02774	0.03668	0.07370	0.10029	0.11891	0.14071	0.03638	0.05655
4000	B	1.2357	1.2762	1.2970	1.3182	1.3618	1.5025	0.8799	0.6582	0.0905	1.4767	1.5150
	STD	0.02937	0.02360	0.02187	0.02141	0.02494	0.05746	0.08471	0.10282	0.12426	0.05320	0.07381
5000	B	1.5906	1.6310	1.6518	1.6730	1.7167	1.8574	1.2348	1.0131	0.4454	1.8316	1.8699
	STD	0.04306	0.03467	0.03066	0.02702	0.02219	0.04242	0.07025	0.08754	0.10844	0.06983	0.09066
6000	B	1.9199	1.9603	1.9811	2.0024	2.0460	2.1867	1.5641	1.3424	0.7747	2.1609	2.1992
	STD	0.05821	0.04894	0.04420	0.03945	0.03040	0.02973	0.05740	0.07327	0.09330	0.08629	0.10725
7000	B	2.2312	2.2716	2.2924	2.3136	2.3572	2.4979	1.8753	1.6536	1.0859	2.4721	2.5104
	STD	0.07389	0.06426	0.05924	0.05410	0.04363	0.02298	0.04716	0.06038	0.07895	0.10268	0.12371
8000	B	2.5287	2.5691	2.5899	2.6111	2.6548	2.7955	2.1729	1.9512	1.3835	2.7697	2.8080
	STD	0.08968	0.07987	0.07471	0.06939	0.05835	0.02653	0.04105	0.04962	0.06560	0.11894	0.14003

Table A5. Continue

$E\left(\frac{CAL}{MOL}\right)$		M=0	M=1/3	M=1/2	M=2/3	M=1	M=2	D1	D2	D3	A2	A3
9000	B	2.8158	2.8562	2.8770	2.8982	2.9419	3.0825	2.4600	2.2383	1.6706	3.0567	3.0950
	STD	0.10551	0.09559	0.09036	0.08495	0.07362	0.03751	0.04102	0.04266	0.05406	0.13507	0.15621
4800	B	1.5221	1.5625	1.5833	1.6045	1.6481	1.7888	1.1663	0.9446	0.3768	1.7630	1.8013
	STD	0.04013	0.03206	0.02833	0.02511	0.02175	0.04534	0.07308	0.09057	0.11160	0.06649	0.08728
5200	B	1.6583	1.6987	1.7195	1.7407	1.7844	1.9250	1.3025	1.0808	0.5131	1.8992	1.9375
	STD	0.04599	0.03735	0.03312	0.02914	0.02307	0.03962	0.06751	0.08459	0.10535	0.07312	0.09398
4600	B	1.4523	1.4927	1.5135	1.5348	1.5784	1.7191	1.0965	0.8748	0.3071	1.6933	1.7316
	STD	0.03726	0.02958	0.02620	0.02351	0.02181	0.04830	0.07592	0.09360	0.11474	0.06315	0.08391
4700	B	1.4873	1.5277	1.5485	1.5698	1.6134	1.7541	1.1315	0.9098	0.3421	1.7283	1.7666
	STD	0.03872	0.03082	0.02726	0.02428	0.02170	0.04677	0.07445	0.09204	0.11312	0.06486	0.08564
4900	B	1.5565	1.5969	1.6177	1.6389	1.6826	1.8232	1.2007	0.9790	0.4113	1.7974	1.8357
	STD	0.04165	0.03341	0.02953	0.02608	0.02192	0.04382	0.07160	0.08899	0.10995	0.06823	0.08905

Table A6. Standard deviation of the B (as defined by Equation 2.24) values (STD) for various reaction mechanisms and activation energies (E) for the second reaction at 40% by weight colemanite

$E\left(\dfrac{CAL}{MOL}\right)$		M=0	M=1/3	M=1/2	M=2/3	M=1	M=2	D1	D2	D3	A2	A3
3000	B	0.9985	1.0595	1.0915	1.1246	1.1939	1.4272	0.7774	0.5948	0.0754	1.2068	1.2111
	STD	0.01544	0.01441	0.01982	0.02738	0.04590	0.11826	0.07843	0.10634	0.14243	0.02408	0.04617
4000	B	1.3966	1.4576	1.4896	1.5227	1.5920	1.8253	1.1755	0.9928	0.4734	1.6048	1.6091
	STD	0.02781	0.01563	0.01241	0.01473	0.03051	0.10219	0.06338	0.09075	0.12655	0.03993	0.06226
5000	B	1.7553	1.8162	1.8483	1.8814	1.9507	2.1840	1.5341	1.3515	0.8321	1.9635	1.9678
	STD	0.04235	0.02787	0.02043	0.01391	0.01673	0.08648	0.04923	0.07566	0.11106	0.05554	0.07798
6000	B	2.0883	2.1493	2.1813	2.2144	2.2837	2.5170	1.8672	1.6845	1.1651	2.2965	2.3008
	STD	0.05725	0.04224	0.03407	0.02561	0.01126	0.07112	0.03673	0.06124	0.09600	0.07093	0.09342
7000	B	2.4032	2.4642	2.4962	2.5293	2.5986	2.8319	2.1821	1.9994	1.4800	2.6115	2.6157
	STD	0.07228	0.05707	0.04869	0.03983	0.02113	0.05591	0.02747	0.04757	0.08117	0.08622	0.10874
8000	B	2.7044	2.7654	2.7974	2.8305	2.8998	3.1331	2.4833	2.3006	1.7812	2.9126	2.9169
	STD	0.08730	0.07199	0.06354	0.05455	0.03507	0.04096	0.02516	0.03545	0.06674	0.10140	0.12394
9000	B	2.9951	3.0561	3.0881	3.1212	3.1905	3.4238	2.7740	2.5913	2.0719	3.2033	3.2076
	STD	0.10224	0.08688	0.07839	0.06935	0.04962	0.02636	0.03101	0.02658	0.05277	0.11648	0.13903

$E\left(\dfrac{CAL}{MOL.}\right)$		M=0	M=1/3	M=1/2	M=2/3	M=1	M=2	D1	D2	D3	A2	A3
5800	B	2.0234	2.0843	2.1164	2.1494	2.2188	2.4521	1.8022	1.6196	1.1002	2.2316	2.2359
	STD	0.05427	0.03932	0.03123	0.02294	0.01093	0.07417	0.03906	0.06408	0.09899	0.06787	0.09035
5600	B	1.9576	2.0186	2.0506	2.0837	2.1530	2.3863	1.7365	1.5538	1.0344	2.1658	2.1701
	STD	0.05125	0.03639	0.02840	0.02035	0.01147	0.07727	0.04151	0.06697	0.10202	0.06477	0.08724
5900	B	2.0559	2.1169	2.1489	2.1820	2.2513	2.4846	1.8348	1.6521	1.1327	2.2641	2.2684
	STD	0.05582	0.04083	0.03270	0.02431	0.01100	0.07259	0.03785	0.06261	0.09744	0.06945	0.09194
5700	B	1.9906	2.0515	2.0836	2.1167	2.1860	2.4193	1.7694	1.5868	1.0674	2.1988	2.2031
	STD	0.05279	0.03788	0.02983	0.02164	0.01107	0.07569	0.04024	0.06548	0.10047	0.06635	0.08882

Table A7. Standard deviation of the B (as defined by Equation 2.24) values (STD) for various reaction mechanisms and activation energies (E) for the second reaction at 50% by weight colemanite

$E\left(\dfrac{CAL}{MOL}\right)$		M=0	M=1/3	M=1/2	M=2/3	M=1	M=2	D1	D2	D3	A2	A3
6000	B	2.2288	2.3397	2.4031	2.4726	2.6321	3.2722	2.1546	2.0600	1.6880	2.4675	2.4126
	STD	0.05981	0.03030	0.01485	0.02567	0.09612	0.47456	0.03395	0.06771	0.16591	0.02023	0.05024
7000	B	2.5429	2.6538	2.7172	2.7868	2.9463	3.5863	2.4688	2.3742	2.0022	2.7817	2.7268
	STD	0.07261	0.04212	0.02250	0.01575	0.08357	0.46249	0.03450	0.05661	0.15282	0.03094	0.06330
8000	B	2.8434	2.9543	3.0177	3.0872	3.2468	3.8868	2.7693	2.6746	2.3027	3.0821	3.0273
	STD	0.08539	0.05445	0.03369	0.01377	0.07148	0.45067	0.03967	0.04679	0.13993	0.04298	0.07628
9000	B	3.1333	3.2442	3.3076	3.3772	3.5367	4.1767	3.0592	2.9646	2.5926	3.3721	3.3172
	STD	0.09815	0.06697	0.04579	0.02167	0.05988	0.43901	0.04785	0.03894	0.12717	0.05541	0.08919
10000	B	3.4148	3.5257	3.5891	3.6586	3.8182	4.4582	3.3407	3.2460	2.8741	3.6536	3.5987
	STD	0.11096	0.07963	0.05827	0.03296	0.04899	0.42743	0.05783	0.03440	0.11448	0.06803	0.10212
11000	B	3.6893	3.8002	3.8636	3.9331	4.0927	4.7327	3.6152	3.5205	3.1486	3.9281	3.8732
	STD	0.12376	0.09235	0.07089	0.04513	0.03936	0.41594	0.06879	0.03447	0.10189	0.08071	0.11501
12000	B	3.9579	4.0689	4.1323	4.2018	4.3613	5.0014	3.8838	3.7892	3.4172	4.1967	4.1418
	STD	0.13646	0.10499	0.08349	0.05752	0.03231	0.40469	0.08024	0.03908	0.08958	0.09334	0.12777

Table A7. Continue

$E\left(\frac{CAL}{MOL}\right)$		M=O	M=1/3	M=1/2	M=2/3	M=1	M=2	D1	D2	D3	A2	A3
13000	B	4.2217	4.3326	4.3960	4.4656	4.6251	5.2651	4.1476	4.0530	3.6810	4.4605	4.4056
	STD	0.14922	0.11772	0.09619	0.07011	0.02933	0.39344	0.09210	0.04688	0.07734	0.10605	0.14060
14000	B	4.4812	4.5921	4.6555	4.7250	4.8846	5.5246	4.4071	4.3125	3.9405	4.7200	4.6651
	STD	0.16185	0.13031	0.10876	0.08262	0.03182	0.38252	0.10400	0.05633	0.06547	0.11867	0.15329
15000	B	4.7369	4.8479	4.9113	4.9808	5.1403	5.7803	4.6628	4.5682	4.1962	4.9757	4.9208
	STD	0.17456	0.14299	0.12144	0.09525	0.03855	0.37161	0.11617	0.06698	0.05395	0.13136	0.16604
13200	B	4.2739	4.3849	4.4483	4.5178	4.6773	5.3174	4.1998	4.1052	3.7332	4.5127	4.4578
	STD	0.15167	0.12015	0.09862	0.07252	0.02946	0.39136	0.09435	0.04851	0.07499	0.10852	0.14307
12700	B	4.1693	4.2802	4.3436	4.4131	4.5726	5.2127	4.0951	4.0005	3.6285	4.4080	4.3531
	STD	0.14670	0.11520	0.09367	0.06761	0.02960	0.39571	0.08970	0.04508	0.07974	0.10356	0.13808
12800	B	4.1955	4.3064	4.3698	4.4393	4.5989	5.2389	4.1214	4.0268	3.6548	4.4343	4.3794
	STD	0.14798	0.11647	0.09494	0.06887	0.02942	0.39456	0.09090	0.04595	0.07851	0.10482	0.13935
12900	B	4.2478	4.3587	4.4221	4.4916	4.6512	5.2912	4.1737	4.0790	3.7071	4.4866	4.4317
	STD	0.15052	0.11900	0.09747	0.07138	0.02935	0.39234	0.09327	0.04769	0.07607	0.10736	0.14191

APPENDIX V: FITTING OF THE POINTS ON FIG. 56 AND 57

X POWER	COEFFICIENT
0	-19999.0013
1	2518.23627
2	-85.4970639
3	.966638716

PERCENTAGE GOODNESS OF FIT = 100

X POWER	COEFFICIENT
0	-252.342474
1	27.3482681
2	-.947228943
3	.0105397707

PERCENTAGE GOODNESS OF FIT = 100

X POWER	COEFFICIENT
0	.229370396
1	-.0249932329
2	8.83021742E-04
3	-9.30306422E-06

PERCENTAGE GOODNESS OF FIT = 100